Thesis for the Degree of Master of Science in Marine Technology

Research on *lift-carry-over* in hull-keel-centre board configurations, to improve the performance prediction of sailing yachts at Dykstra Naval Architects

D.J. Geldermans

Delft University of Technology

December 2018

TU Delft

Thesis for the Degree of Master of Science in Marine Technology

Research on *lift-carry-over* in hull-keel-centre board configurations, to improve the performance prediction of sailing yachts at Dykstra Naval Architects

by

D.J. Geldermans

To obtain the degree of Master of Science
at the Delft University of Technology,
to be defended publicly on Friday december 14, 2018.

Student number:	4242254
Project duration:	November, 2017 – December, 2018
TU Delft, professor and supervisor:	Prof. dr. ir. R. van 't Veer
Dykstra NA, supervisor:	Ir. M. Leslie-Miller

This thesis is confidential and cannot be made public until December 31, 2023.

TU Delft Delft University of Technology

Abstract

This thesis, for the degree of Master of Science in Marine Technology, describes the research commissioned by Dykstra Naval Architects, to graduate at the Delft University of Technology.

Dykstra is regularly designing large classic sailing yachts or motor-sailors, of which the draft is an important design restriction. Therefore, Dykstra is trying to improve the sailing performance by adding lift-generating appendages, without increasing the draft. An example is a retractable centre board, having a big influence on the sailing properties. Predicting the performance contribution of a centre board in a hull-keel-centre board configuration is the subject of this research.

Predicting the performance through commercial VPPs is known to give inaccurate results for yachts with a keel-centre board combination, because these lay outside the scope of the systematic tank test series on which these VPPs are based. Therefore, Dykstra is obtaining all information regarding the performance of the hull through CFD or towing tank tests, after which the centre board is superposed as a lift generating surface.

During the verification of this method for a large yacht with a keel-centre board configuration, it was found that the centre board was working more 'effective' in terms of sideforce and resistance than was expected. This effect has been found in earlier studies as well and is known as the *lift-carry-over*, defined as the ratio between the measured lift and the theoretical lift of the foil. However, these earlier studies were all conducted on conventional hull-keel configurations of small yachts. The goal of this research is to develop a method to predict the performance contribution of a centre board to yachts with a hull-keel-centre board configuration.

Dykstra wants to keep the ability to superpose an appendage to the data of a hull-keel configuration obtained from towing tank experiments or CFD simulations. This means that a method must be developed to estimate the *contribution* of the centre board, in terms of sideforce, resistance and centre of effort.

Both towing tank experiments and CFD simulations are conducted for this research. The Maltese Falcon is used as the 'case ship'. A towing tank model of the Maltese Falcon was already made and tested at the TU delft in 2002. This model is again subjected to towing tank experiments, with a new keel and two new centre boards, resulting in 9 different hull-keel-centre board configurations. The main focus was on the towing tank experiments, executed in the Delft Hydromechanics Laboratory. Extensive preparations, a carefully constructed towing tank setup and elaborate post-processing resulted in good and useful results. The CFD simulations were then done to validate the results of the towing tank experiments and to gain visual insight in the flow around the vessel. The lift-carry-over on the keel and hull above the centre board can clearly be seen, as well as the influence of the centre board on the circulation in the flow around the underwater body of the yacht.

After post-processing all experimental data, the results of the towing tank experiments are used to develop formulations to predict the performance contribution of the centre board. For as far as possible, existing formulations to predict the lift-carry-over, resistance and centre of effort of conventional yachts, have been reconstructed to make them suitable for predicting the centre board contribution. According to the results from the towing tank experiment, the magnitude of the lift-carry-over was even more than was expected. The measured lift of the centre board contribution was roughly a factor 2 higher than the centre would generate according to Wicker & Fehlner theory. It was interesting to see that taking this 'extra' lift into account when calculating the induced resistance, this induced resistance would be largely over estimated. This shows that the lift-carry-over does not only have a positive effect on the generated sideforce, but also on the resistance. Furthermore, it was found that heeling the Maltese Falcon model by 15 degrees, yields the same magnitude of lift-carry-over as for the upright conditions. The theoretical aspects prescribing the lift-carry-over reduction due to heel for conventional hull-keel configurations, are significantly less existent for the centre boards in large yachts. This

resulted in the conclusion that heeling the yacht has no influence on the lift-carry-over from centre board to keel-hull.

The new prediction methods, derived from the towing tank experiment data, are validated on YACHT1 and Adela. These are existing yachts with a hull-keel-centre board configuration, but both very different. This enabled an interesting examination on the influence of certain aspects of the configuration on the performance of the centre board contribution. All in all, it was found that the predicted centre board contribution corresponded really well to the measured data of YACHT1 and Adela. This provides enough trust to implement the new centre board performance prediction methods in the Dykstra performance prediction tool. Every new design cycle of a yacht with hull-keel-centre board configuration will serve as a validation of the derived performance prediction methods.

Preface

Just as the vast majority of Maritime Technology students, I am a passionate sailor. Already in the early days of my study in Delft, I was thinking of doing an internship at Dykstra Naval Architects some day, which I got to know from designing the mighty J-Class yachts. Doing my final internship and writing my master thesis at this fantastic company has been a major privilege, and feels like the perfect ending of my student life.

The week I started the internship at Dykstra Naval Architects, was also the week I became co-founder of a new company, Skoon Energy. It was not always easy to start a company and to write a master thesis at the same time, which is the reason why this research and internship were extended from nine to thirteen months. I greatly appreciate the the support of all the people at Dykstra Naval Architects, and the flexibility which they gave me to be able to start this company.

This research project originated from some findings at Dykstra Naval Architects, during the design phase of a large motor-sailor, in which the predicted performance of the centre board was not in line with the performance according to the CFD simulations. Together with input from Lex Keuning, this led to an interesting research project. Doing towing tank experiments for three weeks in the Delft Hydromechanics Laboratory was the absolute highlight. Many aspects of maritime knowledge we use today are based on systematic towing tank series. However, the methodology of such a research was new to me and much more extensive than I had expected. In general, I feel that during the past year I have learned many things which the study program had only slightly touched upon.

I would like to acknowledge everyone who was involved in the work I did for this research project. Special thanks to Wick Hillege, who supported this research in all aspects at the Delft Hydromechanics Laboratory. Wick coordinated all the experiment preparations, and ensured that all uncertainty factors during the daily operations in the towing tank were eliminated. Also many thanks to Mark Leslie-Miller, who was always available for questions and feedback, guiding me on a daily basis. Finally, I would like to thank Lex Keuning for setting up this research and giving sharp feedback when needed. It was an honour to be his last ever graduate student.

D.J. Geldermans

Delft, December 2018

Contents

Nomenclature

Abbreviations

CB	Centre board
CFD	Computational Fluid Dynamics
CoE	Centre of Effort
DSKS	Delft Systematic Keel Series
DSYHS	Delft Systematic Yacht Hull Series
DVKS	Delft Various Keel Series
LCB	Longitudinal Centre of Buoyancy
LCO	Lift-Carry-Over
VPP	Velocity Prediction Program

Greek Symbols

$\alpha_{e\ keel}$	Effective angle of attack of the keel
β	Leeway angle
β_0	Zero lift drift angle
Λ	Sweepback angle
ν	Dynamic viscosity
ρ	Density

Other Symbols

$A_{lat\ CB}$	Lateral area of the board
$A_{lat\ keel}$	Lateral area of the keel
AR_e	Effective aspect ratio
b_{CB}	Centre board span
b_{keel}	Keel span
c	Chord length
C_D	Drag coefficient
C_F	Friction resistance coefficient
C_L	Lift coefficient
$C_{Dv,fintip}$	Fin tip drag coefficient
C_{D_0}	Viscous drag coefficient
C_{D_i}	Induced drag coefficient
$C_{D_{tot}}$	Total drag coefficient
c_{heel}	Heel coefficient
c_{hull}	Hull coefficient
$C_{L_{(W\&F)}}$	Lift coefficient according to Wicker & Fehlner theory
C_{Res}	Residual drag coefficient
F_D	Drag force
F_L	Lift force
k_i	Induced drag factor
$k_{Hoerner}$	Form factor
$K_{lift\ carry\ over}$	Lift-carry-over factor
R	Resistance
R_i	Induced resistance
R_{res}	Residual resistance
Re	Reynolds number
SF	Sideforce
T	Draft
t	Section profile thickness
T_c	Canoe body draft
T_{eff}	Effective draft
T_e	Effective span
T_{max}	Maximum draft
U_0	Velocity of free stream flow
V_m	Velocity of the model
$V_{e\ keel}$	Effective velocity of the keel
Vs	Velocity of the ship
X_{cp}	Longitudinal centre of pressure
Z_{cp}	Vertical centre of pressure

1

Introduction to the research

This chapter covers an introduction to this research project and the subject matter. The general approach used by Dykstra Naval Architects to predict the performance of sailing yachts will be described. After that, this chapter is concluded by the goal and contributions of this research.

1.1. Research subject and motivation

Dykstra Naval Architects ('Dykstra') brings over 45 years of experience in the design, redesign, naval architecture and marine engineering of classic and modern performance yachts. They offer preliminary and concept designs for both pleasure and commercially operated yachts. Dykstra is regularly designing classic sailing yachts or motor-sailors, of which comfortable cruising is the main objective. The owners of these yachts want to be able to reach every bay and port, so they must not be limited by the draft of their yacht. This results in yacht designs with a (very) long and shallow keel. These types of yachts may lack some sailing performance, especially upwind. Therefore, Dykstra is trying to improve the sailing performance by adding lift-generating appendages, without increasing the draft. Examples are retractable centre boards, winglets and bilge keels. Especially the centre board has a big influence on the sailing properties. The main objective to implementing a centre board in the design is to increase the sideforce production (to windward), to prevent the boat from drifting to leeward. Predicting the performance of a centre board in a hull-keel-centre board configuration is the subject of this research.

Predicting the performance through commercial VPPs is known to give inaccurate results for yachts with a keel-centre board combination, because these lay outside the scope of the systematic tank test series on which these VPPs are based. Therefore, Dykstra is obtaining all information regarding the performance of the hull through CFD or towing tank experiments, after which the appendages are superposed as lift generating surfaces. During the verification of this method, for a large yacht with a keel-centre board configuration, an interesting phenomenon was found. The CFD simulations of the total hull-keel-centre board configuration resulted in a significantly higher sideforce production than was estimated by adding the centre board as a lift generating surface to the sideforce production of the hull-keel only. This suggested an interaction effect, occurring between the hull-keel and the centre board. This effect has been found in earlier studies as well and is known as the *lift-carry-over*. It means that lift generated by the appendage, is transferred to the body on which it is attached. These earlier studies, all conducted on conventional hull-keel configurations, resulted in a few trend formulations to predict the magnitude of the lift-carry-over. However, these formulations are not validated for large yachts with a keel-centre board configuration, and can thus not be used by Dykstra to predict the performance of such yachts. This means that Dykstra must do several CFD simulations before the best configuration for the keel-centre board is achieved. This is computationally expensive and costs significant amount of time. If Dykstra could use performance prediction methods to estimate the contribution of the centre board in such hull-keel-centre board configurations, this would result in a better starting point for the

CFD simulations. A more accurate first estimate means less CFD simulation would be required in total.

When developing (improved) performance prediction methods for hull-keel-centre board configurations, Dykstra wants to keep the ability to superpose an appendage to the data of a hull-keel configuration, obtained from towing tank experiments or CFD simulations. This means that a method must be developed to estimate the magnitude of the lift-carry-over from centre board to keel, and the influence of this lift-carry-over phenomenon on the resistance and centre of effort of the centre board. The lift-carry-over for such configurations is defined as the ratio of the measured lift generated by the centre board when positioned under a hull-keel, to the theoretical lift that the centre board would generate in a free stream[1] flow according to theory.

1.2. Performance prediction at Dykstra Naval Architects

The sailing yacht may be considered as an equilibrium of multiple aero- and hydrodynamic forces and moments. The unsteady behaviour of wind and waves makes this a very complex dynamic equilibrium. Velocity Prediction Programs (VPPs) are used to asses the performance of sailing yachts in varying conditions. In general, a VPP consists of three components [2]:

1. A model for the hydrodynamic characteristics of the boat
2. A model describing the aerodynamic characteristics of the rig
3. Formulations to balance these characteristics with respect to optimum forward speed

Regarding the hydrodynamic aspects, these commercial (standard) VPPs use regression analysis based on systematic series of hulls, keels and rudders. For standard hull shapes and appendage layouts, these VPPs are known to give accurate results. However, if the shape of the hull or appendages lay outside the scope of the systematic series, the results of the VPP are obtained from extrapolation, which results in inaccurate and unusable data. Dykstra is regularly designing vessels laying outside the scope of existing systematic series. These big yachts deviate for instance regarding the beam to draft ratio or the length to displacement ratio. Examples are large classic yachts or 'motor-sailors'. For these kind of yachts, Dykstra uses an inhouse VPP tool, built in Matlab, to estimate the performance. First, all parameters regarding the hull, like resistance, stability, sideforce, etc. are obtained from CFD simulations or towing tank tests, for a varying boat speed, heeling angle and leeway angle. Then, the Matlab tool relates these data to the aerodynamic forces. The rudder(s), keel(s) and optional centre board are to be manually implemented in this tool, of which the interface is presented in an Excel sheet. Finally, a regression analysis will be used to find the optimum forward speed. An important constraint is the equilibrium regarding the yaw moment, which will be satisfied by varying the rudder angle. The sideforce production of all components will result in a certain leeway angle. In the end, the optimum forward velocity for each wind angle and wind speed is found by varying the parameters within the boundary conditions. So, estimating the total performance is a combination of CFD or towing tank tests (hull) and manual input in Matlab (appendages).

The centre board is currently implemented in the VPP simply as a lift generating surface. The theoretical forces generated by the centre board are superposed to the forces generated by the hull, according to CFD data or results from towing tank experiments. Variations in flow velocity and direction, boundary layer effects, downwash or other interaction effects are not considered. Moreover, no contribution of the lift-carry-over phenomenon is being taken into account.

1.3. Goal of the research

The goal of this research is to develop performance prediction methods for the centre board contribution in hull-keel-centre board configurations, to improve the performance prediction of sailing yachts at Dykstra Naval Architects.

[1] Actually, it is not compared to a centre board in total free stream, but to a centre board with it's root chord placed perpendicular to a flat plate. In that case, the effective aspect ratio is twice the geometrical aspect ratio. This is further discussed in section 2.2

1.4. Scientific and practical contributions of the research

Now the problem has been outlined, it is important to clarify why this will be researched. Dykstra is regularly designing classic sailing yachts and motor-sailors, of which the performance is currently predicted as is described in section 1.1. This method is found to be inaccurate for hull-keel-centre board configurations. Moreover, this approach costs significant amount of time since the performance prediction of the keel-centre board layout has to be validated by multiple CFD simulations, before the best configuration is obtained. Instead, Dykstra wants the possibility to make a more accurate estimate of the performance using their inhouse VPP first, before doing CFD simulations for validation. Saving time by using a more accurate VPP, before doing some final CFD simulations to obtain more exact data is the main practical importance of this research for Dykstra.

From a hydrodynamical point of view, it is a very interesting challenge to capture the interaction effect between the hull, keel and centre board, and explain the 'extra' sideforce production. Research has been done on many different types of keels, but not for the combination of a low-aspect ratio keel with a high-aspect ratio centre board. Systematic series on keel-centre board configurations do not exist. Evidently, this research is too short to create such a systematic series and to derive empirical expressions. However, since there isn't any research done on this specific topic, this research can contribute to the hydrodynamical knowledge on this problem. For instance, by examining the influence of some governing parameters qualitatively. If a systematic series will be done on hull-keel-centre board combinations in the future, this thesis can be used as preliminary research. Furthermore, the verification and validation of the test results and the formulation of expressions and trends are fundamental educational elements.

2

Research background

This chapter provides background on the subject matter. The specific lift-carry-over phenomenon found by Dykstra, which was the reason to commission this research, will be discussed in more detail. Furthermore, literature background and previously established prediction methods of the main parameters determining the performance of a sailing yacht will be described.

2.1. Interaction effect of hull, keel and centre board

Dykstra is currently designing a large motor-sailor, which will be equipped with a low aspect keel in combination with a high aspect retractable centre board. The name of this yacht is confidential on the moment of writing this thesis, so it will be referred to as YACHT1. A sketch of this yacht's appendage layout can be seen in figure 2.1.

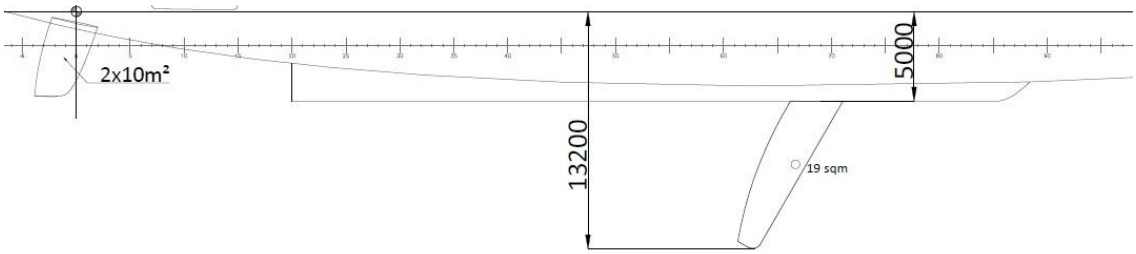

Figure 2.1: The appendage layout of YACHT1.

The performance prediction of this hull-keel-centre board combination was done as is just described in section 1.2. During the verification of this approach, by running multiple CFD simulations, an interesting phenomenon was found regarding the implementation of the centre board. For a leeway angle up to 10 degrees, the sideforce production of the total hull-keel-centre board configuration according to the CFD results is higher than the sideforce production of only the hull-keel according to the CFD results plus the sideforce production of the centre board calculated from theory [18]. This suggests that there is an interaction effect between the hull-keel and the centre board, which has a beneficial effect on the sideforce production. Such an interaction effect was found before in earlier studies regarding different hull-keel combinations and was defined as the lift-carry-over, since lift is carried over from foil to hull. This will be further discussed in section 2.8. For the rest of the research, the regarded interaction effect which yields 'extra' sideforce, is called the lift-carry-over.

2.2. Theoretical lift

The theoretical lift coefficient of an appendage can be calculated with a formula for the lift curve slope, presented by Molland & Turnock, in their book *Marine Rudders and Control Surfaces*[18]. This formula has been verified by experimental data [18].

$$\frac{dC_L}{d\alpha} = \frac{1.95\pi}{57.3\left(1+\frac{3}{AR_e}\right)} \tag{2.2.1}$$

The angle of attack α on the centre board is assumed to be equal to the leeway angle of the ship. AR_e is the effective aspect ratio of the centre board. The end plate effect of the hull on the keel is generally taken into account by doubling the geometrical aspect ratio to obtain the effective aspect ratio, see the following formula, in which b is the span of the foil and c_{mean} is the the mean geometric chord [19].

$$AR_e = 2AR_{geo} = 2\frac{b}{c_{mean}} \tag{2.2.2}$$

A different approach to calculate the lift curve slope of a certain appendage is presented by Whicker & Fehlner [20], see equation 2.2.3. This formula also takes the sweepback angle and a correction factor a_0 into account. Factor a_0 is a correction on the lift curve slope derived from experimental observations.

$$\frac{dC_L}{d\alpha} = \frac{a_0 AR_e}{\cos\Lambda\sqrt{\frac{AR_e^2}{\cos^4\Lambda}+4+\frac{57{,}3a_0}{\pi}}} \tag{2.2.3}$$

With,

$$a_0 = 0.9\,\frac{2\pi}{57.3}$$

In figures 2.4, 2.5 and 2.6 in section 2.5, it can be seen that the theoretical lift curve slope of the centre board of YACHT1 according to Wicker & Fehlner leads to approximately the same results as the Molland & Turnock lift curve slope. Given the fact that both approaches are widely validated and give practically the same results, it can be concluded that these theoretical results regarding the sideforce and resistance are trustworthy. For the remains of this research, the Wicker & Fehlner method is used when calculating the theoretical lift of an appendage.

2.3. Centre of Effort

There are currently no methods to estimate the position of the centre of effort (CoE) of a centre board below a keel. Due to the lift-carry-over it would be incorrect to just take the theoretical CoE of a plain centre board. For regular fin keels, several methods have been developed to estimate the CoE. All methods agree on the longitudinal position, located at 25% of the chord from the leading edge, known as the quarter chord line. Also from aeronautical literature, it is known that the centre of pressure for a conventional 2D foil in an oblique flow is at about 25% of the chord. This called the quarter chord point.

According to Gerritsma's extended keel method, the vertical position is at 43% of the total draft, measured from the waterline downwards[1], see figure 2.2 [4].

In collaboration with the Delft Hydromechanics laboratory, Gerritsma derived in later research another formulation for the centre of effort of the keel. This regards a relationship with the effective draft[2]. According to this method, the centre of effort of the keel is located at the 1/4 chord line, with a vertical position at 60% of the effective draft, measured from the tip of the keel upwards. The effective draft is calculated using the following formula:

$$T_{eff} = T_{max}\sqrt{1-\frac{0.62T_c}{T_{max}}} \qquad \text{measured from the keel tip upwards} \tag{2.3.1}$$

[1] According to *Aero-Hydrodynamics and the Perfromance of Sailing Yachts*, by Fabio Fossati, the vertical position of the CoE proposed by Gerritsma is at 43% of the draft. Larsson and Eliasson describe in their book *Principles of Yacht Design*, that this point lies at 45% of the draft, by the same Gerritsma method [3].

[2] The effective draft is not to be mistaken with the effective span, discussed in section 6.3. The effective span is not a physical measurement, while the effective draft is. The effective draft is a distance measured upwards from the tip of the appendage.

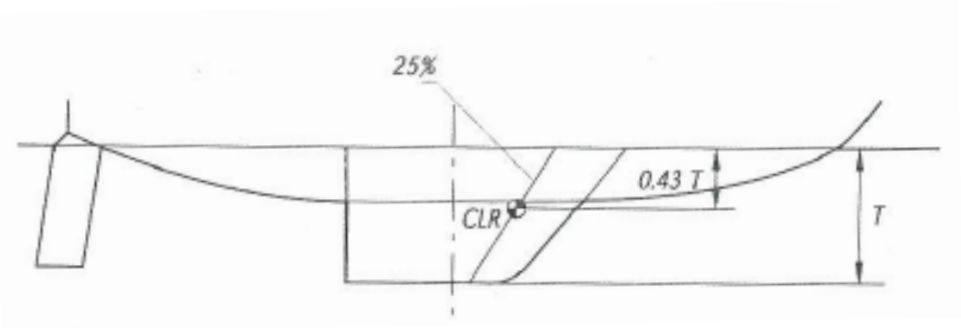

Figure 2.2: According to Gerritsma's Extended Keel Method, the vertical centre of effort lies below the waterline at a distance of 45% of the total draft.

Both methods are examined in this research, to develop a suitable prediction method for the CoE of the centre board in a hull-keel-centre board configuration. The assessment of these methods is discussed in section 7.2.

2.4. Theoretical drag

The drag of a submerged foil consists basically of two components: the viscous drag (also known as profile drag) and the induced drag. The viscous drag coefficient C_{Do} consists of two parts: the frictional resistance and the form drag, depending on the Reynolds number and the section characteristics. The frictional resistance coefficient is calculated according to the ITTC '57 formulation, see equation 2.4.1.

$$C_F = \frac{0.075}{(Log_{10}Re - 2)^2} \tag{2.4.1}$$

The form factor k is dependent on the the section characteristics and is estimated by an empirical formulation as given by Hoerner [9].

$$k_{Hoerner} = 2 \cdot \left(\frac{t}{c}\right) + 60 \cdot \left(\frac{t}{c}\right)^4 \tag{2.4.2}$$

The viscous resistance can now be stated as follows.

$$C_{D0} = C_F\left(1 + k_{Hoerner}\right) \tag{2.4.3}$$

Additionally, Keuning introduces the fin tip drag coefficient, which is calculated using the following equation [12].

$$C_{Dv,fintip} = 0.01875 \cdot \left(\frac{t}{c}\right)^2_{tip} \tag{2.4.4}$$

The induced drag is defined as an additional drag component due to the sideforce production of a wing with finite span. So, the induced drag is a vector of the generated lift, pointing stream downwards, see figure 2.3. In other words: extra resistance due to sideforce.

As known from aeronautical sciences, the induced resistance is related to the loading of the foil, the circulation around the foil and its geometry, by the following formula, in which e is an efficiency factor.

$$C_{Di} = \frac{C_L^2}{\pi \cdot AR_e \cdot e} \tag{2.4.5}$$

So, for a 100% efficiency, the formula would be:

$$C_{Di} = 0.318 \frac{C_L^2}{AR_e}$$

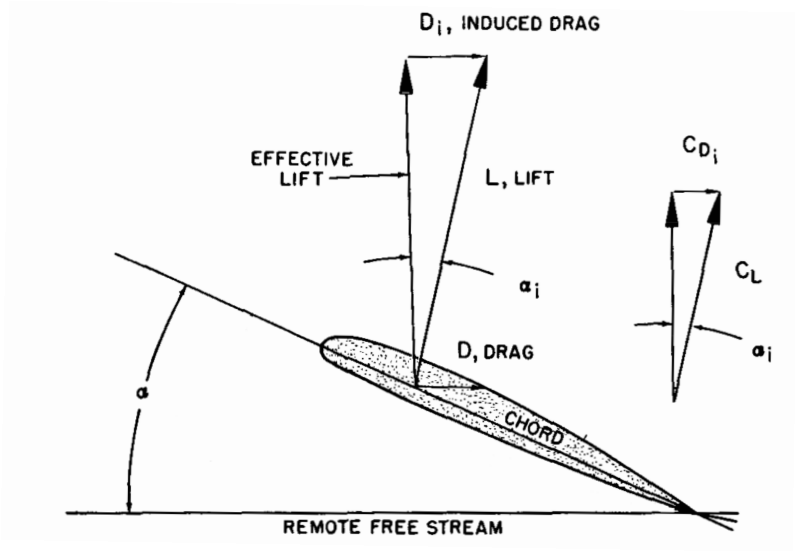

Figure 2.3: The lift can be decomposed in the effective lift (sideforce) and the induced drag.

In maritime studies, the formula of the induced resistance for a foil is often presented as follows.

$$C_{Di} = k_i \frac{C_L^2}{AR_e} \tag{2.4.6}$$

k_i is called the induced drag factor and thus consists of $\frac{1}{\pi}$ and the efficiency factor e. The value of k_i is depended on how nicely the foil is made, the planform of the foil and the closing gap of the foil to the hull or the keel. For this research, the induced drag factor k_i is taken 0.34 [18].
Ultimately, the resistance components are summed to obtain the formula for the total drag coefficient, like can be seen in 2.4.7. The factor '2' in front of the viscous drag and the added fin tip drag is because these components scale with the wetted area, which is roughly twice the lateral area with which the other coefficients scale.

$$C_{Dtot} = 2 \cdot C_{D0} + 2 \cdot C_{Dv,\,fintip} + C_{Di} \tag{2.4.7}$$

It is important to note that for this research, the formulation of the viscous drag will not be modified, since it is not the topic of the research. The focus will be on the induced resistance.

2.5. The case of YACHT1

The lift and drag coefficients according to the CFD simulations are computed by substituting the lift and drag forces in the following formulas. U_0 is the velocity of the free stream flow, ρ is the water density and A_{CB} is the lateral area of the centre board. The lift force is considered as the sideforce.

$$C_L = \frac{F_L}{0.5\rho U_0^2 A_{CB}} \tag{2.5.1}$$

$$C_D = \frac{F_D}{0.5\rho U_0^2 A_{CB}} \tag{2.5.2}$$

These formulas give a non-dimensional number by dividing the lift or drag force by the dynamic pressure multiplied by the lateral area of (in this case) the centre board. The dynamic pressure formulation is part of the Bernoulli equation [18]. The lift and drag coefficients, obtained from both CFD and theory, versus the leeway angle of the ship are plotted in figures 2.4 and 2.5. **Note:** The lift coefficients of the centre board are obtained by subtracting the lift and drag of the hull-keel configuration from the lift and

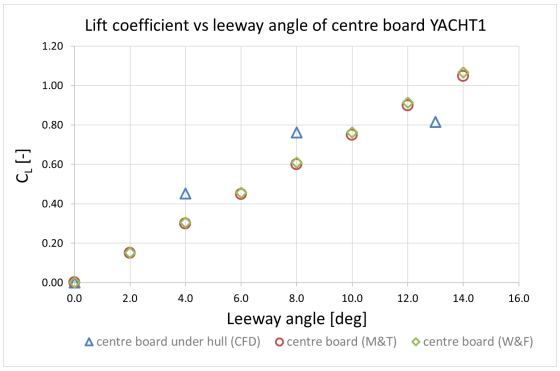

Figure 2.4: The lift coefficient of the centre board according to CFD and according to theory [18].

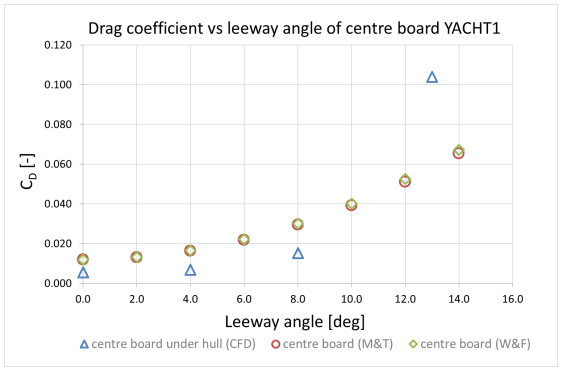

Figure 2.5: The drag coefficient of the centre board according to CFD and according to theory [18].

drag of the total hull-keel-centre board configuration. So, the extra lift generation by the lift-carry-over phenomenon is now completely dedicated to the centre board. In these figures, it can be seen that up to a leeway angle of about 10 degrees, the lift coefficient of the centre board according to the CFD results is higher than according to the theory. Similarly, the drag coefficient is lower through CFD, compared to theory. In contrast, when the leeway angle increases to more than 10 degrees, the lift coefficient is lower and the drag coefficient is significantly higher according to the CFD results, compared to theory. These comparisons were made for a velocity of 12 knots and upright condition.

Another way to visualise this is to plot the total resistance versus the sideforce squared, for each leeway angle. As can be seen in equation 2.4.5, the induced resistance scales with the sideforce squared. So, plotting this relationship, should give a straight, increasing line. This is done for the complete hull-keel-centre board configuration, to capture the result of the total lift-carry-over, see figure 2.6. The

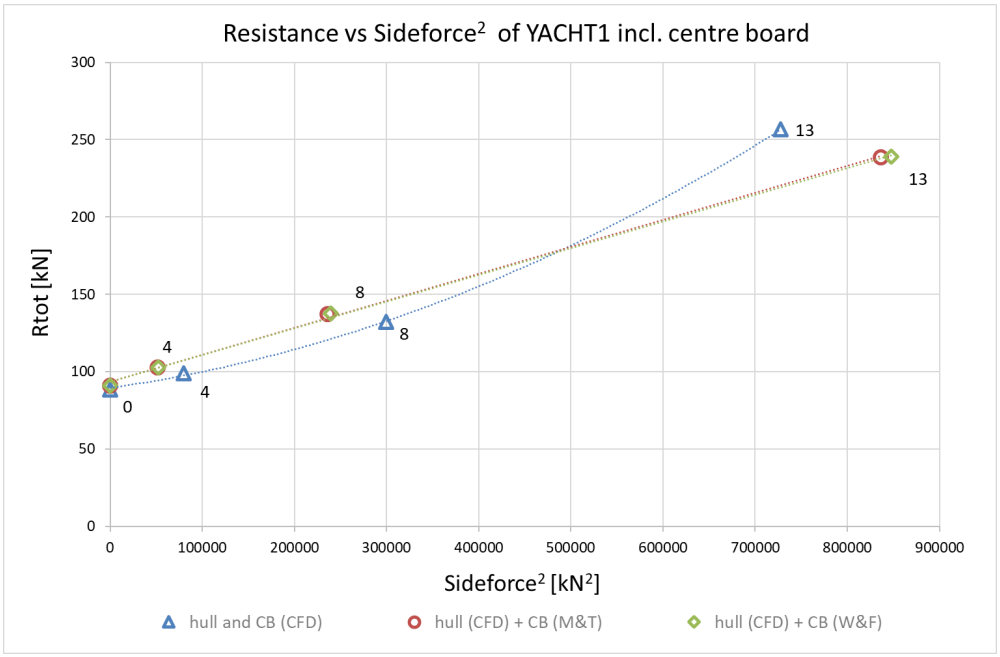

Figure 2.6: The total resistance versus the sideforce squared of YACHT1 including centre board, for leeway angles of 0, 4, 8 and 13 degrees.

results plotted in figure 2.4, 2.5 and 2.6 show that there is a lift-carry-over between the hull-keel and the centre board, which has a beneficial influence on the sideforce production and the resistance, up to a leeway angle of 10 degrees. These findings will be discussed in the next section.

2.6. Analysis

In this section, the methodology of the performance prediction by Dykstra and the verification of this method, discussed in the previous section, will be analysed. An extensive literature study will be discussed afterwards, which was done to find a (theoretical) explanation for the lift-carry-over and to asses other methods used to predict the sideforce.

First of all, Dykstra assumes the angle of attack of the centre board to be equal to the leeway angle of the ship. This assumption is very reasonable, since the centre board is positioned below the keel and will (almost) be in free stream condition. The reason that the lift curve in reality is not a straight line, is because the flow is separating from the foil for a higher angle of attack. This phenomenon is called stalling. The angle of attack at which stalling occurs can vary depending on the geometry of the foil, the properties of the fluid (viscosity and density) and the advance velocity. In general, a common angle from which sailing yacht keels start stalling is about 9 degrees [10]. When the flow is stalling, the lift decreases and the drag increases significantly. Theoretical formulations to calculate the lift do not consider the possibility of stalling, but relate the lift linearly proportional to all angles of attack. In figure 2.4, it can be seen that the centre board starts stalling at a leeway angle of about 8 degrees. In section 2.11, a visual analysis of the CFD simulations will be discussed, confirming the flow separation at 8 degrees leeway. The lift and drag coefficients for a leeway angle of 13 degrees clearly show that the centre board is stalling, see figures 2.4, 2.5 and 2.6. The visualisation in appendix A confirms this statement.

To properly examine the lift-carry-over, it is important to eliminate the stalling region from the analysis. Therefore, only the region up to a leeway angle of 8 degrees will be considered, which is almost a straight line, just as the theory prescribes. In figures 2.4, 2.5 and 2.6 it can be seen that the centre board according to the CFD data behaves better than is expected according to theory, up to a leeway angle of 8 degrees. The centre board produces more lift, has a lower drag and the cost (in terms of resistance) of sideforce is lower. This means that the centre board introduces a beneficial interaction effect. If the centre board is eliminated by subtracting the hull-keel CFD results from the hull-keel-centre board CFD results, it is found that the the centre board itself adds a lift force which is 1.52 times more than the the Wicker & Fehlner theory would predict, at 4 degrees leeway. For the total configuration, this means that for a leeway angle of 4 degrees, the hull-keel according to CFD data plus the centre board regarded as a lift generating surface, produces 20% less sideforce and 4% more total resistance than the complete hull-keel-centre board configuration according to CFD.

In other words, if Dykstra was to predict the performance of this hull-keel-centre board combination using their conventional method, they would underestimate the sideforce production by 20% and overestimate the resistance by 4%. With the use of CFD, Dykstra would in the end find these deviations and redesign the centre board, but this costs extra time. This is essentially the reason why Dykstra commissioned this research; to obtain a more accurate first estimate of the centre board contribution, before doing CFD simulations of the complete configuration.

2.7. Other methods to predict the sideforce and yaw moment

A fundamental and widely used model to calculate the sideforce production is the Extended Keel Method, derived by Gerritsma in 1971[11]. This model isolates the foils and calculates the lift and drag using general wing theory[3]. The sideforce generated by the hull is accounted for by the virtually extended keel inside the canoe body to the waterline [19], see figure 2.7.

So, the aspect ratio and the area of the keel changes. This method yields good results for the calculation of the sideforce versus leeway relationship, but the centre of lateral resistance (CLR) is less well predicted (in general, too far aft) [16]. However, this method is not preferable for the kind of yachts considered in this research, for two reasons. First of all, the EKM predicts the total sideforce of the hull plus keel, while Dykstra is looking for a way to predict the forces on the centre board only, in order to superpose those to the forces of the hull. Second and most importantly, the EKM is not developed for high aspect ratio centre boards extending from (very) low aspect ratio keels. This is the main reason why almost all common (standard) methods are not suitable to use by Dykstra; they are all based on systematic series of ordinary shaped, small to medium sized yachts. It is not necessarily the case that these methods yield incorrect results, but they are just not validated for deviating geometries.

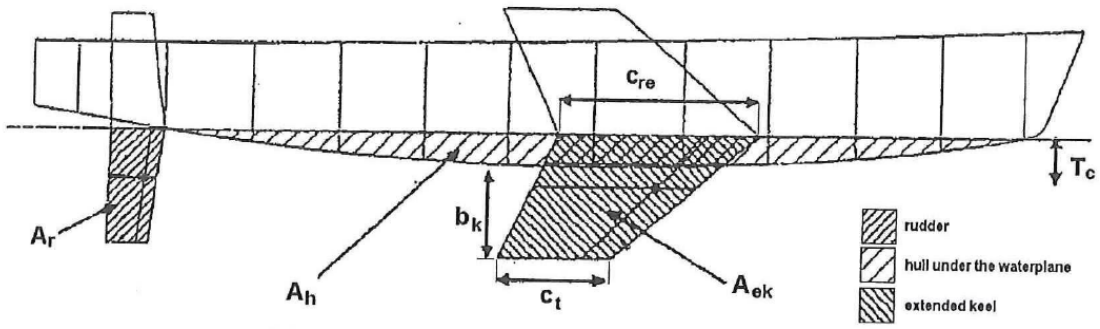

Figure 2.7: The keel virtually extended to the waterline, according to the Extended Keel Method, derived by Gerritsma in 1971.

In the end, the EKM calculates the sideforce of the keel through the same principle of wing theory, which is multiplying the lift curve slope by the angle of attack (leeway angle), the dynamic pressure and the surface of the foil, see the following equation[3].

$$F_{sideforce} = \frac{dC_L}{d\alpha} \cdot \alpha_{keel} \cdot \frac{1}{2} \rho V_s^2 A_{keel} \tag{2.7.1}$$

The only[4] variable parameter in this approach is the lift slope curve, of which there are several different formulas in the field of aero- and hydrodynamics. As discussed in section 2.2, the method of Wicker & Fehlner is used in this research to calculate the lift curve slope of the centre board.

A different approach to estimate the sideforce and yaw moment was presented by Nomoto in 1979. Nomoto tried to improve Gerritsma's method by adding the hydrodynamic forces acting on the underwater hull. These forces and yaw moment were calculated using the so-called slender body theory. This potential contribution to the yaw moment of a body in oblique flow is known as the Munk Moment[16]. The physical explanation of the Munk Moment is that in an ideal (inviscid) fluid, an elongated 3D body at an angle of attack experiences a pure couple, which tends to increase the angle of attack. This couple is composed of two equal but opposing forces acting over the body. This implies that there is no resulting force, but a significant moment. This situation can be seen in figure 2.8. In a real viscous fluid however, vortices and separation will occur downstream along the body, which reduces the pressure on the aft body. The basic idea, adopted by Nomoto is to only integrate the hydrodynamic pressure of the bow half of the slender body, because the lateral flow at the aft body is considered to be too strongly influenced by vortices and flow separation. It was concluded that Nomoto's method still underpredicted the yaw moment, which also caused the CLR to be predicted too far aft. However, the improvement of the yaw moment with respect to Gerritsma's method was significant[16].

Later research by Keuning (2003 and 2008) improved the method of Nomoto using results of the Delft Systematic Yacht Hull Series (DSYHS) [16, 19]. According to the DSYHS, Gerritsma's method yielded better results for the sideforce, where Nomoto's method yielded better results for the yaw moment. In general, Nomoto's method underpredicted the yaw moment, but overpredicted the sideforce.

[3] **Note:** Calculating the lift force using the approach from equation 2.7.1, or calculating the lift and drag coefficients as is done in equations 6.4.1 and 6.4.2, will in this report be referred to as *wing theory*.

[4] There are a number of correction factors to account for heel and downwash, which can be added to this formulation [19]. But again, these correction factors are based on experimental series of yachts, significantly different from the yachts that Dykstra is designing, so not usable.

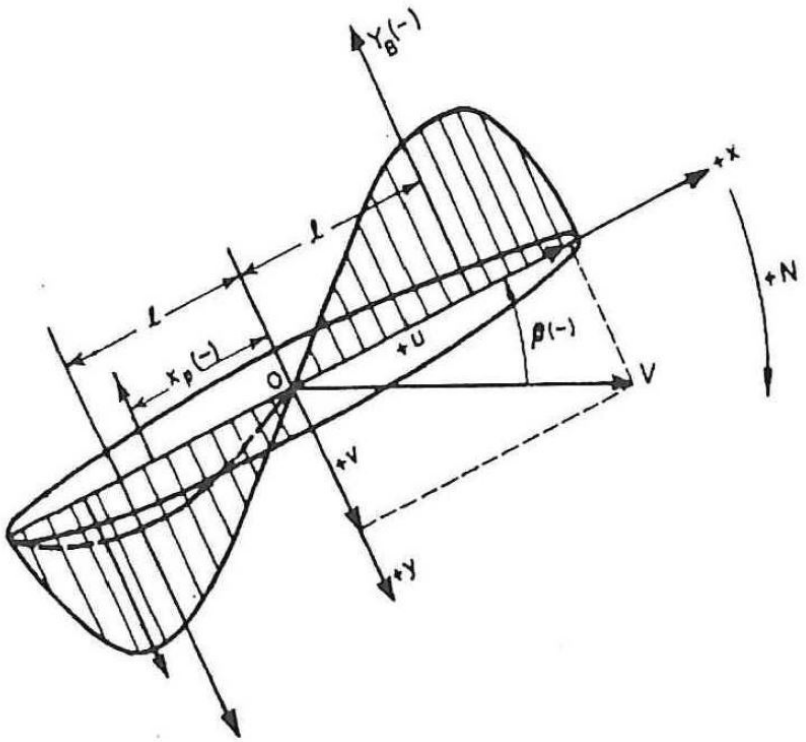

Figure 2.8: The hydrodynamic force distribution on a slender body in potential flow.

2.8. The lift-carry-over

The 'extra' lift generation was also found from earlier measurements on the DSYHS. Keuning and Verwerft tried to capture this lift-carry-over for the entire DSYHS, by calculating the ratio between the total measured lift and the lift generated by the keel and rudder separately using a theoretical expression (like the one from Wicker & Fehlner in equation 2.2.3) [14]. This ratio was referred to as the hull influence coefficient c_{hull}, in which L_t is the total measured lift of the model, L_k is the theoretical lift generated by the keel and L_r is the theoretical lift generated by the rudder [19].

$$c_{hull} = \frac{L_t}{L_k + L_r} \tag{2.8.1}$$

For the keels and hulls in the DSYHS, the following relation was found, with $a_0 = 1.25$ and T_c is the canoe body draft.

$$c_{hull} = a_0 T_c + 1 \tag{2.8.2}$$

However, this formulation of c_{hull} holds for models of the DSYHS with a T_c of $0.1m$ to $0.9m$, while typical Dykstra yachts have T_c values up to about $5m$. Later, the results of two other research projects, the Delft Various Keel Series (DVKS) and the Delft Systematic Keel Series (DSKS), were used to develop the following relationship for the hull influence coefficient, for upright condition, see equation 2.8.1. T_c is the canoe body draft of the yacht, b_k is the span of the keel and $a_0 = 1.80$. This relationship was found for a $\frac{T_c}{b_{keel}}$ ratio of 0.15 to 1.0.

$$c_{hull} = 1.8\frac{T_c}{b_{keel}} + 1 \tag{2.8.3}$$

Additionally, the influence of the heeling angle on the lift has to be taken into account. Keuning and Verwerft state the following: *The influence of the heel angle on the lift production is captured by two mechanisms: one is the lift curve slope reduction due to the fact that the foils are brought closer to the free surface, expressed as heel influence coefficient c_{heel}. The second one is the zero lift drift angle β_0, which originates from the asymmetry of the hull when heeled.*

From experimental data, the following expression was derived for the heel influence coefficient, in which $b_0 = 0.382$ and ϕ is the heeling angle in radians.

$$c_{heel} = 1 - b_0\phi \tag{2.8.4}$$

The zero lift drift angle due to asymmetry of the hull, reduces the effective angle of attack on the appendages. Using the results of the DSYHS, DSKS and the DVKS, an expression has been found for this zero lift drift angle, in which B_{wl} is the waterline beam and $c_0 = 0.405$.

$$\beta_0 = \left(c_0 \frac{B_{wl}}{T_c}\phi\right)^2 \tag{2.8.5}$$

All together, this results in the following equation to approximate the sideforce of the keel. In which the effective velocity of the keel is considered equal to the velocity of the sailing velocity of the yacht: $V_{e\ keel} = V_S$. And, the effective angle of attack of the keel is the leeway angle of the yacht, corrected by the zero lift drift angle: $\alpha_{e\ keel} = \beta - \beta_0$. On the left hand side of the equation, α is the angle of attack of the foil, which is defined as equal to the leeway angle β.

$$L_{keel} = \left(\frac{dC_L}{d\alpha}\right)_{(W\&F)} \alpha_{e\ keel} \cdot \frac{1}{2}\rho V_{e\ keel}^2 A_{lat\ keel} c_{hull} c_{heel} \tag{2.8.6}$$

This formulation can be reduced to the lift coefficient including the terms introduced by the lift-carry-over. This coefficient will be defined as the lift-lift-carry-over coefficient $C_{L_{lift\ carry\ over,\ keel}}$.

$$C_{L_{lift\ carry\ over,\ keel}} = C_{L_{(W\&F)}} c_{hull} c_{heel} \left(1 - \frac{\beta_0}{\beta}\right) \tag{2.8.7}$$

However, for Dykstra it is tricky to use these lift-carry-over formulations, just like all other prediction methods that are based on systematic series. This is because the yachts that Dykstra are designing lay to such an extend outside the scope of the systematic series on which these performance prediction formulations are based. The Dykstra yachts lay outside this scope primarily because of the large dimensions. Secondly, the focus of this research is developing a performance prediction method for hull-keel-centre board configurations, instead of conventional hull-keel configurations on which all currently available performance predictions methods are based.

Nevertheless, these existing prediction methods for the lift-carry-over are examined could potentially be adjusted to make them suited for larger yachts with a keel-centre board configuration. This is described in more detail in chapter 7.

2.9. Tank test data

To validate the findings by Dykstra Naval Architects, data from towing tank experiments with similar setups were analysed. In 1984 and 1985, model tests with seven different keels in combination with one particular hull form have been carried out in the Delft Hydromechanics Laboratory [5–7]. These model tests include a plain restricted draft keel which is tested with and without a centre board, see figure 2.9, [5]. This towing tank model is called the Yonder. The towing tank experiments were done for leeway angles up to 6 or 8 degrees, depending on the keel configuration. In the final paper describing these experiments, the sideforce production of these configurations, as well as the other five configurations, is related linearly proportional to the leeway angle and the velocity squared. By including the area of the keel in the sideforce calculation, each configuration can now be related to one another.

To analyse these towing tank results, the same approach will be used as in the Dykstra VPP tool, which regards the centre board as a lift generating surface. The theoretical lift force of the centre board is added to the sideforce production of the plain restricted draft keel following from the tank test data. This is then compared to the test data of the total hull-keel-centre board configuration. It is found that according to this data, the plain restricted draft keel plus the centre board regarded as a lift generating surface produces 29% less sideforce. This magnitude of of lift-carry-over is even more than was found by Dykstra. Though, these percentages must not be compared to one another since they resulted from a completely different geometry of all aspects of the ship. But, these tank test data do confirm (validate)

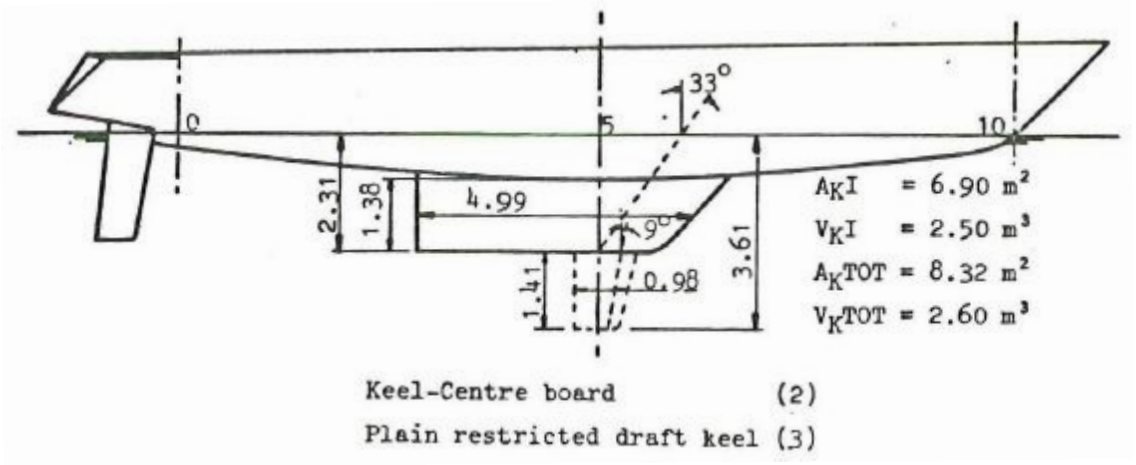

Figure 2.9: The setup of the model which was tested with the plain restricted draft keel only, and with the centre board included.

the existence of the lift-carry-over in hull-keel-centre board configurations. No exact data was provided on the total resistance of both configurations.

2.10. Preliminary research

Several researches on this topic has been done already. Some formulations originating from previous researches have just been discussed, like the method of Gerritsma (EKM) and Nomoto (Munk moment). Most research papers used as literature for this study are written by TU Delft Hydromechanics researchers, like Keuning, Gerritsma, Kapsenberg, Vermeulen, Binkhorst and Verwerft. The people currently working at Dykstra and the TU Delft have provided many useful information and knowledge on the topic as well.

Preliminary research at Dykstra Naval Architects

Multiple graduation interns at Dykstra have worked on researches during the past few years, regarding the performance prediction. Preliminary research theses are:

- *Weather routing of motorsailors*, Daan Sparreboom, 2012. (Sparreboom has also built the Dykstra Matlab VPP tool)
- *Improving the performance of a sail-assisted cargo vessel*, Emile Mobron, 2014
- *Developing a method to analyse the performance of non-standard hulls, using a VPP*, Anne Heerschop, 2016.

These reports present a basic background of the behaviour of sailing vessels and how to predict their performance. However, the physics of the sideforce generation and the lift-carry-over in particular, is only very briefly discussed.

Thesis of B.J. Binkhorst

A thesis with a very similar topic to this research is the one of B.J. Binkhorst; *Keel performance in relation to keel-hull interaction*, written in 1997 [1]. Binkhorst used the results of preliminary research done by Keuning and Kapsenberg, to acquire more detailed information on the behaviour of the keel and rudder fitted under a sailing yacht [15]. During the experiments, Keuning and Kapsenberg measured the loading on the appendages directly. Examination of the influence of the appendage on the complete model was not only done by means of information on the appended and non-appended hull, but also by means of the measured loading on the appendage. Keuning and Kapsenberg already concluded that there is a significant coupling between the flow induced by the hull around the keel and vice versa,

which was called interaction between wing and body, or keel and hull [1]. Binkhorst extended this research by testing another seven keel-hull configurations in the Delft Hydromechanics Laboratory. Just as in this research, Binkhorst intended to show the interaction effect as clearly as possible in terms of influencing parameters.

Binkhorst soon concluded that the foils can not be separated from the hull when calculating the sideforce production, due to the interaction between keel and hull. He also mentioned that the interaction effect is most dominant for ships with a large canoe body draft and a shallow keel, which is the type of ship this research is meant for. However, in this research a centre board is added to the appendage layout, which significantly changes the situation.

Binkhorst did derive very interesting (polynomial) expressions for parameters influencing the drag and lift slope, but these do not hold for the hull-keel-centre board configurations that are considered in this research. Just as was described in section 2.6, these configuration lay outside the scope of previous work. This means that the derived conclusions and expressions from previous work are not trustworthy for these hull-keel-centre board configurations.

2.11. CFD observations

One of the things that initiated this research, were the CFD results of YACHT1. As was already discussed in section 2.1, the vessel with centre board produced more lift than was expected from hydrodynamics theory. In this section, the CFD results of YACHT1 will be discussed qualitatively, by analysing the results visually. The software of CFview, which is part of the NUMECA software, is used to visualise the results of the CFD simulations. Three quantities that are regarded important to visualise the lift-carry-over and the behaviour of the flow are:

- Hydrodynamic pressure (on the surface of the vessel), to analyse the lift production. The hydrodynamic pressure corresponds 1 on 1 with the local velocity.

- The shear in x-direction, which is the viscous stress (in x-direction) to the surface of the vessel. This parameter indicates the amount of frictional (viscous) resistance and possible separation. The nominal value of the shear is negative, because the flow of water is in the negative x-direction. If the value for the shear turns positive, it means the water is locally flowing in the positive x-direction, indicating the water is separating from the body. Therefore, the parameter range in CFview is set to a maximum of 0. Locations where the value of the shear is positive will remain blank, while all negative values are represented by coloured contours. Possible locations where separation occur are thus easy to detect.

- The absolute velocity in the yz-plane, to analyse the amount of circulation in the flow. Especially larger scale vortices will be indicated by this parameter. Energy dissipated in vortices are likely to increase the resistance. In contrast to the previous two quantities, the velocity in the yz-plane is not examined on the surface of the vessel. Instead, it is observed at different cross sections, normal to the X-axis, located every two meters from 8 to 36 meters forward of the aft perpendicular.

Screenshots of the CFD results of YACHT1 with and without centre board can be found in appendix A. The lift-carry-over from centre board to keel and hull can be seen when looking at the shots of the hydrodynamic pressure, see figure A.1. Additionally, visualising the shear in X-direction, provides an easy method to detect the flow separation at the centre board. In appendix A, it can be seen that at a leeway angle of 4 degrees, the flow is still attached. But, when looking at a leeway of 8 degrees, it can be seen that the flow has already separated a bit at the trailing edge of the centre board. At last, it can be seen that the flow has fully separated from the centre board at a leeway angle of 12 degrees. Finally, analysing the absolute velocity in the yz-plane, provides information regarding the circulation in the flow. When at looking figures A.8 to A.11 in appendix A, the tip vortices, shedded by the centre board, can clearly be seen. Secondly, it can be seen that the circulation at the aft of the ship is much less in the configuration with centre board, compared to the configuration without centre board. All in all, it seems that there is less circulation in total in the configuration with centre board.

2.12. Hypothesis

The background of this research, relevant scientific publications on this topic and the CFD results that initiated this research have been analysed and discussed. To be able to properly outline the rest of this thesis, it is important to formulate a hypothesis of how the *extra* lift generation (lift-carry-over) is introduced physically, and what the influence is on the parameters determining the performance of the yacht.

First of all, the lift-carry-over of the centre board to the keel can clearly be seen in figure A.1 of appendix A. The phenomenon of the lift-carry-over has been a topic for several researches, but each for a conventional hull-keel configuration. It is assumed that the lift-carry-over from centre board to keel is even more significant, since both are vertical surfaces. This would suggest that the draft of the keel is an important parameter in the lift-carry-over from centre board to keel. This would be in line with the prediction for conventional hull-keel configurations in which the hull coefficient c_{hull} has the largest contribution to the lift-carry-over magnitude, see equation 2.8.1. In this coefficient, the canoe body draft has a direct influence on the lift-carry-over magnitude. For hull-keel-centre board configurations, this 'function' of the hull is complemented by the keel. Ideally, the draft of the hull including the shallow keel is regarded as canoe body draft, while the centre board is regarded as keel. This will be further discussed in section 7.1.2.

Another parameter which might influence the magnitude of the lift-carry-over is the chord length (and thus aspect ratio) of the centre board. In theory, a wider centre board could carry the lift to a larger area on the keel. However, this is implicitly already taken into account by the hull coefficient. The span of the keel is in the denominator, saying that a longer centre board results in a lower lift-carry-over magnitude.

Secondly, it can be seen that the tip vortex of the keel seems to be much smaller in the configuration with centre board, compared to only the keel-hull configuration. In general, it can be seen that the flow around the keel is more stable when the centre board is added. The centre board seems to stabilise and guide the flow around the ship. A smoother flow increases the efficiency of the lifting objects, resulting in more sideforce. Additionally, less circulation in the wake and less energy dissipation in tip vortices, results in less resistance.

Both hypothetical phenomena will be studied by doing more CFD simulations and towing tank experiments. How the experiments are constructed will be discussed in chapter 3.

3

Methodology

The goal of this research and the analysis of the research background form the basis of the methodology. To begin with, research questions are stated, to outline the structure of this research. After that, the plan of approach for this research project will be discussed.

The answer to some of the research questions will follow from the literature study and (practical) information provided by experts at Dykstra and the TU Delft. First, background information is gathered, and a solid basis is formed regarding the knowledge on the main aspects which determine the performance of a sailing yacht. The lift-carry-over will be further analysed to create insight in how to predict the behaviour of these rather exceptional hull-keel-centre board layouts. This includes further literature study, doing towing tank experiments and CFD simulations. The resulting information and data will then be used to improve existing performance prediction methods, such that they can be used for (large) sailing yachts with a hull-keel-centre board configuration.

3.1. Research questions

These research questions summarise the plan of approach for this research. The first three question have already been discussed in the previous chapters. Question four regards the methodology of the towing tank and CFD experiments, and their contributions to this research in general. The ultimate goal would be to obtain enough data to get clear results and to draw strong conclusions. However, the available time and resources are limited. This means that a test matrix must be designed which is efficient in terms of minimising the test runs, while maximising the useful output. This will be discussed in more detail in the plan of approach. The last question looks beyond the Maltese Falcon towing tank experiments, conducted for this research. It is vital to know whether the new or improved performance prediction methods, based on the results of those experiments, give accurate estimates for yachts other than the Maltese Falcon. In the first place, the results from the experiments must be verified and validated, to be able to say something about the trustworthiness of the resulting data itself. Then when all the data is post-processed, the results are used to improve existing prediction methods, to make them suitable for yachts with hull-keel-centre board configurations. It is also an option to creating new methods and formulations, but this is not the preferred approach since it is considered not wise to diverge too much from established methods. Ultimately, the obtained 'new' methods must be validated on existing yachts with a keel-centre board, to check how well they perform.

1. How is the performance of sailing yachts with a hull-keel-centre board configuration currently predicted at Dykstra, and how accurate is this prediction?

2. According to literature, what could be the theoretical explanation for the lift-carry-over in hull-keel-centre board configurations?

3. Are there other methods to predict the lift (sideforce) and drag of the appendages, and are these appropriate for the type of yachts that Dykstra is designing?

4. How can towing tank experiments and CFD simulations give more insight in the behaviour of the hull-keel-centre board configuration, and the contribution of the centre board in particular?

5. Can the resulting data be formulated in trustworthy trends and formulations, to be implemented in the Dykstra performance prediction tool?

3.2. Plan of approach

The first three research questions have already been answered in the previous section, using literature and information provided by Dykstra and the TU Delft. In the next section, the setup for the towing tank experiments and the CFD simulations and will be discussed. This requires an analysis of the boundary conditions on one end, and the governing parameters on the other. Normally, the boundary conditions are determined by physical limitations, like draft or available space for the centre board construction. However, no boundaries will be set in this research, since the focus will be on the behaviour of the flow and the lift-carry-over, not on the practicality of the design. The driving parameters of the flow will be divided in geometrical parameters and sailing parameters. There are many geometrical parameters that influence the interaction effect. Literally the complete geometry of the ship influences the flow and thus the lift-carry-over. Yet, the following parameters are considered the most important geometrical parameters for this research.

- Canoe body draft
- Span of the keel
- Aspect ratio of the keel
- Area of the centre board
- Aspect ratio of the centre board
- Span of the centre board

The sweepback angle is assumed to be small (less than 15 degrees) and is neglected in future trend formulations because it only has a very small contribution. The sailing parameters are limited to leeway angle, heeling angle and velocity. At this moment, the balance between the desirable information and the available time and resources becomes important, which is quite challenging. Preferably, the tests would consist of a wide variation of hulls, keels and centre boards, tested at several sailing conditions. However, tank time is limited, which means the test matrix must be made sparse to only test the most important combinations of parameters.

Note: Dykstra is not looking for the final 2% or 3% of accuracy in the performance prediction. The objective is to derive indicative formulas to be able to make a more accurate first estimate of the centre board performance. Three weeks of tank testing is too short to develop a complete systematic series in which all influencing parameters can be expressed in trend formulations.

The towing tank experiments will be done before the CFD simulations, mainly because of scheduling reasons[1]. Before the towing tank experiments can start, it is important to know whether the existing model is (still) the same as the digital model[2]. After that, several basic preparations for the towing tank experiments are required, like painting the model and making turbulence strips. Other key preparations are manufacturing two centre boards and a keel. All procedures regarding the towing tank experiments will be discussed in more detail in the following sections and the appended experiment rapport.

Some of the configurations and setups will be tested in CFD, to validate the towing tank experiments. All trends regarding the forces and moments will be examined. Additionally, the CFD simulations could provide visual information on the flow of water around the ship.

[1] Due to the required availability of experiment guides and the planning of some other projects in the towing tank, it turned out to be convenient to finish the towing tank experiments before the summer break.

[2] The towing tank model of the Maltese Falcon is made of wood. Laying still for 16 years can cause the model to deform. More information about the Maltese Falcon and why this model is used in this research is described in the next section.

When all tests are done, the resulting data is post-processed and analysed. Then, verification and validation is done to examine the trustworthiness of the results. Finally, the goal is to use the results to improve the prediction of the centre board contribution in hull-keel-centre board configurations.

3.3. Setup for the towing tank experiments

This section describes the Maltese Falcon model, its appendages and the different configurations. After that, the towing tank setup and the towing tank test matrix is discussed.

3.3.1. Maltese Falcon configurations

The bare hull of the Maltese Falcon was built on speculation in 1990 by Perini Navi, in Turkey. More than 10 years later, the yacht was bought by Tom Perkins, who hired Dykstra Naval Architects to propose a three mast square rig. This resulted in one of the most famous applications of the DynaRig concept. Figure 3.1 shows the Maltese Falcon yacht sailing at St. Barths Bucket regatta.

Figure 3.1: The Maltese Falcon sailing at the St. Barths Bucket regatta. Photo credit: Onne van der Wal.

The Maltese Falcon is the 'case ship' in this research. Because it is a large yacht with a long and shallow keel, it is perfectly suited. The existing model of the Maltese Falcon (scale 1:30) will be used for the towing tank experiments. This model was made by the TU Delft in 2002 and is previously tested in the Delft Hydromechanics Laboratory, see figure 3.2. The main particulars of the Maltese Falcon are listed in table 3.1. The layout of the Maltese Falcon and the key dimensions can be seen in appendix B.

The Maltese Falcon is equipped with a 'two-step' keel. In the towing tank model, the bottom part of this keel is modular. In 2002, the model was tested with and without this bottom part and with two different centre boards. The depth of the bottom part of the keel is very well suited for this research, since the total keel configuration is quite deep with this part, but relatively shallow without. So, two extremes can be tested, which is convenient. In real size, the bottom part of the keel is 1.7 meters deep and 28 meters long (at the top). Due to some damage to the existing keel extension in the Maltese Falcon model, a new one will have to be manufactured.

The two centre boards that have previously been tested were very different from one another. The one in figure 3.2 was meant to be a hinging centre board, able to be folded inside the keel. The other

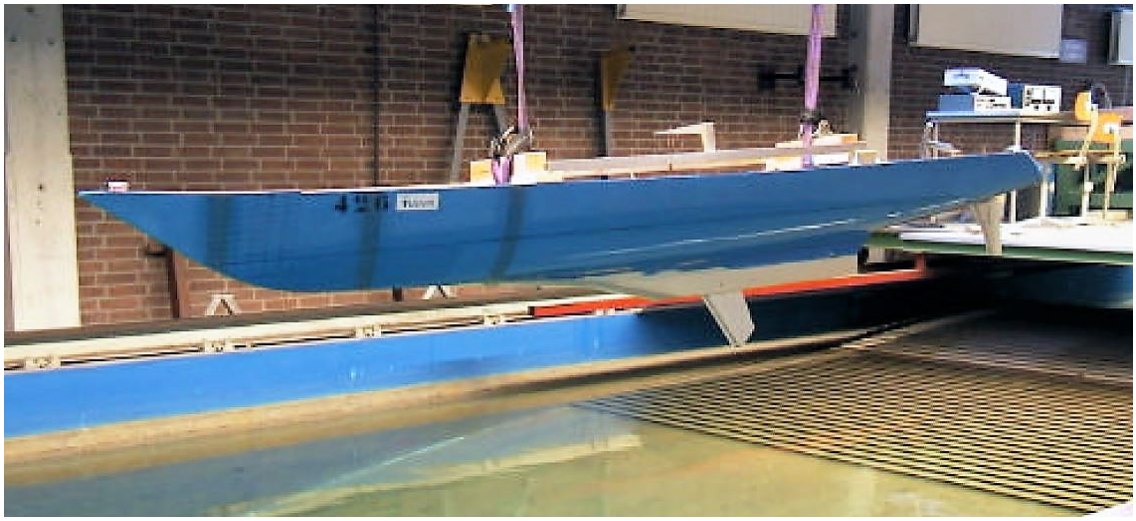

Figure 3.2: The model of the Maltese Falcon, tested in the Delft Hydromechanics Laboratory in 2002

Main particulars		Full size	Model size
Length over all $[m]$	L_{oa}	88.12	2.937
Length between perpendiculars $[m]$	L_{pp}	73.90	2.463
Length of waterline $[m]$	L_{wl}	78.22	2.607
Beam at waterline $[m]$	B_{wl}	10.86	0.362
Canoe body draft $[m]$	T_c	3.41	0.114
Draft (including keel extension) $[m]$	T	6.00	0.200
Displacement	Δ	1240 ton (salt water)	40.33 kg (fresh water)

Table 3.1: The main particulars of the Maltese Falcon in full size and of the towing tank model.

centre board was built neutrally buoyant, so that it can be launched in the water from the deck and then be constructed to the keel by divers. Both centre boards can be seen in figure 3.3, in which the white centre board was the hinging design and the blue centre board the neutrally buoyant. In the end however, no centre board was installed on the Maltese Falcon.

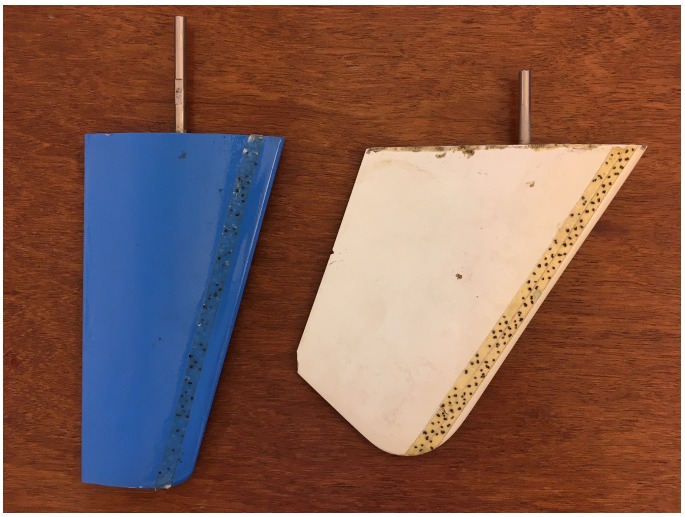

Figure 3.3: Two centre boards, designed for the Maltese Falcon, tested in the Delft Hydromechanics Laboratory in 2002. The white centre board was the hinging design and the blue one was designed neutrally buoyant.

Although the Maltese Falcon has no centre board, the neutrally buoyant centre board has a very nice shape, see figure 3.4. Since it was designed specifically for this yacht, it is assumed that the sideforce production is of the correct order of magnitude. This centre board will be used as a reference to design the centre boards that will be tested. It is decided to test two different centre boards, which are designed to have aspect ratios of 50% and 150% relative to the aspect ratio of this reference centre board.

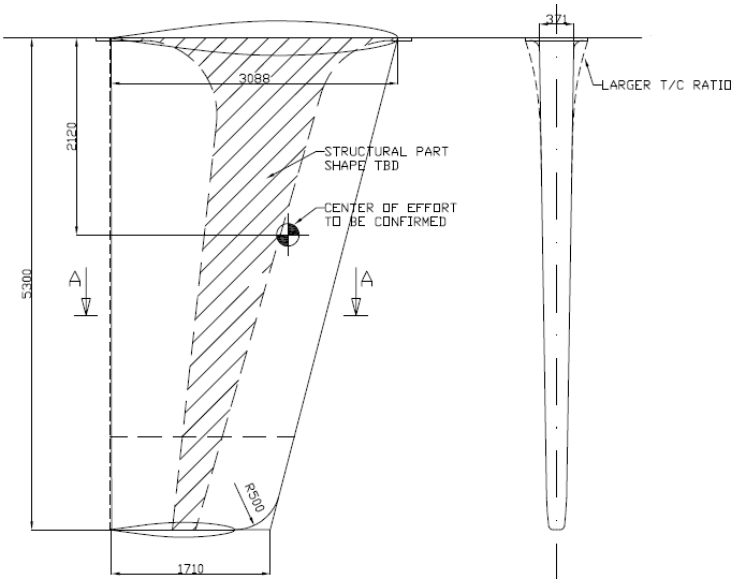

Figure 3.4: The main dimensions of the neutrally buoyant centre board, which will be used as a reference for designing the centre boards that will be tested.

The newly constructed centre boards can be seen in figure 3.5. All parameters of the reference centre board and the two new centre boards are presented in table 3.2. The two new centre boards will both have the same area and sweepback angle, but different aspect ratios. Keeping the area and sweepback angle constant is meant to simplify the relation of the span (and aspect ratio) to other parameters. Keeping the area the same, but differing the aspect ratio means that the (theoretical) lift production of the centre boards will not be equal. The theoretical lift curve slope of the centre boards and the corresponding absolute lift production per degree leeway per velocity squared, are also presented in table 3.2. The lift production relative to the reference centre board is stated as well.

These centre boards will have a NACA 65-015 profile. This is a common profile in rudder and keel applications and has a very similar shape to the existing centre board design. Using Rhino, a digital file of the centre boards is constructed. The centre boards are trimmed to 'vertical slices' and projected in one plane, such that a laser cutting machine can cut out the slices from a 1.5mm thick wooden plate. Then, these slices are assembled together and shaped to the desired centre board shapes. Moulds of these centre boards are also cut and used to ensure the desired shape is achieved.

Centre board dimensions	original (100% AR)	CB1: low aspect (50% AR)	CB2: high aspect (150% AR)
Sweepback angle [deg]	14.6	14.6	14.6
Area [cm^2]	14.2	14.2	14.2
Span [mm]	177	125	217
Average cord [mm]	80	113	65
Aspect ratio [-]	2.21	1.11	3.32
Theoretical lift curve slope (W&F)	0.065	0.046	0.073
Theoretical lift [$N/(deg \cdot V_s^2)$]	0.46	0.32	0.52
Lift compared to original	100%	71%	114%

Table 3.2: The dimensions of CB1 and CB2, based on the original centre board.

Figure 3.5: The newly constructed CB1 and CB2.

Note: It is also considered to keep the theoretical lift of the two centre boards the same as the lift of the original centre board. This would mean that, when choosing a certain aspect ratio, the area has to be corrected to obtain the same theoretical lift production. An advantage of designing two centre boards with equal lift production, would be the possibility to compare the exact amount of lift-carry-over to the area and aspect ratio of the two centre boards. However, it is decided to keep the area equal. This enables the possibility to see what the influence of the nominal lift production is on the relative lift-carry-over, which is considered more interesting.

As stated in the previous section, the number of test runs must be minimised because there is only limited tank time available. This means that the number of physical setups and the number of sailing conditions are limited. Only one hull will be tested, which means that no validated correlation can be made with the canoe body draft, even though this is considered a governing parameter. Testing multiple hulls would be interesting, but would also take significantly more time, both for manufacturing and testing. The model of the Maltese Falcon has a hull with a shallow keel in one piece. Two different centre boards and an extension for this keel are manufactured, to be able to test two different keels in combination with two different centre boards. The centre boards will be tested at one specific longitudinal position only.

The model with the small keel as it originally was built, is called 'bare hull + keel1'. The elongated keel will be called 'keel2', and will have more or less the same dimensions as the bottom part of keel1[3]. There are three requirements for keel2. First, it must fit nicely to keel1. Second, it must have the exact same dimensions as the keel used in the CFD simulations. Finally, it must enable a smart connection of the centre boards. The keel is made in the same way as the centre boards. Only now the keel is cut in horizontal slices from a $6.2mm$ thick wooden plate. The keel is assembled by two bolts, one near the leading edge and one near the trailing edge. During assembly, relatively large holes filled with epoxy enable the fittings of the bolts to move slightly, so that the keel can be aligned perfectly straight and at the correct longitudinal and transverse position. Keel2 can be seen in figure 3.6. More pictures of the construction of the centre boards and all preparations for the towing tank experiment, can be seen in the appended towing tank experiment report.

[3]The existing model keel extension, made in 2002, has too much damage and can not be used for the towing tank experiments. This keel will have to be rebuilt. However, the new keel extension does not necessarily have to be the exact same as the old one, as long as it is the same keel that will be tested in the CFD simulations.

Figure 3.6: The newly constructed keel2

After all test runs with keel1 and keel2 were done, keel 1 will be cut off, to obtain a bare hull[4]. This will be done to test the bare hull and the centre boards below the bare hull, to precisely determine the influence of both keels. So, the bare hull configurations will be tested last. However, the numbering of all hull-keel-centre board configurations will start with the bare hull, since this is the most logic. An overview of all geometrical setups is presented in table 3.3 and figures 3.7 to 3.15.

[4]This was decided during the tests when extra tank time became available because the following project had a delay. Still, it was not sure whether this idea would succeed practically. In the end, keel1 was relatively easy removed, obtaining a neat bare hull. More information and pictures regarding this procedure can be found in the appended towing tank report.

	Bare hull	Keel1	Keel2	CB1 (low-aspect)	CB2 (high-aspect)
Configuration 1	x				
Configuration 2	x			x	
Configuration 3	x				x
Configuration 4	x	x			
Configuration 5	x	x		x	
Configuration 6	x	x			x
Configuration 7	x	x	x		
Configuration 8	x	x	x	x	
Configuration 9	x	x	x		x

Table 3.3: An overview of all setups of the Maltese Falcon that will be tested in the towing tank.

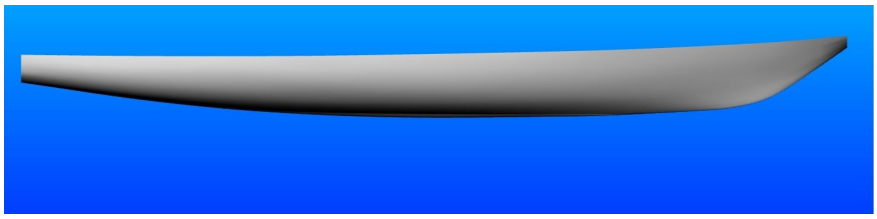

Figure 3.7: Configuration 1. Bare hull

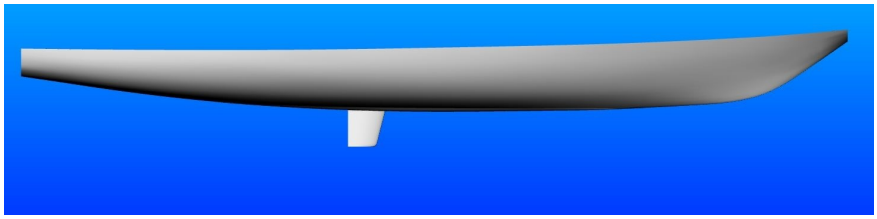

Figure 3.8: Configuration 2. Bare hull + CB1

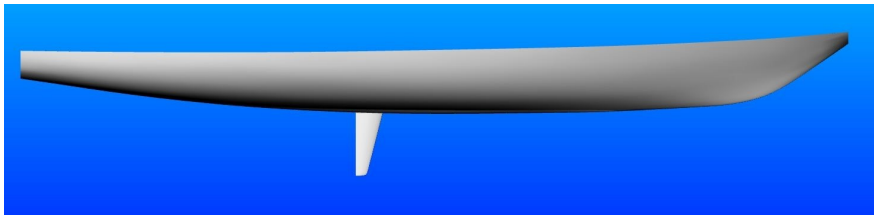

Figure 3.9: Configuration 3. Bare hull + CB2

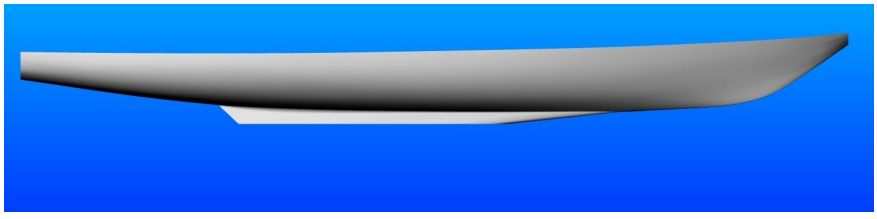

Figure 3.10: Configuration 4. Bare hull + keel1

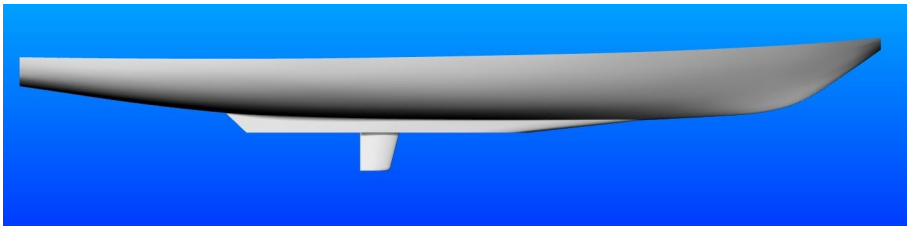

Figure 3.11: Configuration 5. Bare hull + keel1 + CB1

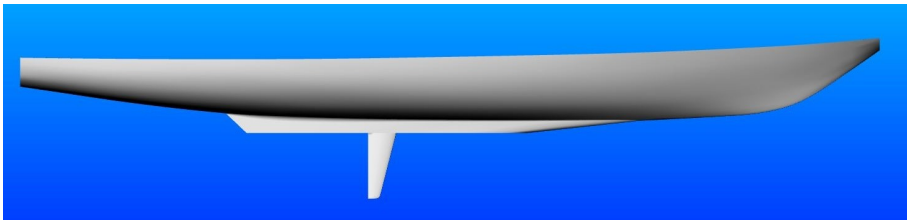

Figure 3.12: Configuration 6. Bare hull + keel1 + CB2

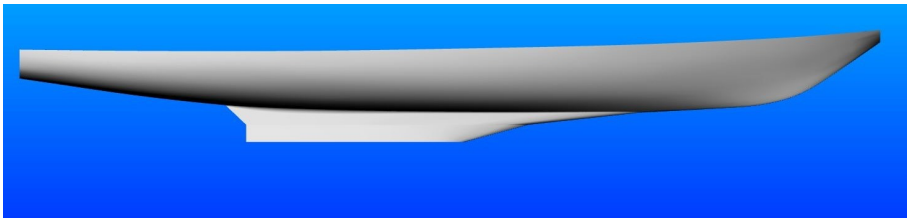

Figure 3.13: Configuration 7. Bare hull + keel1 + keel2

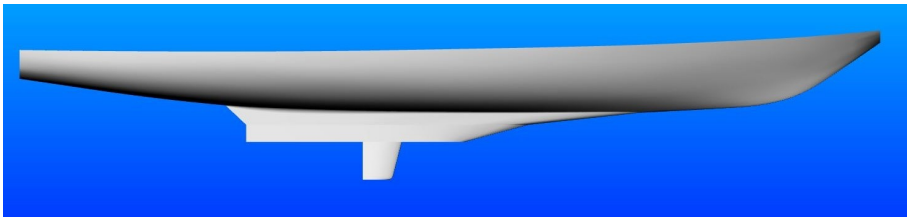

Figure 3.14: Configuration 8. Bare hull + keel1 + keel2 + CB1

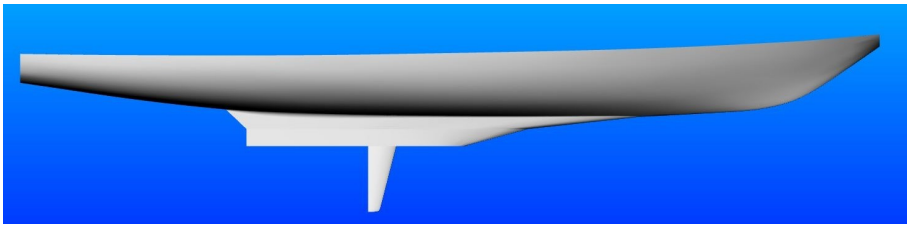

Figure 3.15: Configuration 9. Bare hull + keel1 + keel2 + CB2

3.3.2. Towing tank setup

An important choice is whether to do the experiments with the yacht being able to heave and trim freely using the balance arm setup, or to fix it in a constrained position. For both CFD and towing tank experiments, it is decided to test the model in a fully constrained setup, rather than the balance arm setup. The model is fixed by a hexapod[5] which can move the model in six degrees of freedom with very high accuracy. This fixed setup gives a better control over the position of the model, and provides extra flexibility when designing the arrangement of the force transducers. One reason for using this setup, is to make sure the model experiences the same flow of water during both the CFD simulations and the towing tank experiments. Another important reason for choosing the setup with the fixed 6DOF frame, is the fact that the model has to be taken in and out of the water very frequently, to change configuration. The 6DOF frame gives the ability to quickly disconnect the model, change the appendage layout, and then reconnect the model to the tank setup at the same position with a high accuracy. The 6DOF frame can be seen in the figure 3.16.

Figure 3.16: The Maltese Falcon model, fixed by the hexapod and the 6DOF frame, during the towing tank experiments

[5]This hexapod is also called Notus or 6DOF frame.

Because the model will be held in a fixed position, it is important to choose the correct trim and waterline depth of the model. During the experiments in 2002, the model was tested using the balance arm. Although this was another approach, some interesting data like deplacement and trim was found in the measurement report. But for the experiments in this research, the weight and volume displacement differs for each configuration. Still, for a number of reasons it is decided to use the same heave and trim settings for all nine configurations. Firstly, because it takes significant amount of time to first determine the precise heave and trim for each appendage layout, and then adjust the model setup for each run in which this changes. But most importantly, the experiments are meant to find the relative force between the different configurations, in order to determine the contribution of the centre board.

The movements of the model, induced by the hexapod, are measured by an optical tracking system called Certus. Certus consists of three cameras, measuring the position of the tracker which is mounted on the aft of the Maltese Falcon model. Certus is used to align the Notus (hexapod) and to check/validate the position of the model during the experiments.

3.3.3. Towing tank test matrix

Most towing tank experiments are executed to obtain information on the behaviour of one specific hull and/or appendage layout, tested for many variations in boat speed, leeway angle and heeling angle. However, the objective in this case is to compare different hull-keel-centre board combinations. If all combination are to be tested at all parameter variations, the number of test runs would explode. Therefore, the test matrix must be designed with care. As discussed in section 3.3, there are nine different geometrical setups. These will all be tested at different sailing conditions. all configurations will be tested at heeling angles of 0 and 15 degrees. For all configurations the leeway angle is set at 0, 3, 6 and 9 degrees, which are typical values used in a vast majority of all the towing tank experiments executed at the Delft Hydromechanics Laboratory. Configurations 1, 3, 4, 6, 7 and 9 will also be tested at leeway angles of 7, 8, 10 and 11, to capture the stalling behaviour of CB2[6].

The velocity of the yacht is an important sailing parameter. Though, it is decided to do the runs for only one velocity. The current VPP of the Maltese Falcon shows that the most common boat speed range is 10 to 15 knots. It is decided to take 14 knots as the case boat speed, which corresponds to a Froude number of 0.26. For towing tank tests, this is already a little low. Taking even a lower speed reduces the contribution of the wave resistance and the accuracy of the measurements. Ideally, all geometrical setups are tested for multiple boat speeds. Though, it is decided to do the tests for only one velocity, to keep it simple and straight forward. For the same reason, Dykstra is examining the performance in the inhouse VPP tool for only one velocity as well. The performance is then linearised to other speeds. In the ideal case, all sailing parameters are tested for at least three variations to asses possible non-linearities, but this would result in too many test runs.

An estimate of the total number of runs can be seen in table 3.17. Some setups will be tested both at starboard and port side, to check the symmetry/accuracy of the model and the experiment setup. Additionally, some runs will be done more than once, to verify the outcome. Obviously, no run can be done at the exact same conditions, resulting in the exact same outcome. But, it is important to check the accuracy of the measurements and to determine a standard deviation. Additionally, an error for some reason or the other is always possible. The results will be checked immediately after each run. If the outcome seems unnatural, the run can be done again. Which specific runs will be done multiple times will be determined during the tests and will be a bit arbitrary. It was estimated that about 25% of the all runs will be done to check the symmetry, or to repeat a previous run for verification.

An overview of the towing tank test matrix is presented in table 3.17. Another matrix listing the order of all runs is presented in the appendix. It is estimated that the total of 120 test runs will take about two to three weeks.

[6]Originally, the plan was to test only at leeway angles of 0, 3, 6 and 9 degrees. However, when analysing the results during the experiments, it seemed as if CB2 was stalling at a leeway angle of 9 degrees. It was then decided that all configurations with CB2 and the configurations with no CB would be tested at additional leeway angles. By doing this, CB2 could be eliminated to analyse the stalling behaviour.

	Fn [-]	Vm [m/s]	Heeling angle [deg]	Leeway angle [deg]	No. of runs
Configuration 1 Bare hull	0.26	1.315	0 15	0 3 6 7 8 9 10 11	16
Configuration 2 Bare hull + CB1	0.26	1.315	0 15	0 3 6 9	8
Configuration 3 Bare hull + CB2	0.26	1.315	0 15	0 3 6 7 8 9 10 11	16
Configuration 4 Bare hull + keel1	0.26	1.315	0 15	0 3 6 7 8 9 10 11	16
Configuration 5 Bare hull + keel 1 + CB1	0.26	1.315	0 15	0 3 6 9	8
Configuration 6 Bare hull + keel1 + CB2	0.26	1.315	0 15	0 3 6 7 8 9 10 11	16
Configuration 7 Bare hull + keel1 + keel2	0.26	1.315	0 15	0 3 6 7 8 9 10 11	16
Configuration 8 Bare hull + keel1 + keel2 + CB1	0.26	1.315	0 15	0 3 6 9	8
Configuration 9 Bare hull + keel1 + keel2 + CB2	0.26	1.315	0 15	0 3 6 7 8 9 10 11	16
			Total number of runs, excluding symmetry runs and repetition runs:		**120**

Figure 3.17: The towing tank test matrix, excluding the repetition and symmetry runs.

In the end, the towing tank experiment lasted for three weeks, doing about 14 runs per day on average. 186 runs were done in total, of which 30 runs were conducted to align the model and setup, and to measure the strip resistance. 156 runs remain, of which 120 runs were planned according to the test matrix. So, 36 runs were done to check the symmetry of the model or the towing tank setup, or to repeat a previous run for verification. This is 30% of the planned number of runs.

3.4. Setup for the CFD simulations

Doing CFD simulations brings two main contributions to this research. Firstly, it can be used to validate the results of the towing tank experiments. Trends regarding the forces and moments will be examined. Secondly, the flow of water around the model can be analysed in detail, which is not possible in the towing tank.

Not all runs that were done in the towing tank will be done in the CFD as well. That would take too much time and is not necessary for the purpose of doing CFD simulations. Only configurations 4 and 6 will be simulated, with and without heel, for leeway angles up to 11 degrees.

The CFD simulations will be done with *FINE Marine - NUMECA*, which is available both at Dykstra and at the TU Delft. The ISIS-CFD flow solver of NUMECA makes use of the incompressible unsteady Reynolds-Averaged Navier-Stokes equations (RANS) [17]. RANS equations are time averaged equations of motions for fluid flow. The quantities of the flow are decomposed into time averaged and fluctuating quantities. The solver is based on the finite volume method to build the spatial discretization of the transport equation. The velocity field is obtained from the momentum conservation equations and the pressure field is extracted from the mass conservation constraint, or continuity equation, transformed into a pressure equation [17].

The meshes will be build using Hexpress, which is also part of the NUMECA software. Hexpress has been developed to ensure a quick management of the grid generation process for external and internal configurations. The software is able to generate an unstructured hexahedral mesh in any "water-tight" computational domain [17]. The Hexpress software provides an interactive and user friendly interface, based on a wizard approach, in which the mesh is generated step by step. During those steps, the mesh can locally be refined at curves and edges. Then after the mesh is constructed, the flow and boundary conditions are set in FINE Marine. The SST k-omega model is selected as the turbulence model. A k-

omega model is a two equation model, which means that it includes two extra transport equations to represent the turbulent properties of the flow. This allows a two equation model to account for effects like convection and diffusion of turbulent kinetic energy. The addition of the shear stress transport (SST) formulation improves the prediction of separation and reattachment of the flow, compared to k-epsilon and the standard k-omega model. Furthermore, no additional features like transition models, adaptive grid refinement, etc. have been implemented. More about the used settings, parameters and the resulting data of the CFD simulations, are presented in chapter 5.

3.4.1. Construction of the Maltese Falcon digital model

Several digital models of the Maltese Falcon were already built a while ago at Dykstra Naval Architects. To be able to compare the CFD data to the data from towing tank experiments, it is important that the digital model of the Maltese Falcon exactly matches the towing tank model. The towing tank model of the Maltese Falcon (in this research defined as configuration 4; bare hull + keel1) is built in 2002, about 16 years ago. Laying still for such a period could affect the shape of the model, since it is built from wood. To check the shape of the towing tank model, a special 3D pen is used to make a scan. Sections at every $10cm$ were drawn on the model with a permanent marker, as well as a centre line and a deck line. Then, the 3D pen was to zigzag over all lines on the hull. Meanwhile, the 3D pen was in contact with three cameras[7] to monitor it's position. This system writes a text file of the coordinates of the tip of the pen with a frequency of 100Hz. These coordinates are then filtered to obtain a neat point cloud, covering only the sections, keel line and deck line. When this point cloud was compared to the digital models present at Dykstra, it was clear that the towing tank model differs significantly. Therefore, a new digital 3D geometry had to be constructed. Furthermore, it was noticed that the model showed some significant deviations in the starboard and port side symmetry[8]. For the CFD simulations, an exactly symmetrical model should be used. So, one half of the measured hull is used to construct the digital model. This is done by shaping the section lines to the measured points on one half of the model only, and copying this over the centre line. The point cloud is converted into a hull shape, using Maxsurf, AutoShip and Rhino. Keel2 and both centre boards are constructed in Rhino, made from scratch, and can be added to the model. The filtered point cloud can be seen in figure 3.18

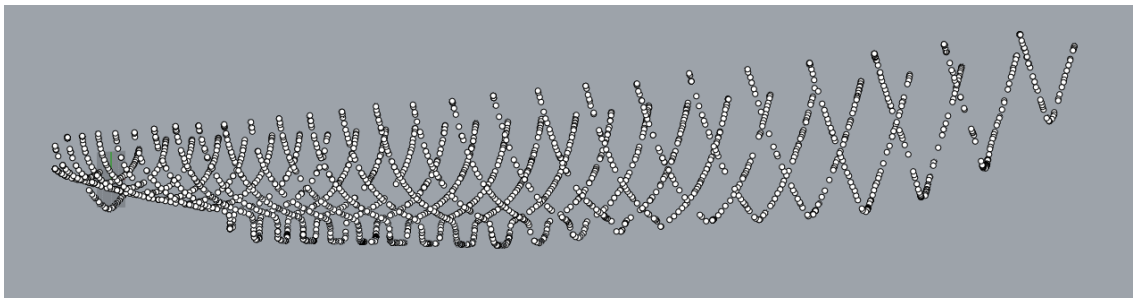

Figure 3.18: The filtered point cloud covering the Maltese Falcon model.

3.5. Improving the performance prediction

The obtained data from the towing tank experiments and the CFD simulations will be compared to validate the results. Verification will be done by examining and discussing the uncertainty of the experiments and the resulting data. After that, the data resulting from the experiments will be analysed extensively. After this analysis, performance prediction methods that are currently available will be tested on this data where possible. In the end, the data obtained from the Maltese Falcon towing tank experiments will be used to improve existing performance prediction methods, to make them suitable for hull-keel-centre board configurations. Methods will be derived to estimate the sideforce, resistance

[7] This system is called Certus and was mentioned previously in section 3.3.2. It is the same camera setup used in the towing tank to monitor the position of the model.

[8] Examining the asymmetry of the Maltese Falcon model in the towing tank is described in section 4.2

and centre of effort of the centre board contribution. Finally, it is important to examine how trustworthy these new methods are. Therefore, they will be validated on data from YACHT1 and Adela.

4

Towing tank tests

The main information about the setup of the towing tank tests has already been discussed in section 3.3. A separate report about the towing tank experiments is appended to this thesis report, containing the daily processes, encounters, decision making and photographs of the setups and alignment and calibration of the model and the towing tank components. The results of the experiments will be presented in this chapter. The analysis of the results will be done in chapter 6, after a comparison to the CFD data and a conclusion regarding the uncertainty.

Before the real experimental runs can start, the experiment setup must be aligned and calibrated. First, the 6DOF frame is calibrated by applying forces in sheer X-, Y-, and Z-directions and examining the measured forces. Then, the 6DOF frame is aligned with the model and the model is aligned with the tank, using Certus. Several runs upright and without leeway are done, while the position of the model is tweaked until the sum of the forces in Y-direction are zero. Then, symmetry runs will be done to check the symmetry of the experiment setup and the symmetry of the model itself. After that, the resistance of the turbulence strips are to be determined, which will take approximately one full day.

4.1. Frame of reference

When analysing the results, it is important to choose the correct frame of reference. The 6DOF frame measures the forces on the model through six force transducers; 1 in x-direction, 2 in y-direction and 3 in z-direction[1]. The measured forces on each transducer are together converted to x, y and z forces and moments in the ship's axis system. But, this must be translated to the tank axis system, since the resistance and sideforce of the ship are defined parallel and transverse to the flow of water. The following translation matrix is used to convert the forces in the ship's axis system to the forces in the tank axis system [8]. The forces in the ship's axis system are denoted by the small 'f', while the forces in the tank axis system are denoted by a capital 'F'. The same holds for the axis denotations. Translating the moments from the ship bound axis system to the tank axis system is done using the same method and the same translation matrix.

$$\begin{bmatrix} F_X \\ F_Y \\ F_Z \end{bmatrix} = \begin{bmatrix} cos\psi cos\theta & -sin\psi cos\phi & sin\psi sin\phi \\ sin\psi cos\theta & cos\psi cos\phi & -cos\psi sin\phi \\ -sin\theta & cos\theta sin\phi & cos\theta cos\phi \end{bmatrix} \cdot \begin{bmatrix} f_x \\ f_y \\ f_z \end{bmatrix}$$

4.2. Alignment of the towing tank construction and model

The 6DOF frame and rest of the experiment setup is calibrated and aligned with the tank. Photos of the procedures can be found in the appended towing tank report. Before the runs to determine the resistance of the turbulence strips can start, the exact starting position of the model must be determined. This is the position which the model always returns to when taking it in and out of the water, having

[1] The lower case axis denotations x, y and z, indicate the ship bound axis system.

no leeway and no heel. More about determining this position will be described in section 6.2. When a position is found where the model has no heel and generates no sideforce, the symmetry of the model and construction is examined by doing several runs with both positive and negative leeway and heeling angles. Positive leeway angles correspond to a positive heeling angle and vice versa, to simulate a realistic sailing condition. The symmetry checks, both without and with heel, are presented in figure 4.1 and 4.2. Some runs are repeated to verify the results. This can be seen in the graphs where two values are denoted at some points. The repetition runs resulted in very similar values. Also, the values of the sideforce and resistance at positive and negative leeway angles are about the same[2]. It can be seen that for negative leeway angles, the model generates a little more sideforce than for positive leeway angles, both with and without heel. However, these margins were considered as acceptable. It was decided to continue with the positive leeway and heeling angles for the rest of the experiments.

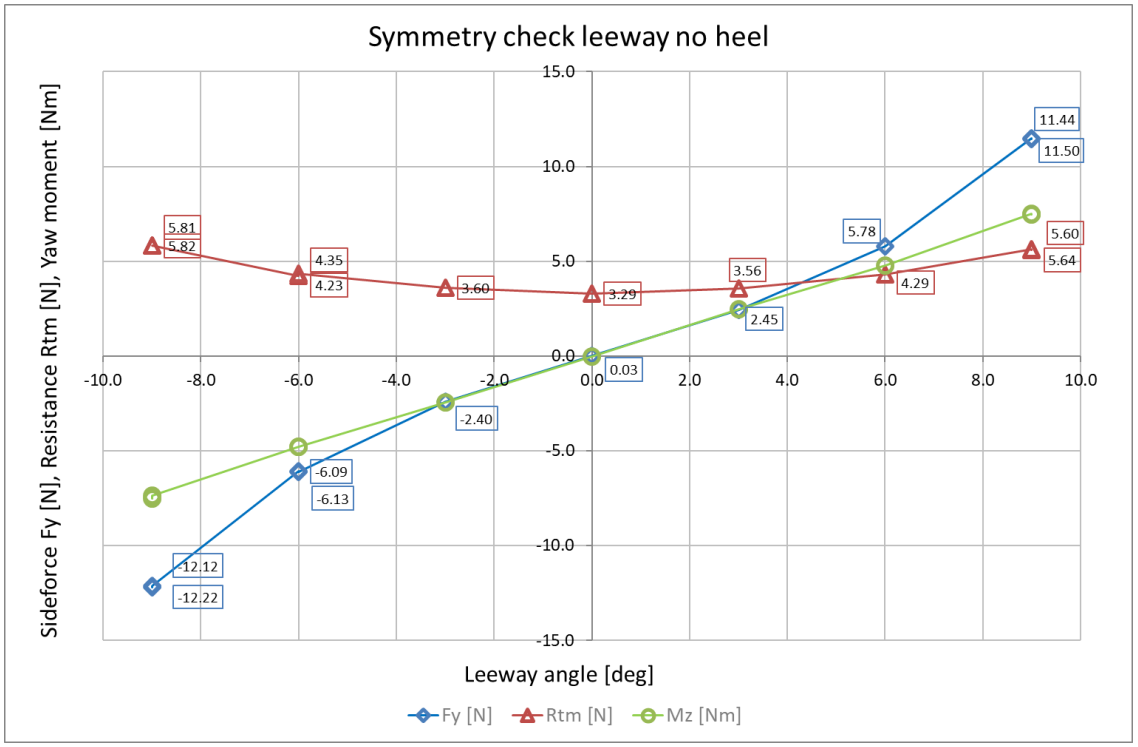

Figure 4.1: Checking the symmetry of the model, for upright conditions

[2]Some asymmetry of the towing tank model was earlier noticed, during the construction of the Maltese Falcon digital model, described in section 3.4.1

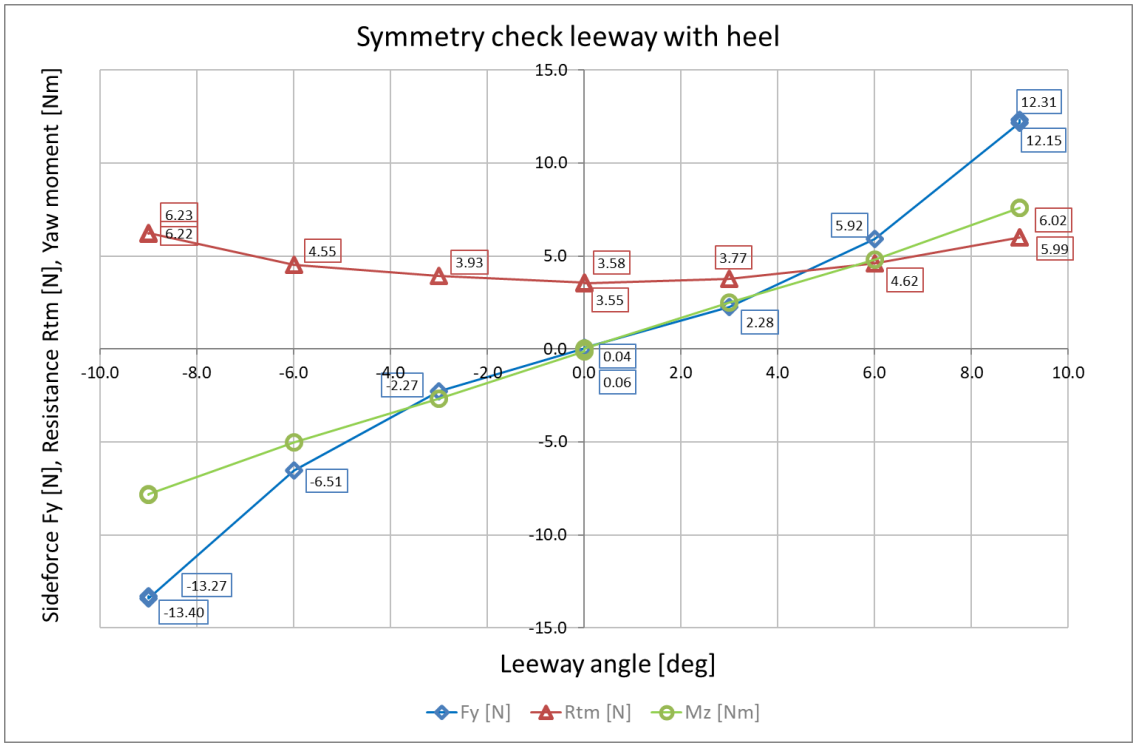

Figure 4.2: Checking the symmetry of the model, for heeled conditions

4.3. Turbulence strips

In full scale, the flow of water is always turbulent at cruising speeds on open water. However, in the towing tank the water can remain laminar, resulting in a different frictional resistance profile. Therefore, so called Carborundum strips are attached to the bow of the model and to the leading edge of the appendages, to start a turbulent flow. But, these turbulence strips increase the total resistance of the model. The ship in full scale does not have such turbulence strips and thus this little extra resistance of the model must be corrected for. Before the experiment runs can start, the resistance of the turbulence strips will be derived. The model is first tested with a single turbulence strip at each strip location. After that, second strips are added and the model is tested again, with the exact same parameters. The model both with one and two strips will be tested at 5 different velocities. All runs will be repeated at least once to verify the outcome. This results in at least 20 runs to determine the strip resistance. The resistance of the runs with one turbulence strip will then be subtracted from the resistance with two strips, to obtain the resistance of one turbulence strip. This will then be reduced to a resistance factor per cm^2, to be able to estimate the resistance of the turbulence strips on the hull and on all the appendages. Or, a resistance coefficient for the turbulence strips in general, having a value of 0.0031. The resistance of the model with a single strip and a double strip can be seen in figure 4.3.

If one wants to be most precise, this procedure should repeated for all 9 hull-keel-centre board configurations separately. But instead, it is decided to test the resistance of the turbulence strips only for configuration 4 (bare hull + keel1). Mainly because it would take too much time considering a full day testing per configuration. Secondly, it was found that when the obtained resistance coefficient of the turbulence strips on configuration 4 is used to predict the resistance of the strips on the appendages, the strips on the appendages cause a resistance increase of only 0.015N for keel 2, 0.010N for CB1 and 0.020N for CB2. But, in order to measure the strip resistance, the model must be taken out of the tank to add the second strip. It is assumed that taking the model out of the tank and putting it back in would result in a measurement error which is bigger than the difference in resistance of one strip and two strips. Nico van der Kolk tested the error of taking the model out and putting it back in at the same location. Van der Kolk found that after 10 runs with in between each run disconnecting and connecting the

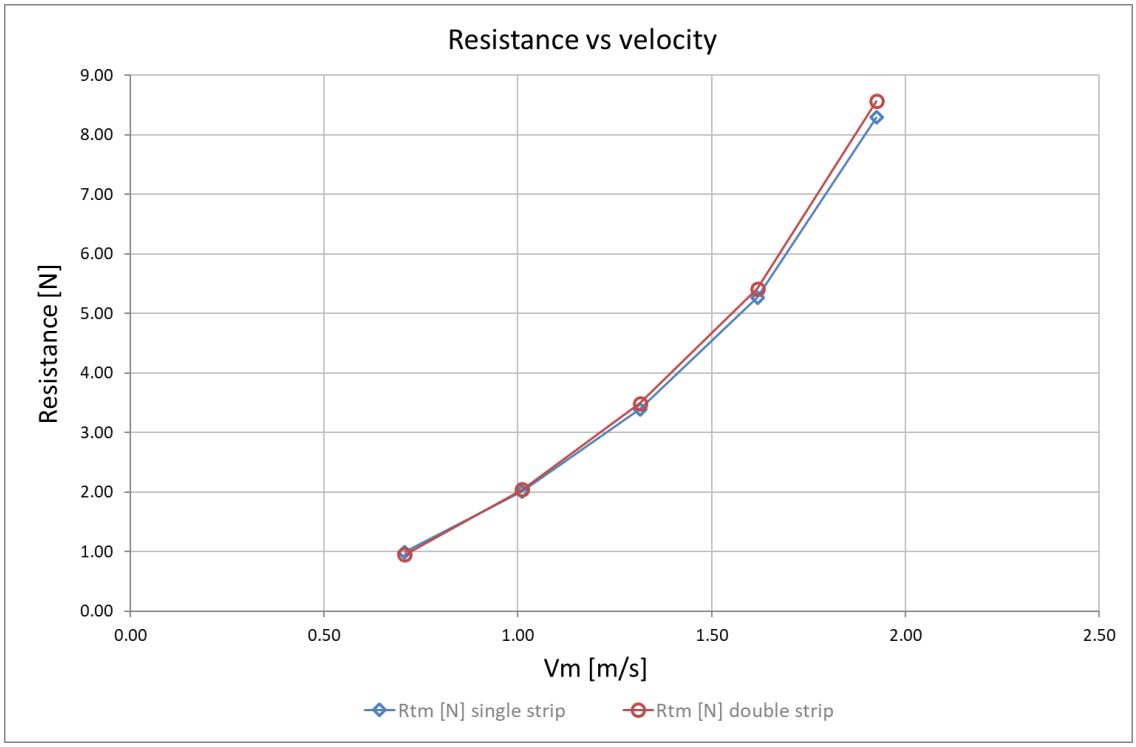

Figure 4.3: The resistance of the model with a single strip and with a double strip for five different boat speeds.

model to the 6DOF frame, the error in resistance was 0,96% on average. In case of the Maltese Falcon model, this would be around 0.040N, which is more than double of the expected increase in strip resistance. This confirms the assumption that it is not worth testing the strip resistance on the appendages. Instead, the resistance coefficient of the turbulence strips on configuration 4 is used to predict the resistance of the strips on the appendages. The appendages are not experiencing the exact same flow as the hull, so the resistance coefficient is not exactly the same. But still, this is considered as the most accurate method available to estimate the resistance of the turbulence strips on the appendages. Knowing the known surface of the turbulence strips on the hull and on all of the appendages, results in a resistance estimate of the turbulence strips for each configuration. For each run, this strip resistance will be subtracted from the measured total resistance of the model.

The strip resistance was determined for sailing upright and without leeway. For simplification reasons it is assumed that the resistance of the turbulence strips is the same for all sailing conditions. The estimated resistance of all turbulence strips is now subtracted from the calculated resistance.

4.4. Results

Only the resistance, sideforce and yaw moment versus leeway for the upright conditions are presented in the following two subsections. An analysis of these results and the influence heel will be discussed in chapter 6, after the results from the towing tank experiments have been validated by the CFD simulations.

4.4.1. Resistance

After the resistance of the turbulence strips has been determined, it was time to start the experimental runs. The resistance of all configurations versus leeway angles up to 9 degrees is plotted in figure 4.4. Note that this graph alone is not a good indication of the performance of each configuration, since the sideforce and the moments must also be taken into account. Again, qualitative representations of the results, like the resistance relative to the sideforce, are presented in chapter 6.

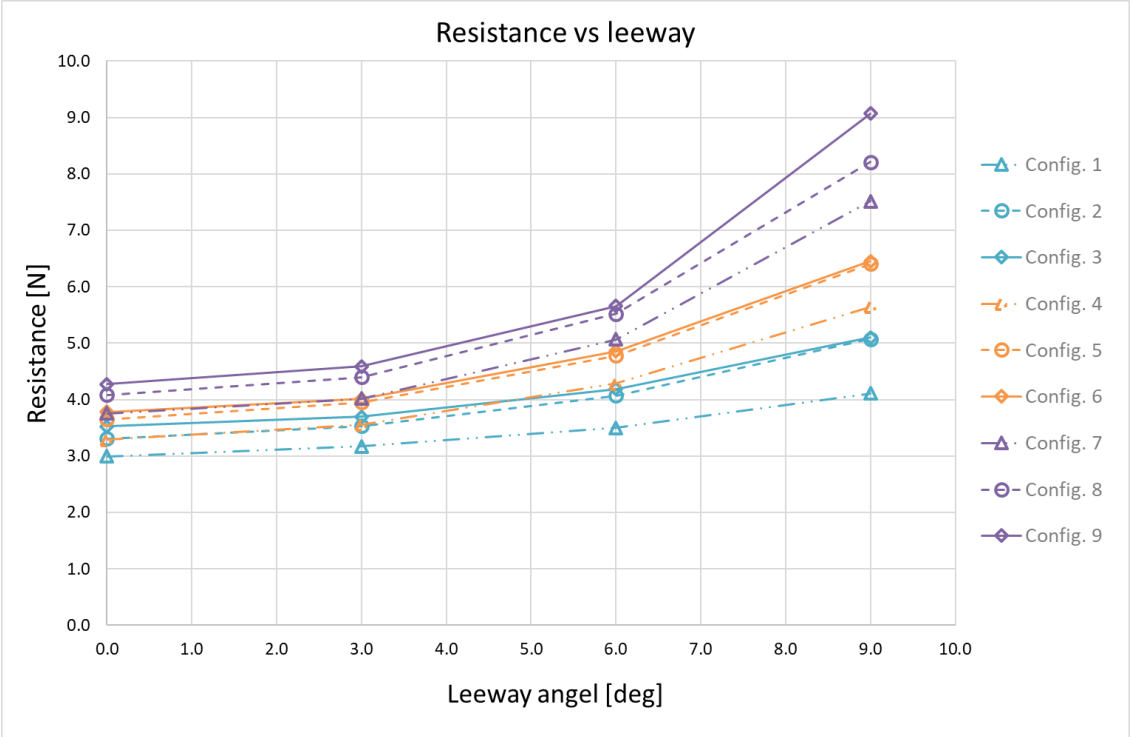

Figure 4.4: The resistance of all configurations for leeway angles up to 9 degrees.

4.4.2. Sideforce and yaw moment

The sideforce and yaw moment of all configurations for leeway angles up to 9 degrees are plotted in figure 4.5 and 4.6. In figure 4.5, it can be seen that all configurations result in a linear trend, except for the configurations 1, 4 and 7, which do not have a centre board. For those configurations, the sideforce is increasing exponentially for increasing leeway angles. This is not a surprise, since it is known from previous studies and literature that low aspect ratio bodies in general are more effective, in terms of sideforce, at higher angles of attack. Then it could be argued why the other configurations, having the same hull and keels, do not show such a trend. In chapter 6 it will be discussed that this is due to the influence of the centre board. The yaw moment is for each configuration a linear relationship with the leeway angle of the ship, see figure 4.6.

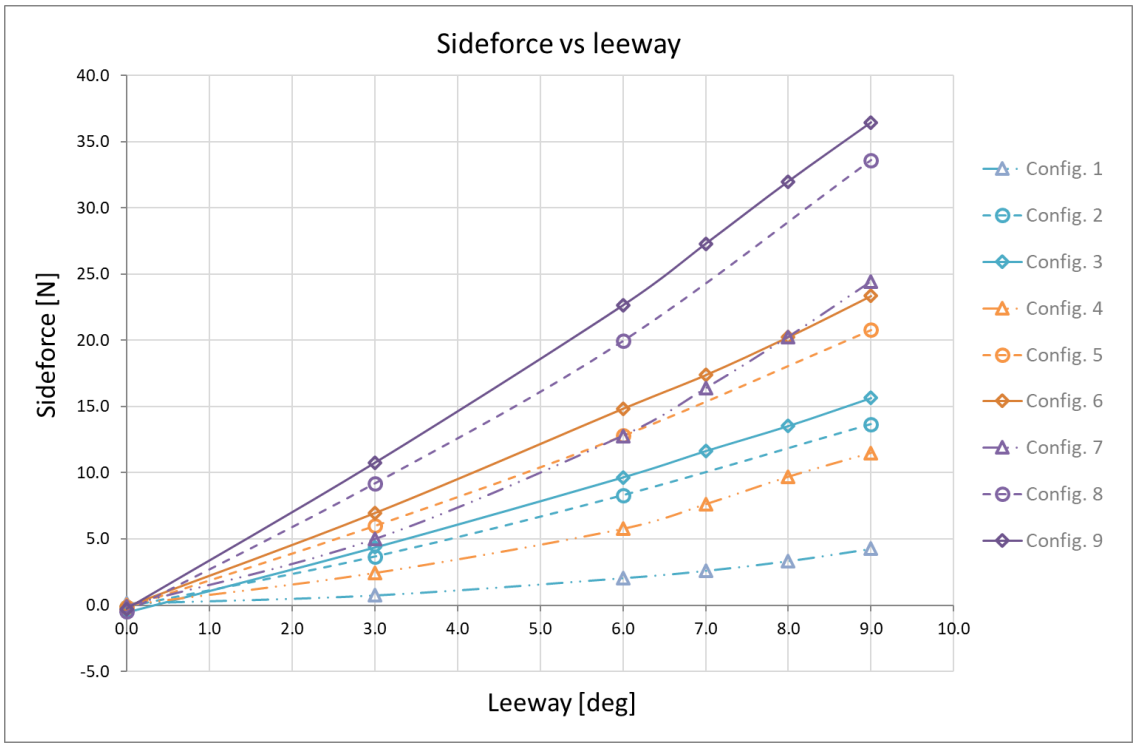

Figure 4.5: The sideforce of all configurations for leeway angles up to 9 degrees.

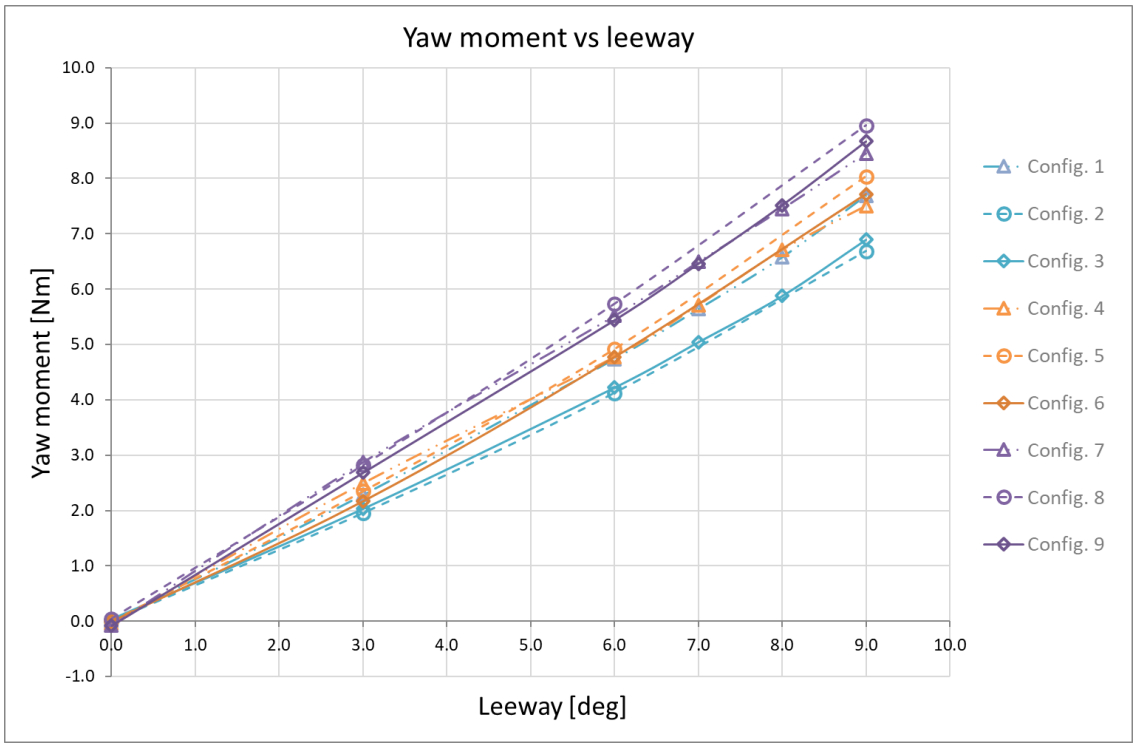

Figure 4.6: The yaw moment of all configurations for leeway angles up to 9 degrees.

5

CFD simulations

There are two main reasons to simulate the model of the Maltese Falcon with Computational Fluid Dynamics (CFD). First, to validate the results from the towing tank experiments. Secondly, CFD can visualise the flow, providing extra information that can not be obtained from the towing tank experiments. As discussed in section 3.4.1, a new digital 3D model had to be constructed for the CFD simulations. The setup of the CFD simulations and the used software have been discussed in chapter 3. This chapter further discusses the used settings and parameters for the CFD simulation of the Maltese Falcon model. After that, the resulting data and visualisations that show the effect of the centre board, are presented. An analysis of these results and a comparison will be made in the next chapter. The CFD simulations on YACHT1 and Adela have been carried out before this research started and will therefore not be discussed in detail, regarding the CFD settings.

5.1. Computational mesh

As discussed in section 3.4, the mesh is constructed using the Hexpress software. In this section, details on the mesh are presented, for configuration 6. The simulated configuration 4 has a similar mesh, only without the centre board. The initial mesh of the domain is constructed of 15 cells in X-direction, 9 cells in Y-direction and 6 cells in Z-direction. This results in cubic cells, with dimensions of 0.833 x 0.833 x 0.833 meters. The cell size is refined at locations with large curvature and expected large pressure/velocity gradients. The cell refinements of surfaces with curvature have been adapted based on their curvature. The number of cell size refinements that have been applied to certain surfaces of the yacht's body can be seen in table 5.1. The corresponding cell size is stated in table 5.1 as well. The deck and transom surfaces have not been refined. Besides the surface refinements, some curves are refined as well. These

Surface	No. of refinements	Cell size [mm]
Hull	9	1.628
Hull keel intersection	12	0.203
Keel	10	0.814
Keel tip	9	1.628
Keel trailing edge	11	0.407
Centre board	9	1.628
Centre board tip	10	0.814
Centre board trailing edge	11	0.407

Table 5.1: The refinements on each surface and the corresponding cell size.

are curves where two surfaces come together and where pressure/velocity gradients are high, like the hull centre line at the bow, keel leading edge and the centre board leading edge. These refinements are summarised in table 5.2.

Curve	No. of refinements	Cell size [mm]
Hull centre line at bow	9	1.628
Keel leading edge	9	1.628
Centre board leading edge	9	1.628

Table 5.2: The refinements on three curves where two surfaces come together and where pressure/velocity gradients are high

The waterline is refined as well, with a cell height set to $\frac{L_{wl}}{500} = 0.005m$. With a maximum aspect ratio of 125, this results in cell sizes of $0.625m$ in X- and Y-direction.

The value of Y+ was set to 30, resulting in a first layer thickness of $0.804mm$. The following figures show the mesh on the surface of the Maltese Falcon model, in configuration 6. After meshing, the domains consist of 2 million and 2.3 million cells for configuration 4 and 6 respectively.

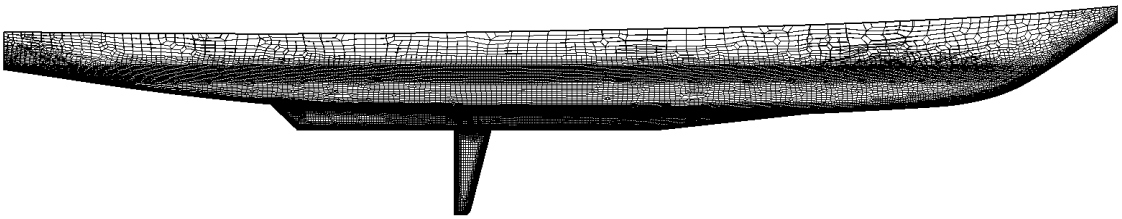

Figure 5.1: Side view of the mesh

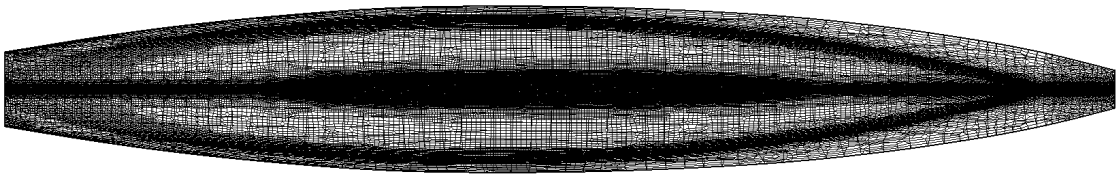

Figure 5.2: Bottom view of the mesh

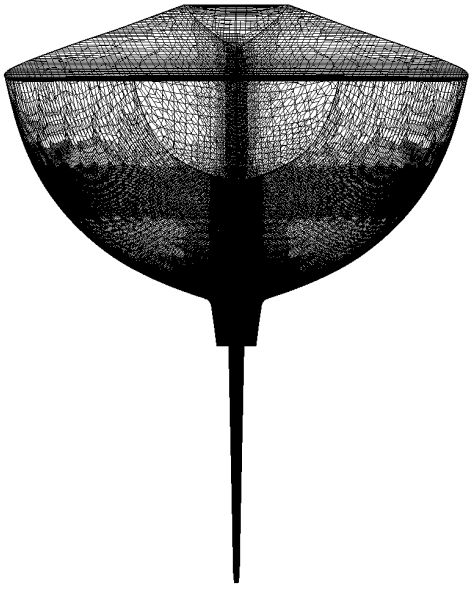

Figure 5.3: Forward view of the mesh

5.2. Domain and boundary conditions

The domain around the hull is constructed such that the boundaries are far enough away not to influence the flow around the yacht. Dykstra uses a rule of thumb to set the domain size, based on the waterline length of the model. The longitudinal domain size is chosen such that there is about one boat length in front of the hull, and three boat lengths in the wake. The 'beam' of the domain is set to three boat lengths in total. In Z-direction, the distances from the waterline to the bottom and top face are set to 1.5 and 0.5 boat lengths respectively. The dimensions of the computational domain, relative to the reference point of the Maltese Falcon model (aft perpendicular on the waterline), are presented in table 5.3. These dimensions are based on a waterline length of the Maltese Falcon model, approximated to $2.5m$.

Direction	Minimum [m]	Maximum [m])
X-direction (longitudinal)	-7.5	5
Y-direction (beam)	-3.75	3.75
Z-direction (height)	-3.75	1.25

Table 5.3: Domain sizes relative to the reference point of the yacht.

All hull and appendage surfaces had a no-slip boundary condition, using wall functions to capture the boundary layer. On the top and bottom of the domain, the pressure is prescribed. All other domain faces have a far field boundary condition, with a prescribed speed of $V = 0\ m/s$, in all directions.

5.3. Solver setup

Just as in the towing tank experiments, the Maltese Falcon model was in a fixed position. Only in surge and sway direction, the motion was imposed to simulate a forward speed with a certain leeway angle. Properties of the fluids can be seen in table 5.4. Just as in the towing tank, the water properties are set to fresh water at 21 degrees Celsius. Details on the solver have already been described in section 3.4.

Fluid	Density [kg/m3]	Dynamic viscosity [Pa·s]
Water	998.0	9.78e-004
Air	1.2	1.85e-005

Table 5.4: Fluid properties, based on fresh water at 21 degrees Celsius.

5.4. Results

As discussed in section 3.4, only configuration 4 and 6 are tested with the CFD simulations. The results of the simulations and the visualisations are presented in the following subsections.

5.4.1. Sideforce and resistance

The total sideforce and resistance of configurations 4 and 6, for leeway angles up to 11 degrees, are plotted in the following figures.

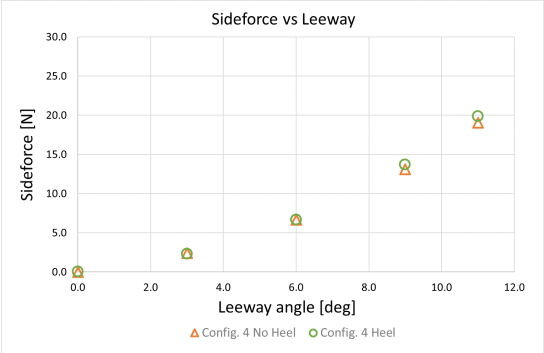

Figure 5.4: Sideforce versus leeway angle of configuration 4 upright and heeled.

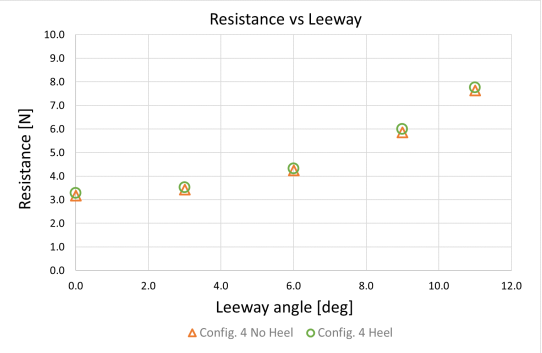

Figure 5.5: Resistance versus leeway angle of configuration 4 upright and heeled.

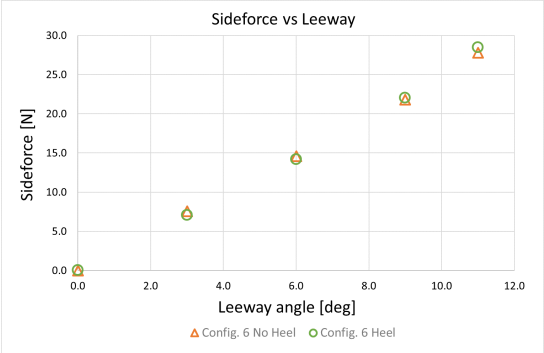

Figure 5.6: Sideforce versus leeway angle of configuration 6 upright and heeled.

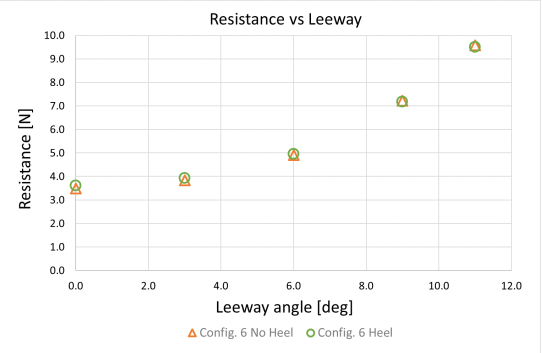

Figure 5.7: Resistance versus leeway angle of configuration 6 upright and heeled.

5.5. Visualisation

There are many parameters and variables that can be made visible using the results of the CFD simulations. CFView is the software that is used for this. This program is part of the NUMECA software as well. The visualisations of configuration 4 and 6 are presented next to each other, to be able to clearly see the influence of the centre board. Only the visualisations for the upright setups with a leeway angle of 6 degrees are presented in this chapter. The flow on the centre board is still attached for this leeway angle and all phenomena can clearly be seen. The images for all other setups can be found in the appendix. First, the hydrodynamic pressure on the hull, keel and centre board is presented. The lift-carry-over can clearly be seen, especially on the suction side, where the iso contours of the hydrodynamic pressure show that the keel generates more sideforce directly above the centre board.

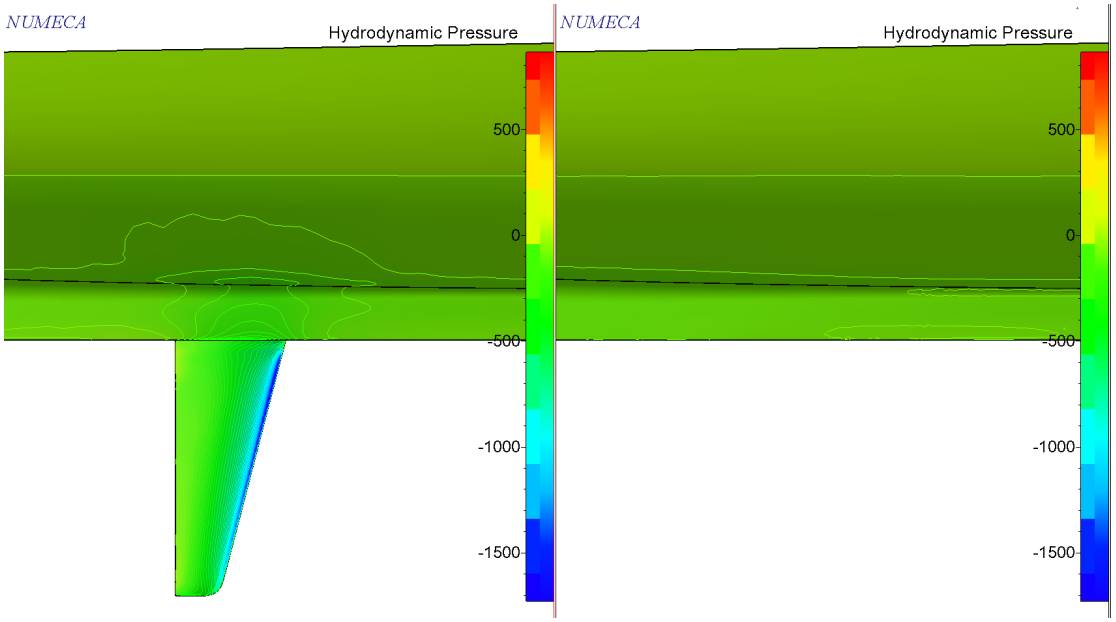

Figure 5.8: The hydrodynamic pressure on the hull's surface, shown at the suction side of the model.

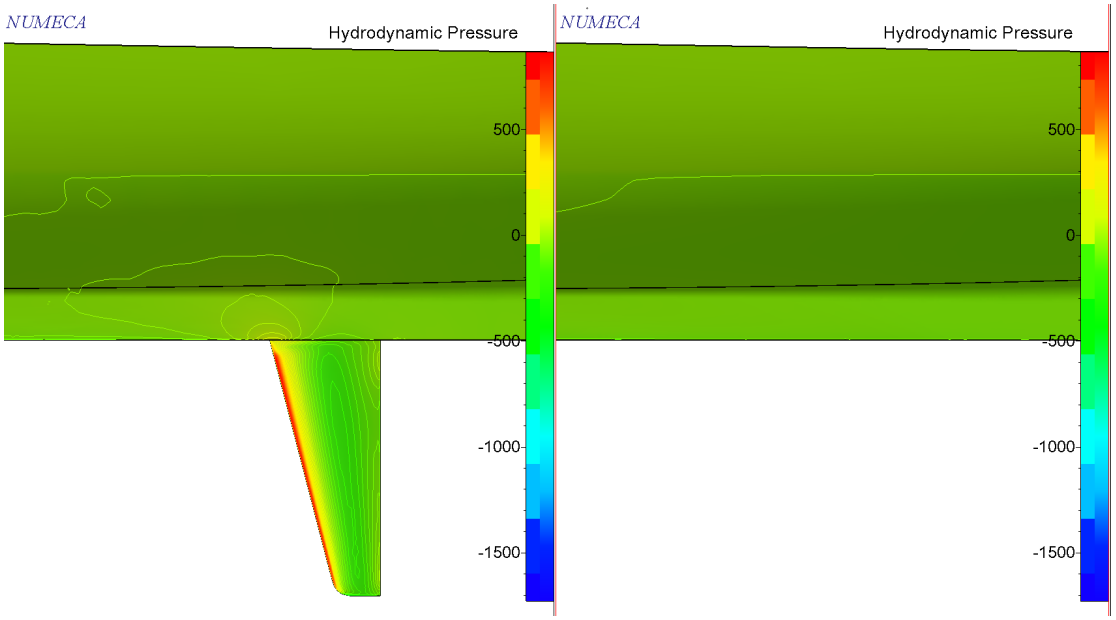

Figure 5.9: The hydrodynamic pressure on the hull's surface, shown at the pressure side of the model.

A second parameter that can give interesting insight in the behaviour of the flow is the shear on the hull in x-direction. This tells something about the resistance and the direction of the flow. If the shear in x-direction is positive, it can be assumed that the flow separates from the hull and flows locally in the positive x-direction. A black iso contour is introduced at the zero value of the shear in x-direction to make this transition visible. It can be seen for a leeway angle of 6 degrees that the flow is still attached. In appendix C, it can be seen that the flow does separate for leeway angles of 9 and 11 degrees.

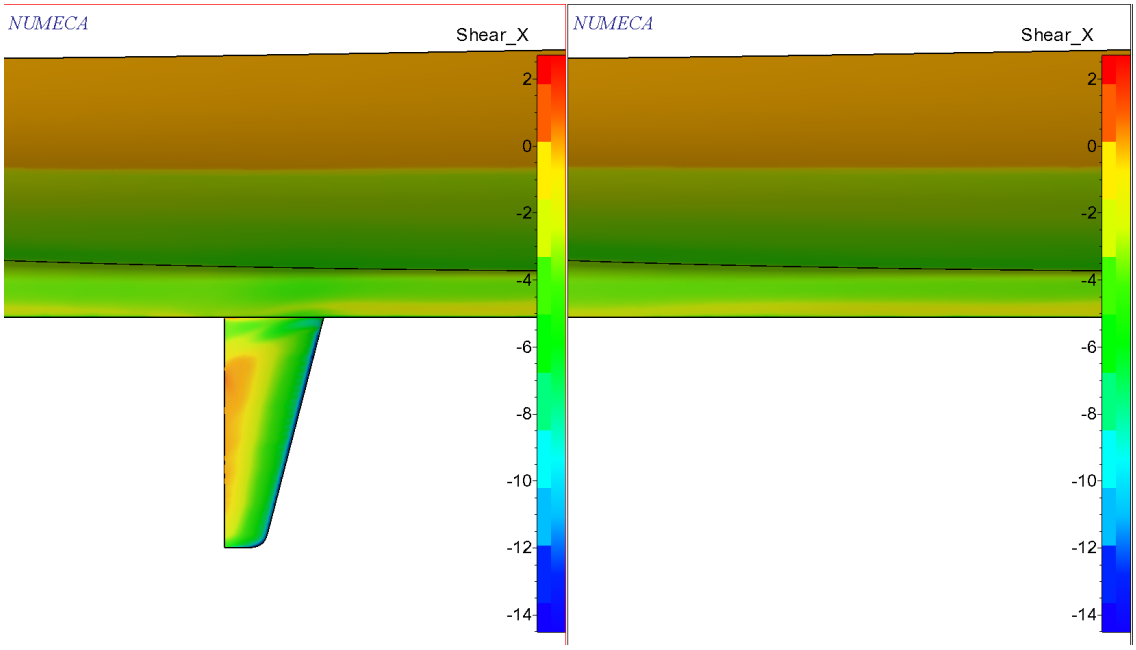

Figure 5.10: The shear (in X-direction) on the hull's surface, shown at the suction side of the model.

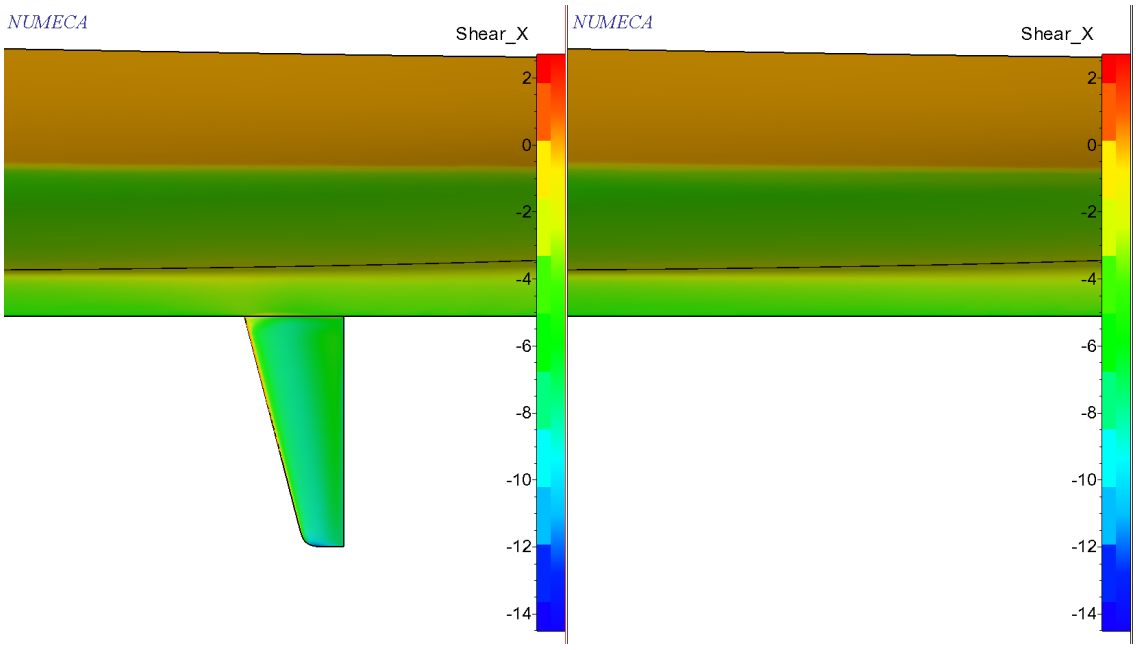

Figure 5.11: The shear (in X-direction) on the hull's surface, shown at the pressure side of the model.

A repeating thought during this research is that energy is dissipated in the circulation of the flow, causing the resistance to increase. The circulation can be interpreted as the turbulence on a bigger scale, showing the distortion of the flow. The centre board largely affects the circulation of the flow around the ship, which can be seen in the figure 5.12. Cross sections are made every $10cm$, starting at $1m$ aft of the aft perpendicular, until the leading edge of the keel. The circulation is made visible by showing the absolute velocity in the yz-plane, using the following formula.

$$V_{yz} = \sqrt{V_y^2 + V_z^2} \tag{5.5.1}$$

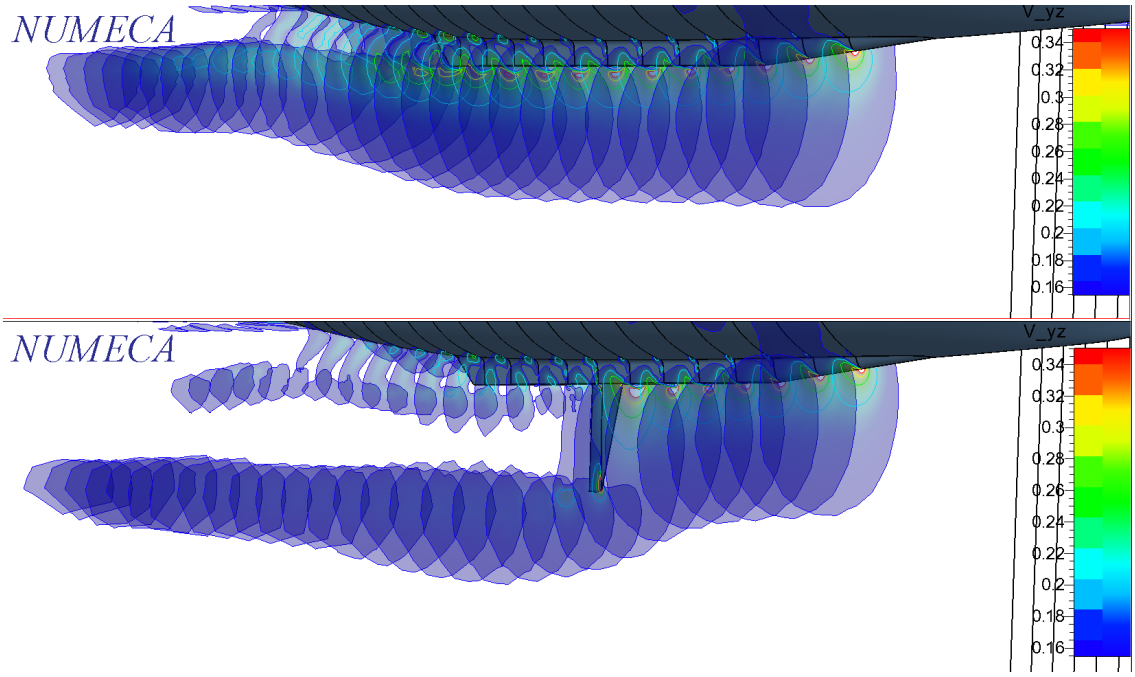

Figure 5.12: The magnitude of circulation in the flow around the model, made visible at cross sections at every 10cm, from the leading edge of the keel to the aft of the ship.

Figure 5.13 shows the circulation in the flow at a cross section $10cm$ behind the centre board trailing edge. Figure 5.14 shows the circulation $10cm$ aft of the keel trailing edge.

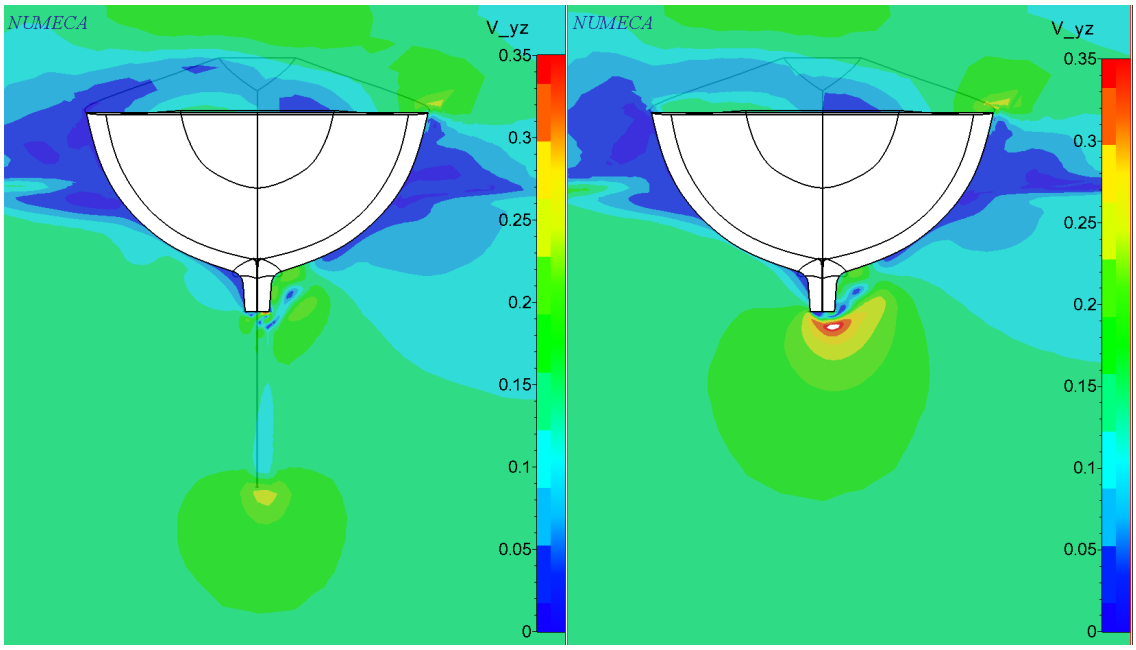

Figure 5.13: The circulation in the flow at a cross section $10cm$ behind the centre board trailing edge

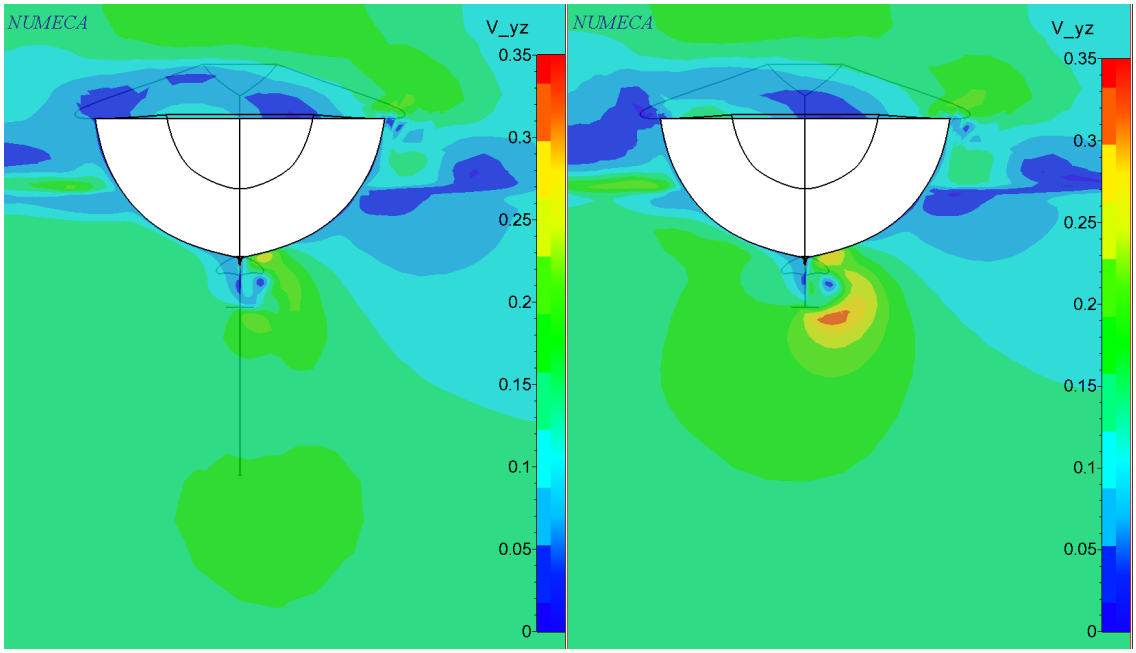

Figure 5.14: The circulation in the flow at a cross section $10cm$ behind the keel trailing edge

In figures 5.12, 5.13 and 5.14, it can be seen that the circulation is translated from the keel down to the centre board. The tip vortex originating from the centre board can clearly be seen as well. All in all, it seems that there is a little less total circulation in the configuration with centre board, compared to the configuration without.

6

Post Processing and result analysis

This chapter first describes how trustworthy the results are. Then when the results from the towing tank experiments are validated, all findings are analysed. In general, it was found that up to the stalling point of the centre boards, the towing tank experiments and the CFD simulations give very similar results. Only for leeway angles of 9 and 11 degrees, the stalling behaviour of the centre boards start showing discrepancies between the results from the towing tank experiments and the CFD simulations. So, when validating the results, the data up to 9 degrees is used to compare the complete configurations. Regarding the centre boards, only the data up to 6 degrees is used to to compare the results from the towing tank experiments to the CFD simulations.

Above all, it is important to state that in chapter 7, only the experimental data of the centre boards up to a leeway angle of 6 will be used to improve the performance prediction methods. The assumption is made that the sideforce increases linear with the leeway angle, up to 6 degrees[1].

6.1. Validation

Only configurations 4 and 6 are tested in the CFD simulations. As could already be seen in chapter 4 and 5, the results from the towing tank experiments and the results from the CFD simulations show very similar trends regarding the sideforce and resistance versus the leeway angle. In figures 6.1 to 6.4, the sideforce and resistance according to both the towing tank experiments and the CFD simulations are plotted in the same graphs.

There are some small discrepancies. For leeway angles up to 9 degrees, the resistance in the towing tank is 3.1% higher and the sideforce is 3.6% lower than in the CFD simulations. Those discrepancies, and the slightly bigger deviations in the stalling region, might be caused by incorrectly simulating the roughness of the centre board and the detachment of the flow[2]. The following section will elaborate on the potential uncertainty in some aspects of the research.

[1] Existing lift prediction methods for foils, both in aero- and hydrodynamical studies, relate the lift production directly linear to the angle of attack.

[2] It must be said that the nominal differences between the towing tank and the CFD results are still small numbers, in the order of $1.0N$.

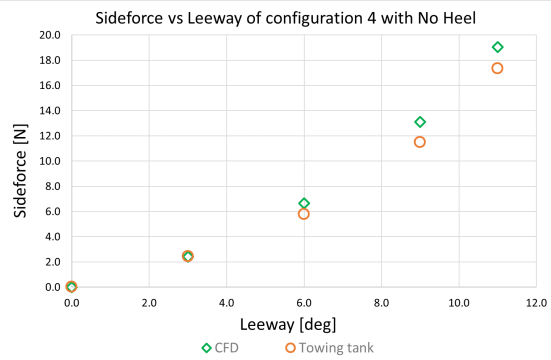

Figure 6.1: The sideforce versus leeway angle of configuration 4 according to the CFD simulations and the towing tank experiments.

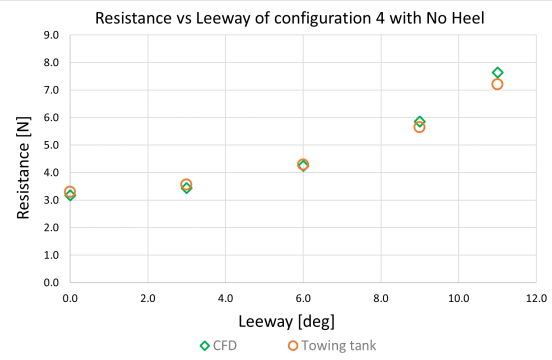

Figure 6.2: The resistance versus leeway angle of configuration 4 according to the CFD simulations and the towing tank experiments.

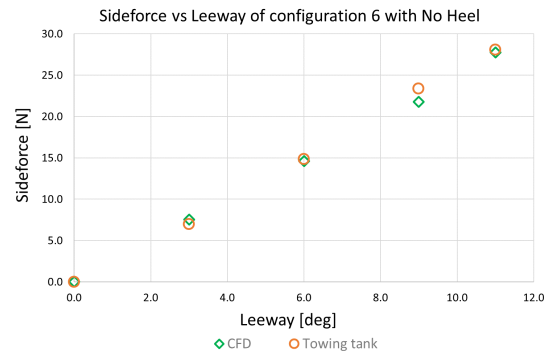

Figure 6.3: The sideforce versus leeway angle of configuration 6 according to the CFD simulations and the towing tank experiments.

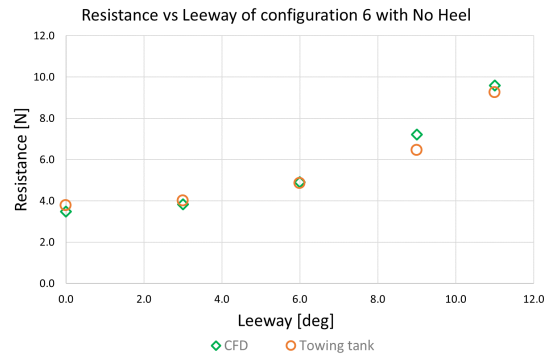

Figure 6.4: The resistance versus leeway angle of configuration 6 according to the CFD simulations and the towing tank experiments.

6.2. Uncertainty

The uncertainty of the obtained data is an important parameter which says something about how trustworthy the results of the experiments are. Verification of the towing tank experiments is usually done by doing multiple repetition runs and analysing the standard deviation. This will then lead to an uncertainty of measurement. In CFD, the largest contribution to the numerical uncertainty is the discretization error. Therefore, verifying the CFD results can be done with a grid refinement study. The same geometry will be tested in the same flow conditions, only the number of cells in the mesh will be different. The difference in the resulting data is then related to the mesh refinement, extrapolated to the theoretical exact solution.

To begin with, the uncertainty in the towing tank experiments was minimised as much as possible on before hand, by calibrating all testing equipment and carefully aligning the appendages on the model and the model in the tank. All (daily) procedures during the preparations for the towing tank experiments and during the experiments itself, can be found in the appended towing tank experiment report.

About 25% of all runs were repetition runs or symmetry runs. Repeating some runs more than once was done to check the standard deviation, to verify the results. Testing the model on the opposite heel and/or leeway angles was done to check the symmetry of the model and towing tank setup. The standard deviation is calculated through the following formula.

$$s = \sqrt{\frac{\sum_{i=1}^{N} \left(x_i - \overline{x}\right)}{N-1}} \tag{6.2.1}$$

For all configurations, the standard deviation of the repetition run(s) was on average only $0.02N$ regarding the resistance and $0.06N$ for the sideforce. The symmetry runs showed an average standard deviation of $0.19N$ for the resistance and $0.51N$ for the sideforce.

Even though it was a planned aspect of this research, it is decided not to do a grid refinement study, or another procedure to verify the CFD results. The results up to a leeway angle of 6 degrees are very similar for the towing tank experiments and the CFD simulations. The purpose of the CFD simulations was to check whether the results of the tank experiments showed strongly deviant results, and to visualise the flow around the yacht. Due to a shortage of time and a priority to focus on improving the performance prediction methods, no procedures to verify the CFD results have been conducted. Still, there is enough trust in the towing tank results, to use them for improving and developing the performance prediction methods.

6.3. Performance analysis

The results from the towing tank experiments have already been presented in terms of sideforce, resistance and yaw moment per degree leeway. However, for this research it is more interesting to know what the additional resistance is due to the generated sideforce (induced resistance). So in this section, the resistance versus the sideforce is examined, to get an impression on the effectiveness of the configurations. Additionally, the sideforce normalised to the leeway angle gives an impression of how effective each configuration is for increasing leeway angles. The latter approach is an ideal way to compare the sideforce of the centre boards to the theoretical lift curve slope $\frac{dC_L}{d\alpha}$

As discussed in section 2.4, the induced resistance scales with the sideforce squared, see equation 2.4.5. Plotting the resistance versus the sideforce squared should give a linear line like can be seen in figure 6.5 [13]. The flatter the line, the more effective the geometry is. The translation on the vertical axis is depended on the viscous resistance of the foil.

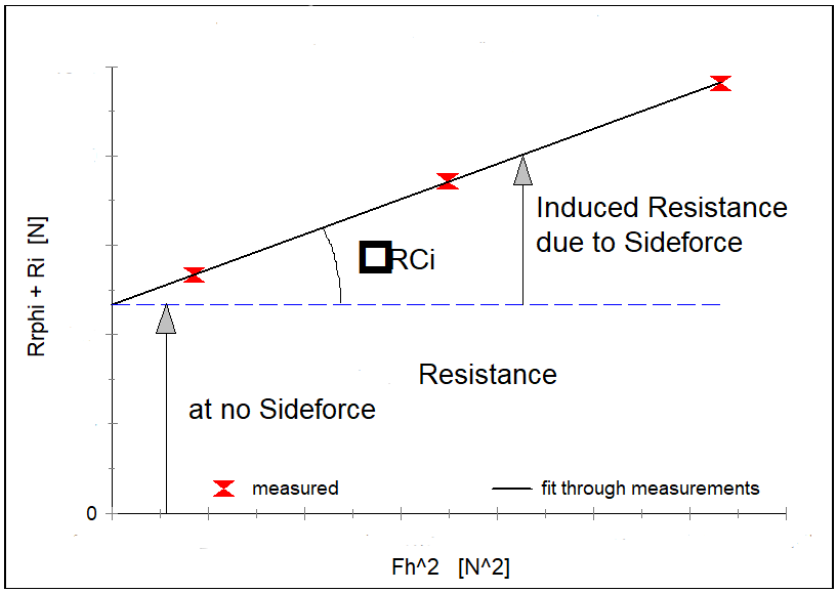

Figure 6.5: An overview of how the resistance scales with the sideforce squared.

An addition to this, is the expression of the effective span T_e of the configuration. This is another way to relate the resistance to the sideforce. The effective span is in agreement with the effective aspect ratio and is the equivalent total effective draft of the hull-keel-centre board combination [13]. The addition 'effective' originates from the fact that a reduction (or sometimes increment) of the geometrical span is found which is dependent on the free surface-, hull-, keel-centreboard interaction and endplate effects.

The effective span can be calculated using the following formula.

$$T_e = \sqrt{\frac{SF^2}{\pi R_i \frac{1}{2}\rho V_s^2}} \tag{6.3.1}$$

Or, to include the induced drag factor k_i:

$$T_e = \sqrt{k_i \frac{SF^2}{R_i \frac{1}{2}\rho V_s^2}} \tag{6.3.2}$$

Which can also be written as the following equation, using the slope of the induced resistance, see figure 6.5.

$$T_e = \sqrt{k_i \frac{1}{RC_i \frac{1}{2}\rho V_s^2}} \tag{6.3.3}$$

Equation 6.3.2 will be used in this research to calculate the effective span of the configurations or the centre boards. Plotting the effective span vs the leeway angle should give a horizontal line. The higher the effective span, the more effective the configuration is in terms of sideforce vs resistance. The effective span has been calculated for all nine configurations and is presented in the following three graphs. It can clearly be seen by the increasing trends of configurations 1, 2 and 3, that those configurations without a keel work more effective at bigger leeway angles than they do at lower leeway angles. This was previously noticed and discussed in section 4.4. Furthermore, it can be noticed that the effective span of the configurations with the high aspect ratio centre board (3, 6 and 9) start decreasing at bigger leeway angles. This could mean that the centre board starts stalling. This will further be examined by eliminating the centre boards from the configurations, which will be discussed in the next section. In the end, the performance prediction methods assume a linear trend between the sideforce and leeway angle, and a quadratic relationship between the induced resistance and the sideforce. Those two boundary conditions would result in a horizontal line of the effective span versus the leeway angle. Therefor, a horizontal trendline is placed through the data points that show this linear relationship. As already discussed in the introduction of this chapter, in the end only data up to a leeway angle of 6 degrees will be used for improving the performance prediction methods of the centre board contribution.

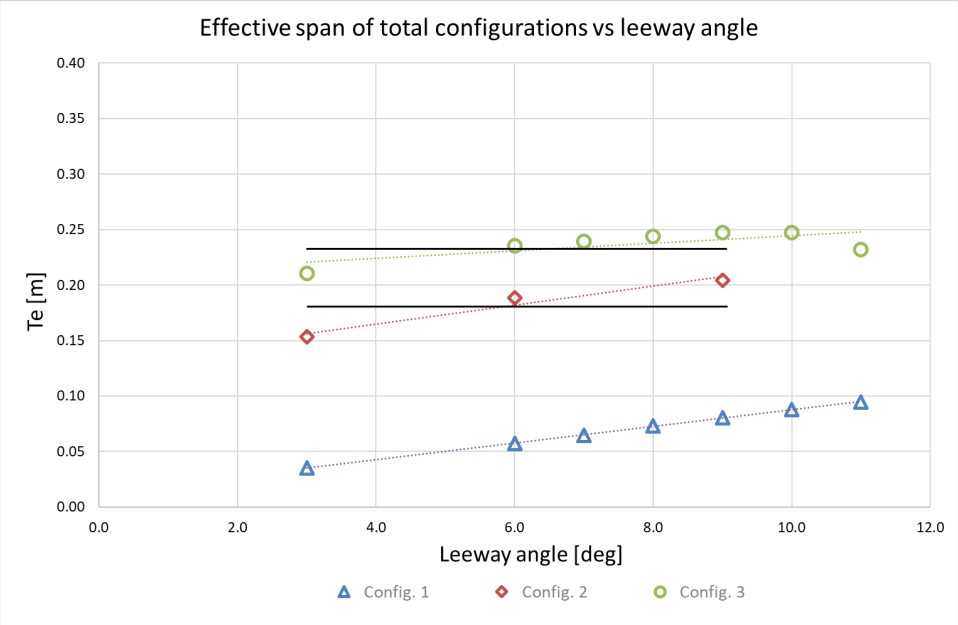

Figure 6.6: The effective span of configurations 1, 2 and 3, versus the leeway angle.

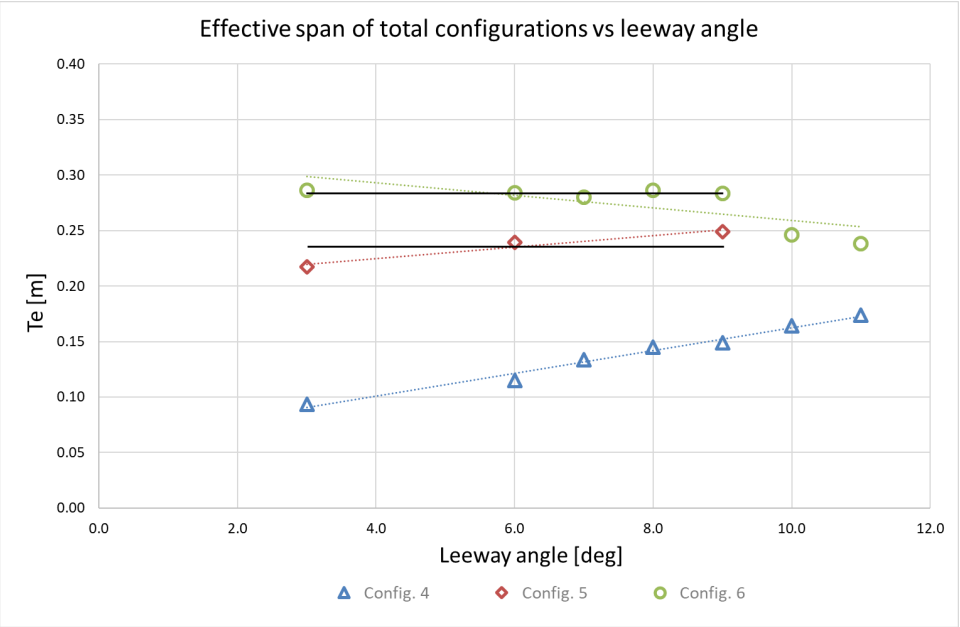

Figure 6.7: The effective span of configurations 4, 5 and 6, versus the leeway angle.

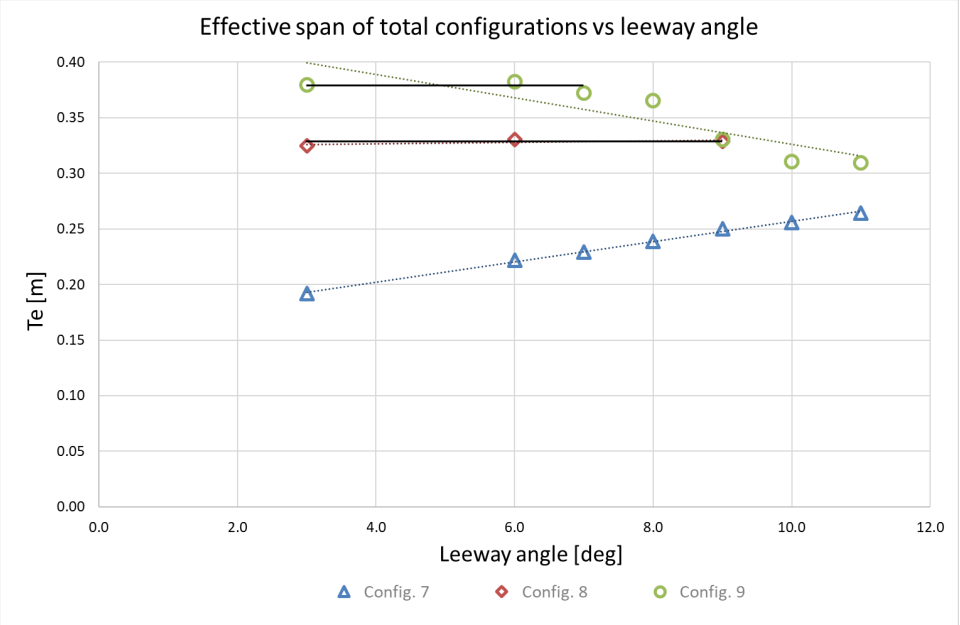

Figure 6.8: The effective span of configurations 7, 8 and 9, versus the leeway angle.

6.4. Eliminating CB1 and CB2

During the towing tank experiments, it seemed that the centre boards were (partly) stalling at a leeway angle of 9 degrees. This section will analyse this presumption. After all test runs, CB1 and CB2 could be eliminated from the configurations. By doing this, the exact behaviour of the centre board under a specific configuration can be examined. First, the lift and drag coefficients of the centre boards are plotted, according to the results of the towing tank experiments. After that, other parameters are plotted to examine the effectiveness of the centre boards.

6.4.1. Lift and drag coefficients

A common approach to examine the behaviour of a foil in a flow, is to determine the lift and drag coefficients versus the angle of attack, or leeway angle in this case. The coefficients for the experimental data are calculated using the following equations, previously discussed in section 1.2. These equations are filled in with the properties of the centre boards and the resulting data from the towing tank experiments. The results can be seen in figures 6.9 and 6.10 for CB1 and in figures 6.11 and 6.12 for CB2.

$$C_L = \frac{F_L}{0.5\rho U_0^2 A_{CB}} \tag{6.4.1}$$

$$C_D = \frac{F_D}{0.5\rho U_0^2 A_{CB}} \tag{6.4.2}$$

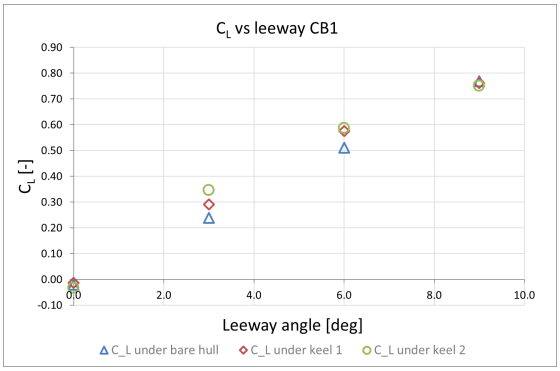

Figure 6.9: The lift coefficients of CB1 in configurations 2, 5 and 8, versus the leeway angle.

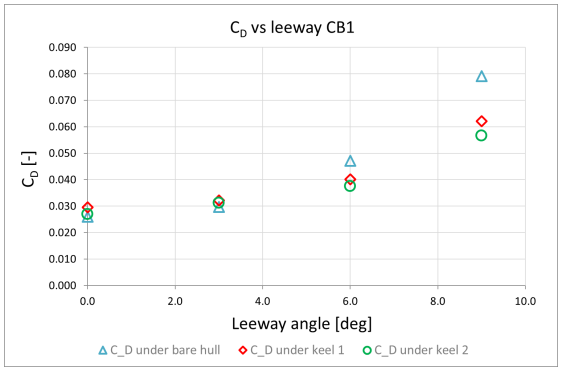

Figure 6.10: The resistance coefficients of CB1 in configurations 2, 5 and 8, versus the leeway angle.

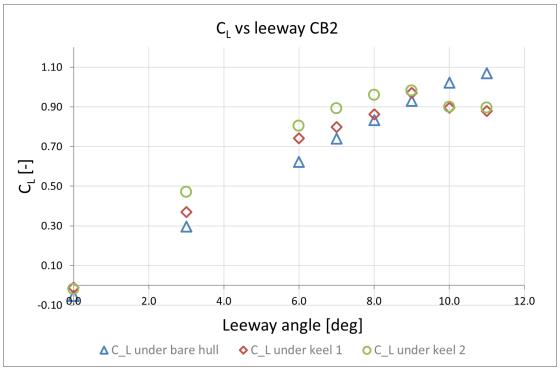

Figure 6.11: The lift coefficients of CB2 in configurations 3, 6 and 9, versus the leeway angle.

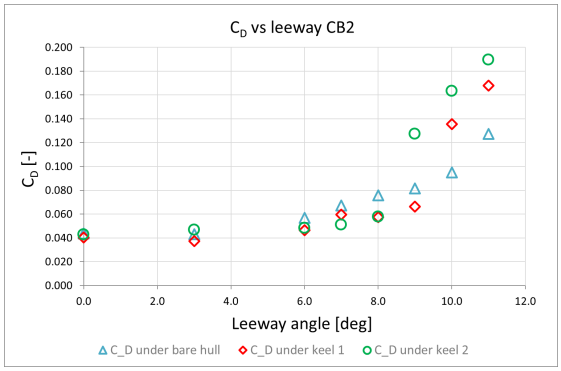

Figure 6.12: The resistance coefficients of CB2 in configurations 3, 6 and 9, versus the leeway angle.

6.4.2. lift curve slope

One way to examine how effective these centre boards are in terms of lift, is to check the lift per degree leeway, versus the leeway angle. Besides, this is a good way to compare the lift of the centre boards with the theoretical lift curve slope $\frac{dC_L}{d\alpha}$.

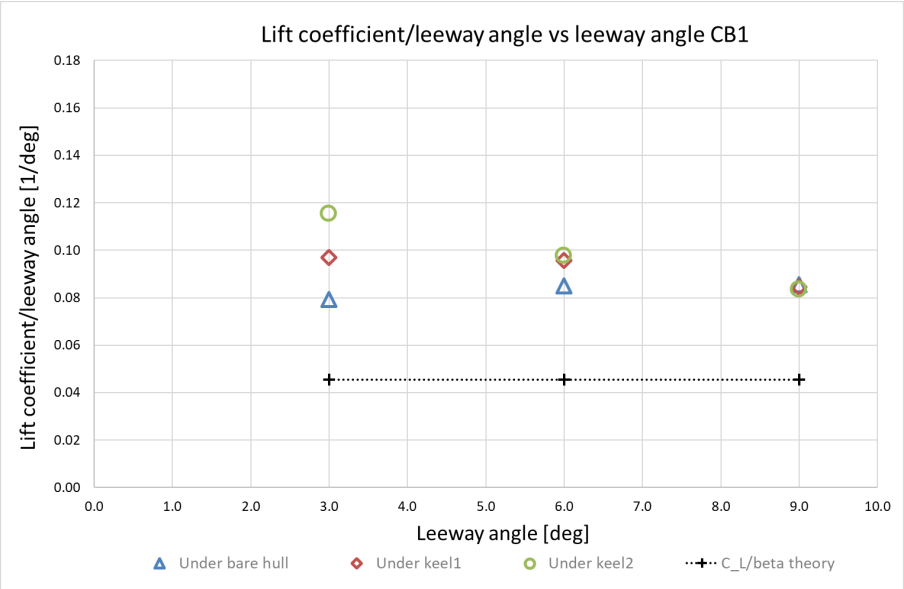

Figure 6.13: The lift coefficient per degree leeway of CB1, versus the leeway angle of the model.

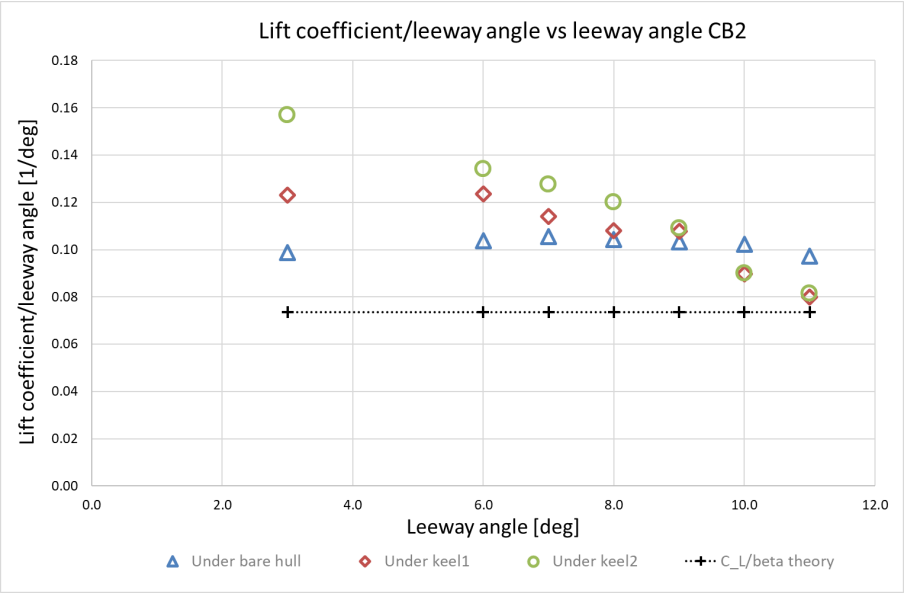

Figure 6.14: The lift coefficient per degree leeway of CB2, versus the leeway angle of the model.

The influence of the lift-carry-over can clearly be seen, as the lift generated by the centre boards is obviously much higher that the theoretical lift. The drag coefficients per degree leeway and the theoretical drag are not presented here. The induced drag largely depends on the lift coefficient, so a formulation for the theoretical lift including the lift-carry-over have to be found first, before a realistic theoretical approximation of the drag coefficient can be presented.

6.4.3. Resistance vs sideforce^2

It was previously discussed that the induced resistance scales with the sideforce squared. So, plotting this relationship should result in a straight line. Figures 6.15 and 6.16 show this relationship for the results of the towing tank tests for the centre boards eliminated from the rest of the configurations.

For the low-aspect centre board positioned under the bare hull, it can be seen that this does result in a straight line, which means that the centre board is at each leeway angle just as effective. Under keel1 and keel2 however, this is not the case. For a leeway angle of 9 degrees, the resulting points lay a little 'higher' in the graph than the proposed linear trend, set by the previous leeway angles of 0, 3 and 6 degrees. This is an indication that the centre board could be (partly) stalling at a leeway angle of 9 degrees.

When examining the high aspect ratio centre board in figure 6.16, it can be seen that the flow remains attached up to a leeway angle of 10 degrees for the bare hull configuration. When the centre board is positioned below keel 1 and keel 2, the flow remains attached up to 9 and 8 degrees leeway respectively.

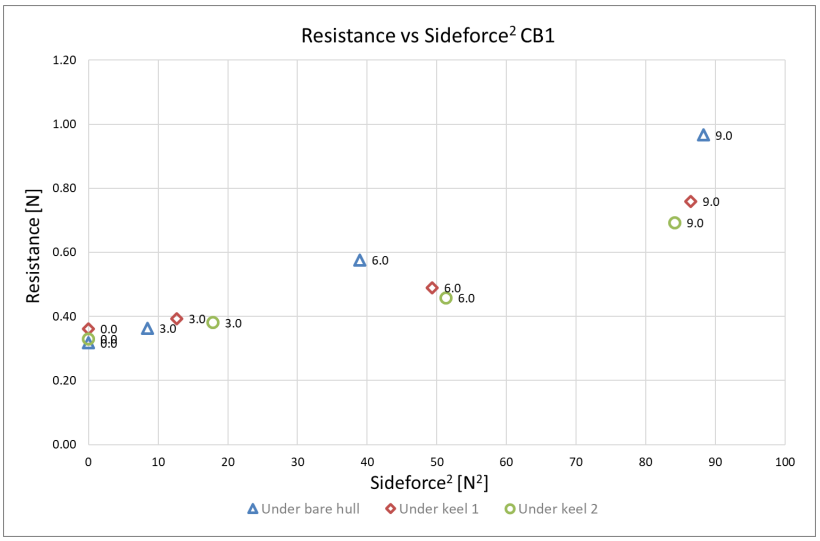

Figure 6.15: The resistance versus the sideforces squared, of CB1.

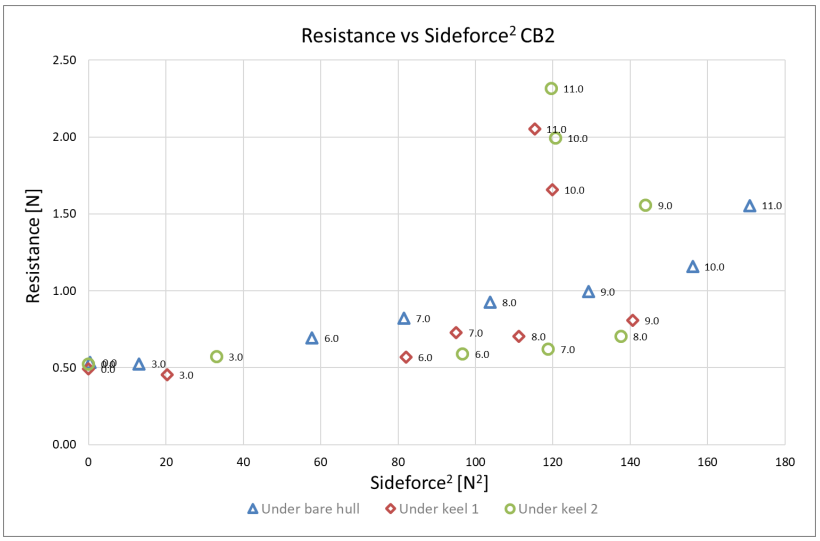

Figure 6.16: The resistance versus the sideforces squared, of CB2.

6.4.4. Conclusion

Looking at all previous graphs in section 6.4, a few clear conclusion can be drawn. First of all, the low aspect ratio centre board generates less sideforce than the high aspect ratio centre board, but also less resistance. Again, this is because the sideforce largely contributes to the induced resistance. Secondly, both centre boards generate more sideforce and less resistance when positioned below a keel, compared to the bare hull configurations. The configurations with the deepest keel show the most beneficial characteristics.

Another important aspect is the stalling behaviour of the centre boards. To begin with, CB2 starts stalling a little sooner than CB1. Besides that, the centre boards stall later when placed below the bare hull compared to the configurations with keel. The centre board below the deepest keel stalls the soonest, in terms of the leeway angle. Figures 6.15 and 6.16 clearly illustrate that up to the stalling angle, the centre boards work most effectively when positioned below a keel.

Finally, the lift coefficients of the centre boards are compared to the theoretical values. This shows a big discrepancy, which is not surprising. The fact that the centre boards below the Maltese Falcon model generate more sideforce than the theory prescribes, is due to the lift-carry-over. This is what Dykstra had found before, and this is what essentially led to this research.

However, in those findings, the theoretical drag coefficient was higher than the obtained values from the CFD simulations. Now, the theoretical drag of the centre boards is significantly lower than the drag coefficients following from the towing tank experiments. For leeway angles of 9 degrees and higher this is obvious since the centre boards are stalling. But also for smaller leeway angles, the centre boards have a drag coefficient almost twice as high as the theory prescribes. The extra sideforce due to the lift-carry-over contributes significantly to the induced resistance. But, also the setups without leeway (so with no induced resistance) result in a higher viscous resistance for the centre boards in the towing tank than the theoretical viscous resistance of the centre boards.

One possible explanation is that the turbulence strips haven't worked sufficiently and the flow around the centre board was still laminar[3]. The Reynolds number of the centre boards is calculated using the following formula, in which V_m is the velocity of the model, L is the average cord length of the centre boards and ν is the dynamic viscosity of water.

$$Re = \frac{V_m \cdot c_{av}}{\nu} \tag{6.4.3}$$

For CB1 and CB2 this results in Reynolds numbers of about 152,000 and 87,000 respectively. The ITTC '57 friction coefficients are 0.0074 and 0.0087 for CB1 and CB2. In figure 6.17, it can be seen that the centre boards for those Reynolds numbers and friction coefficients lie relatively close to the turbulent-laminar transition area. Nevertheless, after consultation of several experts at the TU Delft Hydromechanics laboratory, the assumption that the centre boards operate in a fully turbulent flow is held.

Another reason for why the viscous drag of the centre boards according to the towing tank experiments is higher than the theoretical form drag, could be that the roughness of the manufactured centre boards is relatively high. This hypothesis was also derived after the comparison of the CFD results to the results of the towing tank experiments. The viscous resistance of the centre boards measured in the towing tank experiments is also higher than according to the CFD results.

[3] In a laminar flow, the frictional resistance is higher than in a turbulent flow.

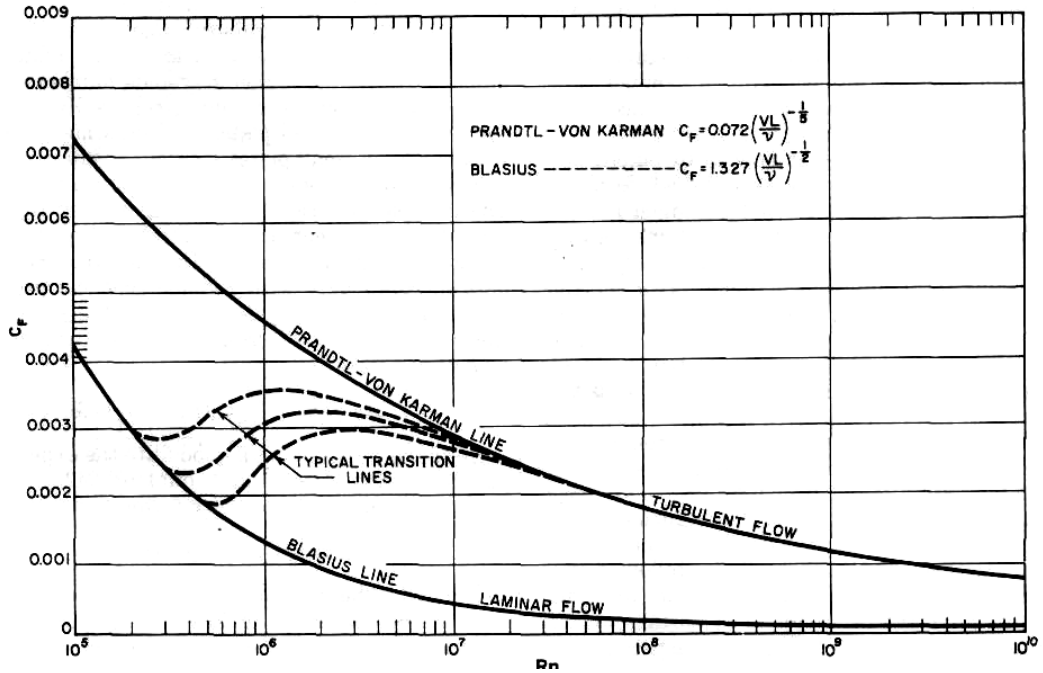

Figure 6.17: The Prandtl - Von Karman and Blasius friction lines for turbulent and laminar flow.

6.5. The influence of heel on the behaviour of the centre boards.

All configurations were tested upright and with 15 degrees heel. This was primarily done to examine the influence of heel on the lift production of the centre board and the lift-carry-over. As discussed in section 3.3.2, the model was fixed by the hexapod and the 6DOF frame, and could not trim and heave freely. When the model was heeled, it was rotated around the ship's x-axis at a vertical position on the waterline. This resulted in the model being in an unnatural trimmed position, relative to the upright position. This procedure caused the model to have a larger deplacement when heeled, compared to upright. So, obviously the resistance of the heeled model was higher than for the model tested upright. The difference in sideforce, resistance and yaw moment between the heeled and upright configurations would be irrelevant, and will therefore not be discussed in this report. However, the centre boards can be eliminated from the heeled configurations, which does provide relevant information.

For the centre boards eliminated from configurations with keel (5, 6, 8 and 9), the sideforce at leeway angles of 3 and 6 degrees was found to be on average 3.9% lower when heeled. The resistance of these centre boards was 11.6% higher with heel compared to upright, averaged over leeway angles 0, 3 and 6 degrees. For those configurations, this influence of heel on the centre boards is made visible by plotting the resistance versus the sideforce squared at leeway angles up to 9 degrees, for the eliminated centre boards, see figures 6.18 to 6.21. It can be seen in the graphs that the data points of the setups with heel lie slightly higher and more to the left, compared to the data points for the setups with no heel.

The setups with heel were not tested for leeway angles of 7, 8, 10 and 11 degrees, like the setups with upright condition. So, a conclusion about the stalling behaviour of the centre boards under heel is hard to draw. But for the other leeway angles up to 9 degrees, the centre boards show a very similar behaviour when heeled, compared to upright. This will later be reflected upon in section 7.1.1.

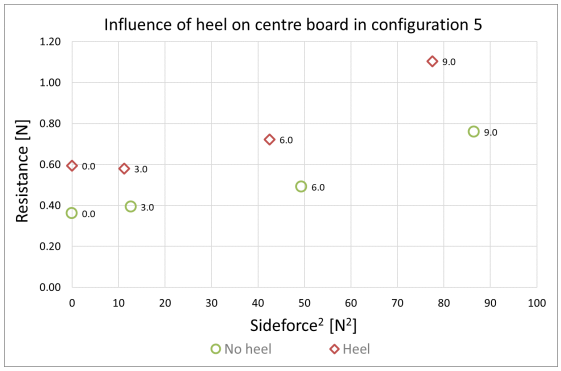

Figure 6.18: The resistance versus the sideforce squared for the centre board in configuration 5, in upright and heeled condition.

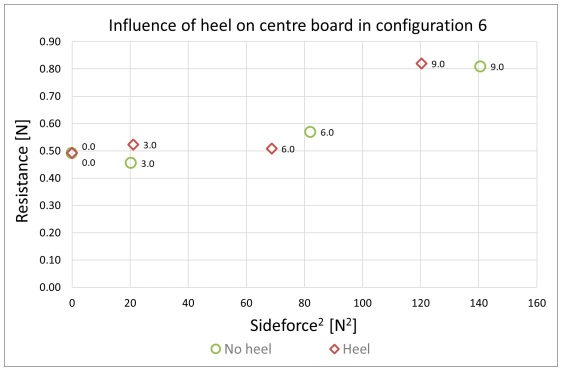

Figure 6.19: The resistance versus the sideforce squared for the centre board in configuration 6, in upright and heeled condition.

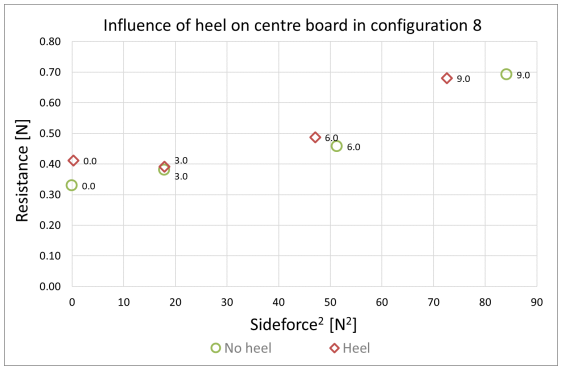

Figure 6.20: The resistance versus the sideforce squared for the centre board in configuration 8, in upright and heeled condition.

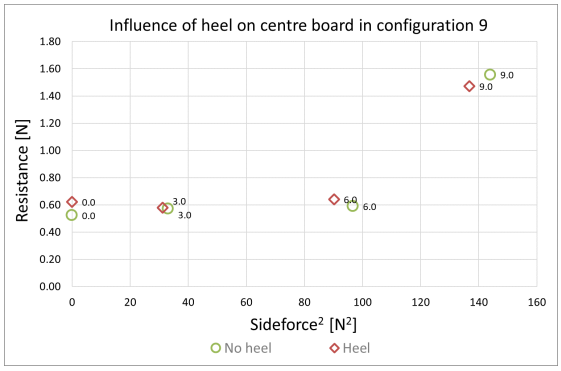

Figure 6.21: The resistance versus the sideforce squared for the centre board in configuration 9, in upright and heeled condition.

7

Improving the performance prediction

In the previous chapters, the results from the Maltese Falcon towing tank experiments and the CFD simulations have been discussed. The goal is now to use these results to improve the performance prediction for hull-keel-centre board configurations. First, the existing formulations to predict the lift-carry-over from keel to hull will be adjusted in an attempt to make these suitable for predicting the lift-carry-over from centre board to hull-keel. That will be the basis for developing new methods to predict the sideforce, resistance and centre of effort of the centre board contribution. Finally, when these methods have been developed, they will be tested on other yachts with a hull-keel-centre board configuration, to examine the trustworthiness.

Regarding the development of a new sideforce prediction equation, it is important to state that it is assumed that the centre boards behave as effective for every leeway angle until the stalling region, just as is done in existing prediction methods. For that reason, only the data for leeway angles of 3 and 6 degrees are used to fit the new prediction equation[1]. The new prediction equations for the resistance and the lateral centre of effort will also be fitted to the data points up to a leeway angle of 6 degrees. This means that for all parameters regarding the performance, a prediction method will be developed that is independent of the leeway angle.

7.1. lift-carry-over

The extra lift generation, induced by the hull-keel-centre board interaction effect, was earlier described as the lift-carry-over. All contributions to the lift-carry-over formulation have been described in section 2.8. To summarise (and repeat) the most important; these contributions together resulted in the following equation to approximate the sideforce of the keel. The effective velocity of the keel is considered equal to the sailing velocity of the yacht: $V_{ekeel} = V_S$. And, the effective angle of attack of the keel is the leeway angle of the yacht, corrected by the zero lift drift angle: $\alpha_{ekeel} = \beta - \beta_0$. On the left hand side of the equation, α is the angle of attack of the foil, which is defined as equal to the leeway angle β.

$$L_{keel} = \left(\frac{\mathrm{d}C_L}{\mathrm{d}\alpha}\right)_{(W\&F)} \alpha_{ekeel} \cdot \frac{1}{2}\rho V_{ekeel}^2 A_{latkeel} c_{hull} c_{heel} \tag{7.1.1}$$

This formulation can be reduced to the lift coefficient including the terms introduced by the lift-carry-over. This coefficient will be defined as the lift-lift-carry-over coefficient $C_{L_{lift\ carry\ over,\ keel}}$.

$$C_{L_{lift\ carry\ over,\ keel}} = C_{L_{(W\&F)}} c_{hull} c_{heel} \left(1 - \frac{\beta_0}{\beta}\right) \tag{7.1.2}$$

This theoretical lift-lift-carry-over coefficient will be compared to the lift coefficients obtained from the towing tank experiments. The last three coefficients in equation 7.1.2, will together be called the

[1] In case the data at these two points show significant discrepancies, the data point at a leeway angle of 3 degrees will be governing, since it is assumed that the centre board will be 100% effective in terms of sideforce and resistance at small leeway angles.

lift-carry-over factor $K_{lift\ carry\ over}$, which is the ratio between the measured (real) lift coefficient and the theoretical lift coefficient of the centre board. This can then be written as:

$$C_{L_{lift\ carry\ over}} = C_{L_{(W\&F)}} \cdot K_{lift\ carry\ over} \tag{7.1.3}$$

The lift-carry-over factor obtained from the towing tank results is defined as follows:

$$K_{lift\ carry\ over} = \frac{C_{L_{CB,\ towing\ tank}}}{C_{L_{CB,\ theory}}} \tag{7.1.4}$$

The main goal is now to use the obtained data from the towing tank experiments, to adjust this formulation in an attempt to make it applicable for predicting the lift-carry-carry-over factor of the centre board $K_{lift\ carry\ over,\ CB}$.

The lift carry over factor, obtained from the towing tank data is presented in figure 7.1, for all centre board configurations.

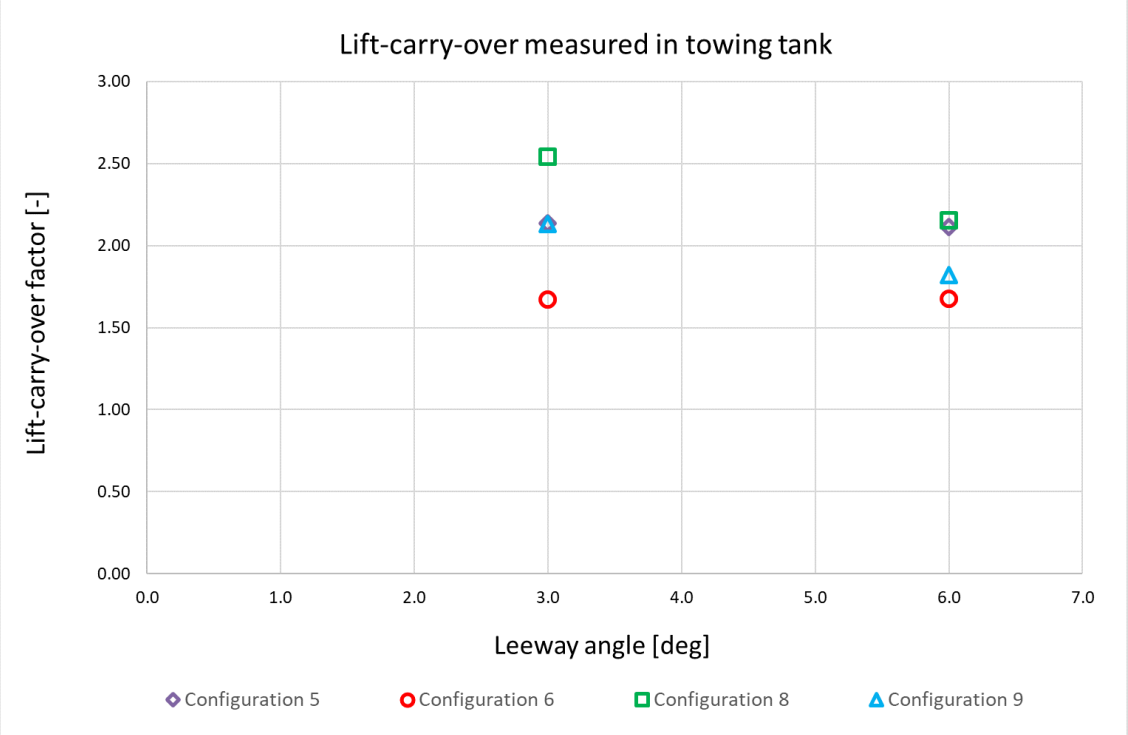

Figure 7.1: The lift-carry-over factor of the centre boards in configurations 5, 6, 8 and 9.

It can be seen that for configurations 5 and 6 the lift-carry-over of the centre boards is about the same at both leeway angles. However, for configuration 8 and 9, the lift-carry-over at a leeway angle of 3 degrees is bigger than at a leeway angle of 6 degrees. This is probably due to the fact that the centre boards below keel2 are more effective at lower leeway angles, which was already concluded in the previous chapter. As stated in the introduction of this chapter, the data point at a leeway angle of 3 degrees will be governing when fitting the prediction equation.

7.1.1. Influence of heel on the lift-carry-over

In chapter 6 it was stated that heeling the ship with 15 degrees resulted in a decrease in total sideforce production of only 1.9%. When discarding the bare hull configurations and only examining the configurations with keel-centre board configurations, the decrease in sideforce of the centre boards itself is 3.9%. The theoretical lift of the centre board decreased with $1 - cos(\phi) = 3.4\%$ due to heel. This already

implies that the lift-carry-over when heeled, is about the same as for the upright condition. Indeed, the lift-carry-over factor is only 0.3% lower if the ship is heeled, compared to upright. In figures 7.2 to 7.5 it can clearly be seen that the measured lift-carry-over for upright and heeled condition is in each configuration very similar.

This is not in line with the theoretical lift-carry-over, in which the coefficients introduced to account for heel, c_{heel} and β_0, give a reduction on the lift-carry-over of 10% and 2% respectively. So, following the test data, these coefficients could be discarded. And also physically, omitting these coefficients can be justified. The heeling coefficient c_{heel} was introduced by Keuning and Verwerft to account for the fact that the foils are brought closer to the free surface. However, in the keel-centre board configurations on the yachts that Dykstra are designing, the distance of the centre board to the free surface is in general relatively large. Regarding the Maltese Falcon, the centre of effort of the centre boards are about 5.5 and 7.5 meters down from the free surface for the keel1 and keel2 configurations respectively. So, the centre boards are far away from the free surface anyway. Secondly, the zero lift drift angle was introduced to account for the asymmetry of the hull when heeled. But, those large sailing yachts like the Maltese Falcon, have a higher length to beam ratio, resulting in a relatively symmetrical hull with regard to heel. This means that the shape of the submerged body does not differ much when the ship is heeled. Following the tank test data and these qualitative arguments, it is decided to omit both the heel coefficient c_{heel} and the zero lift drift angle β_0[2]. The final lift-carry-over factor thus consists only of the (modified) hull coefficient, both for upright and for heeled conditions.

7.1.2. Adjusting the hull influence coefficient

As already stated in section 2.8, the hull coefficient for hull-keel configurations is defined as can be seen in equation 7.1.5, with $a_0 = 1.80$

$$c_{hull} = a_0 \frac{T_c}{b_{keel}} + 1 \tag{7.1.5}$$

In regular hull-keel configurations, the canoe body draft T_c and the span of the keel b_{keel} are very straight forward parameters. But in the case of this research, there is a very long and shallow keel, in combination with a centre board. So, how must this formula be used for these hull-keel-centre board configurations? And can this formula be used at all for these configurations?

This formula was based on experimental data of conventional hull-keel configurations, in which the lift generated by the keel was carried over to the hull. So, configurations with a keel-centre board combination would fall outside the scope. Still, with a few minor assumptions, this formula could be used to give an approximation. Firstly, the lift generated by the centre board is carried over to the hull and keel, instead of the hull only. So, so the numerator in equation 7.1.5 is complemented by the span of the keel b_{keel}. Then secondly, the span of the centre board b_{CB} is used as the denominator in the formula of c_{hull}[3], instead of the span of the keel b_{keel}. In the end, the coefficient a_0 is set to 0.90, to fit the lift-carry-over prediction as close to the tank data as possible.

$$c_{hull} = 0.90 \frac{T_c + b_{keel}}{b_{CB}} + 1 \tag{7.1.6}$$

Finally, this gives the following new formula for the lift-carry-over factor, both for upright and for heeled conditions.

$$K_{lift\ carry\ over} = c_{hulll} = 0.90 \frac{T_c + b_{keel}}{b_{CB}} + 1 \tag{7.1.7}$$

The value of the coefficient a_0 was determined while fitting this formula to the 'real' lift-carry-over, found by the following ratio:

$$\frac{C_{L_{CB,\ towing\ tank}}}{C_{L_{CB,\ theory}}}$$

[2] In case of a ship with a relatively asymmetrical hull, the zero lift drift angle β_0 should be included in the lift-carry-over prediction for heeled conditions. But, this has not been verified or further examined.

[3] **Note:** Several other ways to implement the keel, centre board and even the hull, in this formula have been tried. After extensive analysis, it was found that implementing the span of the keel and the span of the centre board as described in this section, in the end fits best to the results from the towing tank experiments

How this new prediction method for the lift-carry-over factor corresponds to the real lift-carry-over from centre board to keel, can be seen in the following four graphs.

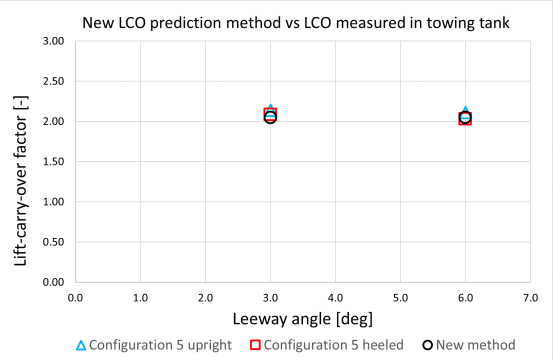

Figure 7.2: The new method to predict the lift-carry-over factor and the measured lift-carry-over factor in configuration 5, for leeway angles of 3 and 6 degrees.

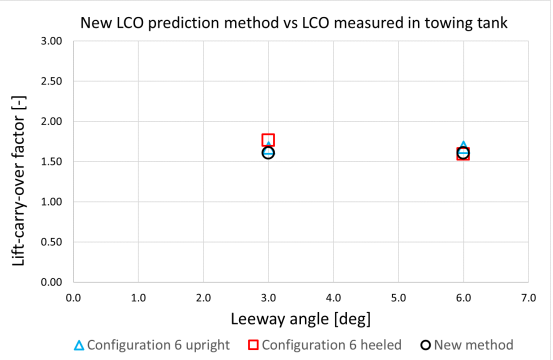

Figure 7.3: The new method to predict the lift-carry-over factor and the measured lift-carry-over factor in configuration 6, for leeway angles of 3 and 6 degrees.

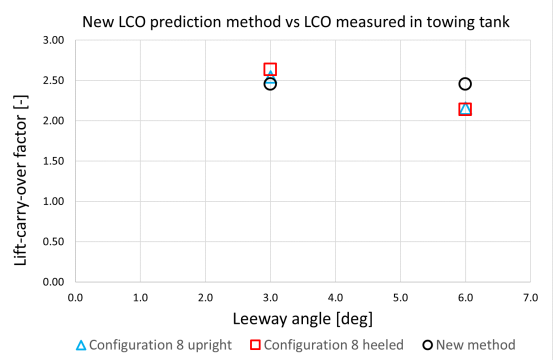

Figure 7.4: The new method to predict the lift-carry-over factor and the measured lift-carry-over factor in configuration 8, for leeway angles of 3 and 6 degrees.

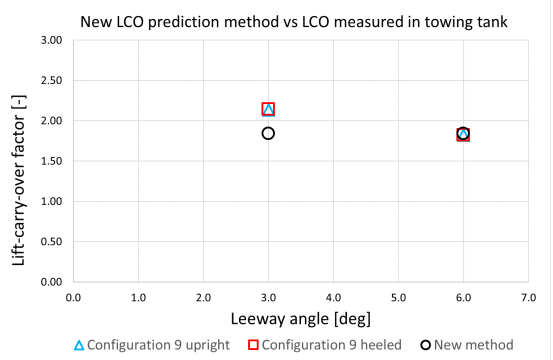

Figure 7.5: The new method to predict the lift-carry-over factor and the measured lift-carry-over factor in configuration 9, for leeway angles of 3 and 6 degrees.

7.2. Centre boards centre of effort

The yaw and roll moments of the sailing yacht are very important parameters regarding the performance. In order to superpose the centre board to a hull-keel configuration, it is more convenient to predict the centre of effort of the centre board, rather than these moment itself. The predicted sideforce of the centre board, together with the predicted centre of effort, can then be used to calculate contribution of the centre board to the moments of the yacht, orientated in the ship's axis system. The centre of effort (CoE) is also referred to as centre of pressure.

In section 2.3, it was discussed that the longitudinal centre of pressure (X_{cp}) of a conventional keel is assumed to be at the 25% chord line. Regarding the vertical centre of pressure (Z_{cp}), two methods by Gerritsma have been discussed in section 2.3, relating the vertical location of the CoE to the draft and the effective draft respectively. These methods will now be assessed, by a comparison to the data resulting from the towing tank experiments. Hypothetically, the magnitude of the lift-carry-over has an influence on the vertical centre board CoE.

The centre of effort of the centre boards according to the towing tank experiments can easily be calculated, using equations 7.2.1 and 7.2.2. The moments and forces substituted in these equations are from the eliminated centre boards.

$$X_{cp} = \frac{M_Z}{F_Y} \tag{7.2.1}$$

$$Z_{cp} = \frac{M_Z}{F_Y} \tag{7.2.2}$$

The data resulting from the towing tank experiments, show that the longitudinal position of the centre board CoE varies a little for different leeway angles. This is not surprising given the fact that the flow around the hull changes for varying leeway angles. Moreover, the relative contribution of the Munk moment to the total yaw moment, changes with increasing leeway angles. This is because the contribution of the sideforce generated by the keel and centre board to the total yaw moment increases significantly, while the Munk moment remains similar. So, at bigger leeway angles, the contribution of the appendages to the yaw moment is more dominant than the contribution of the Munk moment.

The scatter in the data makes it difficult to justify a reliable assessment for the longitudinal CoE position. But, when taking the mean of the values at 3 and 6 degrees leeway, a relationship to make a rough estimation can be established. It is found that the longitudinal position lies in front of the centre board top leading edge. From the towing tank data, it was found that this distance depends both on the chord length of the centre board and the lift-carry-over factor. How much this distance is, can be calculated using the following formula:

$$X_{cp} = 0.125 \cdot C_{r,\,CB} \cdot K_{lift\ carry\ over} \qquad \text{Measured from the top leading edge forwards} \tag{7.2.3}$$

The vertical centre of effort, seemed independent of the leeway angle. For each Maltese Falcon configuration, the Z_{cp} resulted in the same values for all leeway angles. The next step is to find out whether the relationships presented by Gerritsma (discribed in section 2.3) hold. The first method is straight forward, being 43% of the total draft.

$$Z_{cp} = 0.43 \cdot T_{max} \qquad \text{Measured from the waterline downwards} \tag{7.2.4}$$

For the second method, the effective draft must be calculated for each configuration. Just as is done in calculating the hull coefficient c_{hull} in section 7.1.2, the canoe body draft is taken as the draft including the keel(s), so the equation becomes like the following:

$$T_{eff} = T_{max}\sqrt{1 - \frac{0.62(T_c + b_{keel})}{T_{max}}} \qquad \text{Measured from the CB tip upwards} \tag{7.2.5}$$

Then, the results of both methods are examined and compared to the Z_{cp} resulting from the towing tank experiments. The first method, being independent of the lift-carry-over, resulted in a position of Z_{cp} being very close to 43% of the total draft, for all configurations.

The second method seemed not to have a direct relationship with the calculated effective draft. But, further assessment showed that including the lift-carry-over, does result in a reasonable approximation of the vertical CoE. For all keel-centre board configurations, the distance from the tip of the centre board to the Z_{cp} of the centre board was close to 50% of the effective draft multiplied by the lift-carry-over:

$$Z_{cp} = 0.50 \cdot T_{eff} \cdot K_{lift\ carry\ over} \qquad \text{Measured from the CB tip upwards} \tag{7.2.6}$$

However, the first method of Gerritsma showed a little more accurate prediction than the second method. Moreover, after validation of both methods on two other yachts with a keel-hull-centre board configuration, the first method showed significantly better results than the method based on the effective draft. This validation procedure will be discussed in section 7.4.

Again, it is important to note that equation 7.2.3 only gives a rough approximation of the longitudinal CoE position, averaged for all leeway angles up to the stalling point. Nonetheless, when the obtained approximated values for X_{cp} and Z_{cp} are plotted next to the obtained data from the towing tank experiments, it can be seen that the approximations are fairly accurate. For each configuration, the measured CoE of the centre boards are plotted both for leeway angles of 3 and 6 degrees, to show the difference between the two leeway angles. The yellow markers indicates these CoE obtained from the towing tank

data, while the yellow dot represents the approximated position of the CoE of the centre boards using equations 7.2.3 7.2.4, see figures 7.6 to 7.9.

Since the estimation for the Z_{cp} is more accurate than the estimation for X_{cp}, the contribution of the centre board to the roll moment can be calculated with more accuracy than the contribution to the yaw moment.

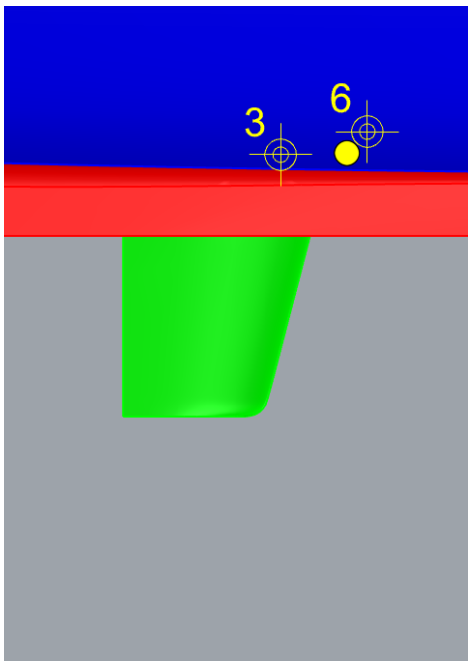

Figure 7.6: The measured CoE at 3 and 6 degrees leeway and the predicted CoE of the centre board in configuration 5.

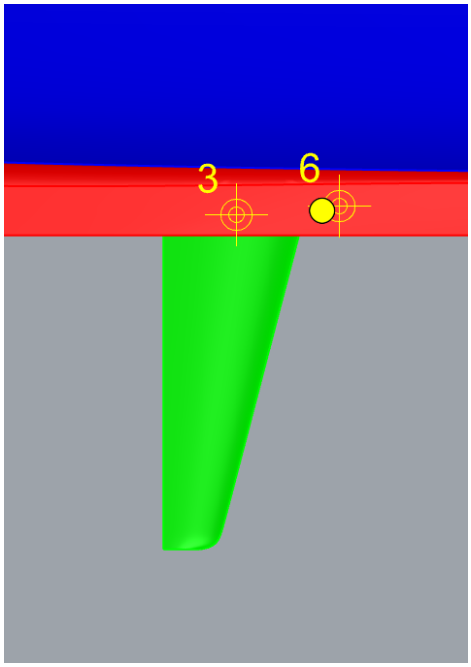

Figure 7.7: The measured CoE at 3 and 6 degrees leeway and the predicted CoE of the centre board in configuration 6.

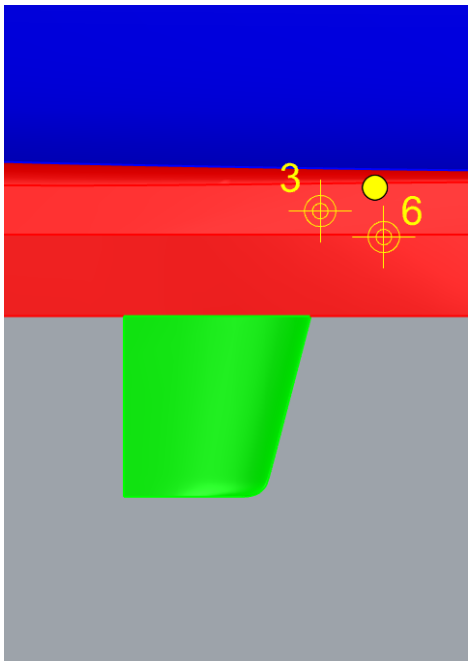

Figure 7.8: The measured CoE at 3 and 6 degrees leeway and the predicted CoE of the centre board in configuration 8.

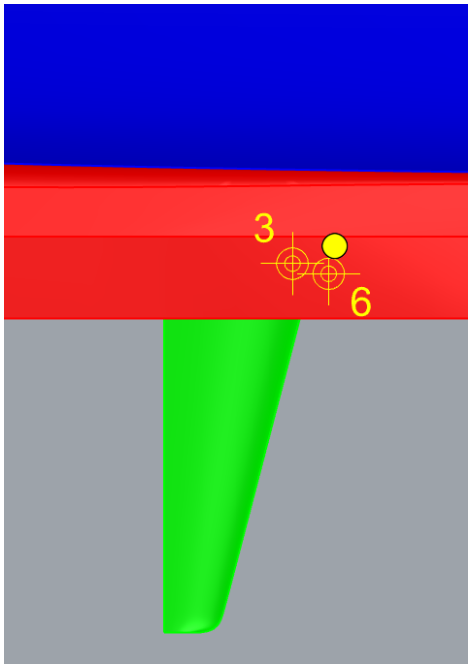

Figure 7.9: The measured CoE at 3 and 6 degrees leeway and the predicted CoE of the centre board in configuration 9.

7.3. Resistance

The resistance calculation for a centre board in a hull-keel-centre board configuration does not differ much from how it was first described in section 2.4, to calculate the theoretical drag coefficient for a foil in general. The viscous drag and fin tip drag of the centre board are calculated just as described in section 2.4. Only now, the hypothesis is that an increased lift coefficient of the centre board should be used to calculated the induced resistance, to account for the lift-carry-over. Following this hypothesis, the induced drag coefficient is calculated as follows, with the induced drag factor taken as 0,34:

$$C_{Di} = k_i \frac{C^2_{L_{lift\ carry\ over}}}{AR_e} \tag{7.3.1}$$

When the formula for the total drag coefficient (see equation 2.4.7, in section 2.4) is filled in with this new induced resistance formulation, the following results are obtained for the centre boards in configurations 5, 6, 8 and 9. The drag coefficients resulting from the towing tank experiments are plotted in the same graphs, just as the theoretical drag coefficients *excluding* the lift-carry-over. The blue triangles represent the total drag coefficient calculated from the towing tank data. The green diamonds and black circles show the estimated drag coefficients, excluding and including the lift-carry-over respectively.

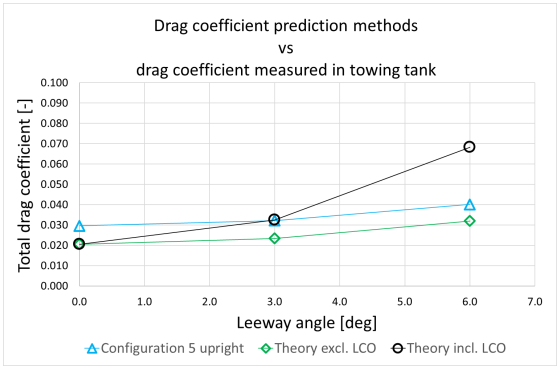

Figure 7.10: The measured and theoretical drag coefficients of the centre board in configuration 5

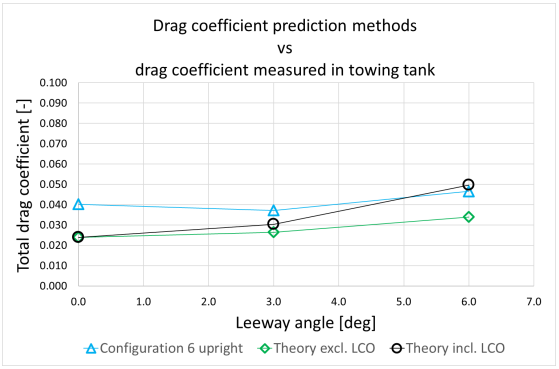

Figure 7.11: The measured and theoretical drag coefficients of the centre board in configuration 6

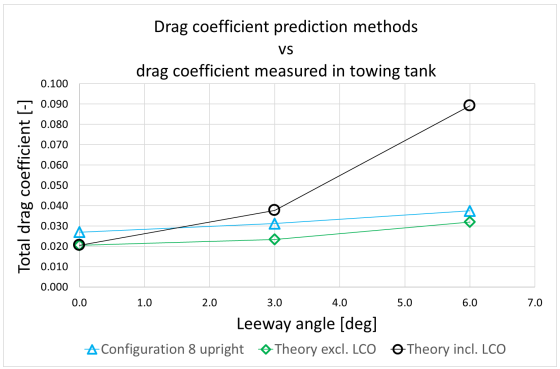

Figure 7.12: The measured and theoretical drag coefficients of the centre board in configuration 8

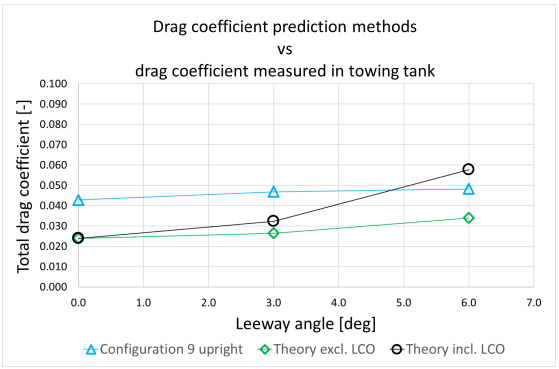

Figure 7.13: The measured and theoretical drag coefficients of the centre board in configuration 9

First of all, it can clearly be seen that the resistance is largely overestimated when the lift-carry-over is included in the calculation of the induced resistance. Apart from the vertical translation in the graph, due to the difference in viscous drag, the induced drag is actually quite accurately predicted when using the theoretical lift from Wicker & Fehlner *excluding* the lift-carry-over. All in all, the hypothesis to use an increased lift coefficient in the calculation of the induced resistance is found to be incorrect. This shows that the lift-carry-over phenomenon not only causes a positive effect regarding the sideforce production, but also regarding the induced resistance.

Secondly, the theoretical viscous drag of the centre boards is lower than the drag which was measured in the towing tank. This can be seen by the vertical translation at 0 degrees leeway, where the induced drag is by definition zero and the total drag thus only consists of viscous drag. The CFD simulations also resulted in a lower viscous drag than the measurements in the towing tank do. One reason for this could be that the roughness of the centre boards in the towing tank is relatively high, compared to the roughness assumed in theory and in the CFD program.

The calculation of the viscous drag will not be adjusted, since it is assumed that the centre boards in the towing tank setups cause a higher viscous drag than would normally be the case. More importantly, the viscous drag is not considered a focus point in this research.

To give some background information on this phenomenon; publications by Binkhorst have previously described the existence of a residuary resistance component [1]. This resistance component is calculated by subtracting the theoretical total resistance from the total measured resistance. The results of the towing tank experiments in relation to the theoretical drag confirm the presence of such a resistance component. Binkhorst also states that there is a relationship between the residuary resistance and distance of the vertical center of buoyancy of the keel to the free surface. A larger distance yields a higher residual resistance. This can be seen in the results of the towing tank experiments as well, where the residual resistance of CB2 is higher than that of CB1. Regarding the residual resistance of the centre boards, the following equations hold.

$$R_{res} = R_{measured} - C_{Dtot,theory} \cdot 0.5 \rho V_m^2 A_{lat\ CB} \tag{7.3.2}$$

Or,

$$C_{Dres} = C_{Dtot,measured} - C_{Dtot,theory} \tag{7.3.3}$$

7.4. Validation of the improved prediction methods

At this stage, formulations have been derived based on the Maltese Falcon experiment results to predict the sideforce, resistance and centre of effort of the centre board in a hull-keel-centre board configuration. Now, it is important to validate these prediction methods, by testing them on other yachts with a hull-keel-centre board configuration, to check if the derived methods also hold for other yachts. YACHT1 and Adela, both designed by Dykstra, have such configurations and have previously been tested by doing CFD simulations. The sideforce, resistance and centre of effort of the centre board according to the new/improved prediction methods will now be compared to the results from the CFD simulations of both yachts.

7.4.1. Lift-carry-over

The sideforce (lift-carry-over) prediction will be assessed first. For both YACHT1 and the Adela, the predicted lift coefficients are plotted in one graph with the lift coefficients according to the CFD results, see figures 7.14 and 7.15. It can be seen that the lift (and thus the lift-carry-over factor) is quite well predicted, especially for the small leeway angles.

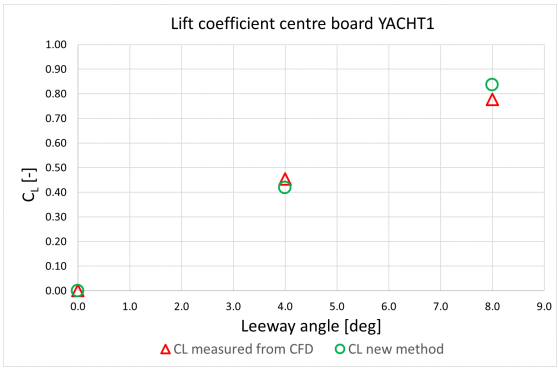

Figure 7.14: The lift coefficient versus the leeway angle of the centre board below YACHT1 measured from CFD, and according to the new prediction method.

Figure 7.15: The lift coefficient versus the leeway angle of the centre board below Adela measured from CFD, and according to the new prediction method.

7.4.2. Centre of effort

The CoE of both yachts according to the CFD simulations is displayed, together with the CoE of the hull according to CFD, superposed with the centre board CoE obtained from the prediction equation, see figure 7.16 and 7.17. During the design phase, this is the way the centre board is added to the configuration to obtain a first estimate of the forces and moments contributed by the centre board. Most favourable dimensions of the centre board and its position relative to the hull and keel will be estimated using the performance prediction methods, before doing CFD simulations of the complete configuration. The CoEs are plotted only for 3 degrees leeway. The yellow marker gives the location of the CoE measured in CFD, and the white dot represents the estimated location. The CoE for 6 degrees lies very close and would only make the representation unclear. It can be seen that adding the centre board estimation to the CFD data of the hull, gives a pretty accurate location for the total centre of effort.

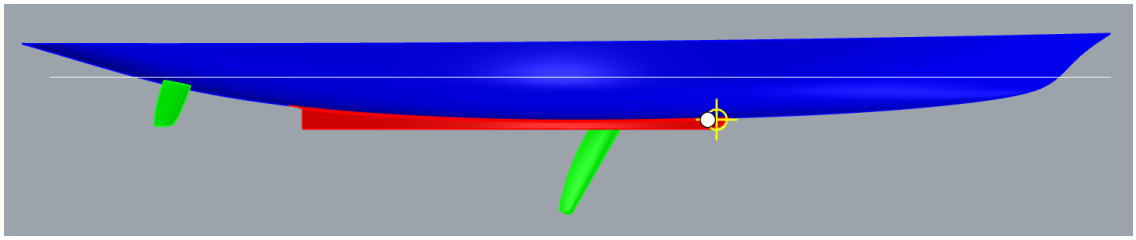

Figure 7.16: The centre of effort of YACHT1

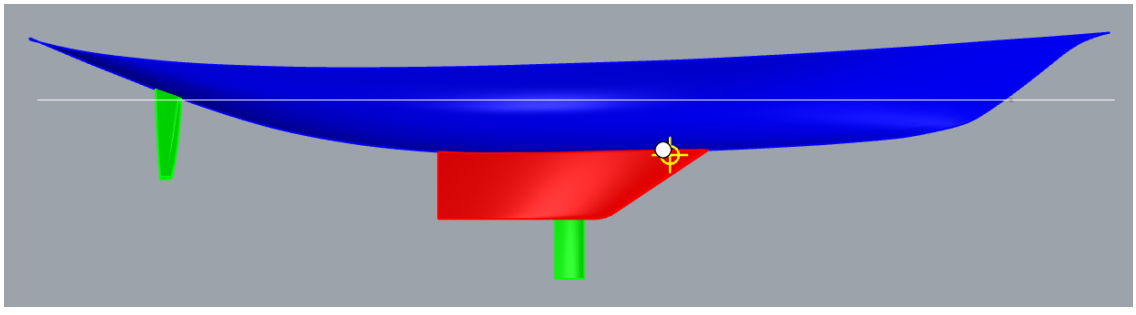

Figure 7.17: The centre of effort of Adela

7.4.3. Resistance

The resistance seemed more difficult to predict. From the Maltese Falcon experiment results, the latest hypothesis was introduced saying the lift coefficient *without* the lift-carry-over should be used for calculating the induced resistance coefficient, as described in the previous section. This method was tried for calculating the drag coefficients of the YACHT1 and Adela centre boards as well. It can be seen in figure 7.18 that the resistance is (still) largely overestimated when compared to the measured drag coefficient. However, for the Adela centre board it can be seen in figure 7.19 that the measured resistance is much higher than the predicted resistance. So, these two yachts give opposites results regarding the measured drag and the predicted drag.

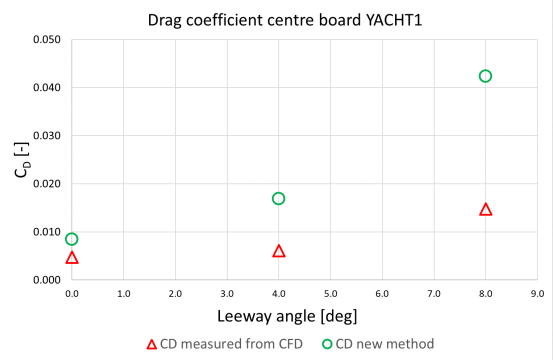

Figure 7.18: The drag coefficient versus the leeway angle of the centre board below YACHT1 measured from CFD, and according to the new prediction method.

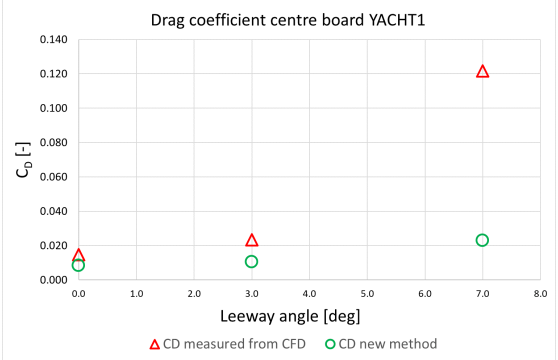

Figure 7.19: The drag coefficient versus the leeway angle of the centre board below Adela measured from CFD, and according to the new prediction method.

How come the measured drag of YACHT 1 is so low and the measured drag of Adela is so high? First, it must be repeated that the measured drag of the centre board is obtained by subtracting the data of the configuration without centre board from the configuration with centre board. By doing this, the total contribution of the centre board to the total yacht is obtained. So for example, if the centre board is reducing the circulation in the flow (as was described in section 5.5), being beneficial for the total resistance, this is reflected on the centre board drag coefficients.

Note: This approach could therefore be misleading, since it is the *contribution* of the centre board that is being measured and estimated. The exact forces on the centre board itself are not determined. But, it is important to keep in mind the required ability of superposing the centre board to the data of the hull. It is the purpose of this research to be able to add the estimated contribution of the centre board to the data of the hull acquired from CFD simulations of towing tank experiments.

Another reason why the resistance is difficult to predict, is because of the large contribution of the induced resistance, being proportional to the lift force squared (see equation 7.3.1). So, small deviations in the values of the lift coefficients, results in larger effects on the (induced) resistance.

Still, the resistance of the Adela centre board at 7 degrees leeway is considered to be very high. Therefore, the flow around the centre board is visualised to see if the flow could be stalling. Just as was described in sections 2.11 and 5.5, the shear in x-direction is plotted to visualise potential stalling, see figure 7.20. When the shear in x-direction is positive, it means the flow is detaching from the centre board and locally flowing in the positive x-direction.

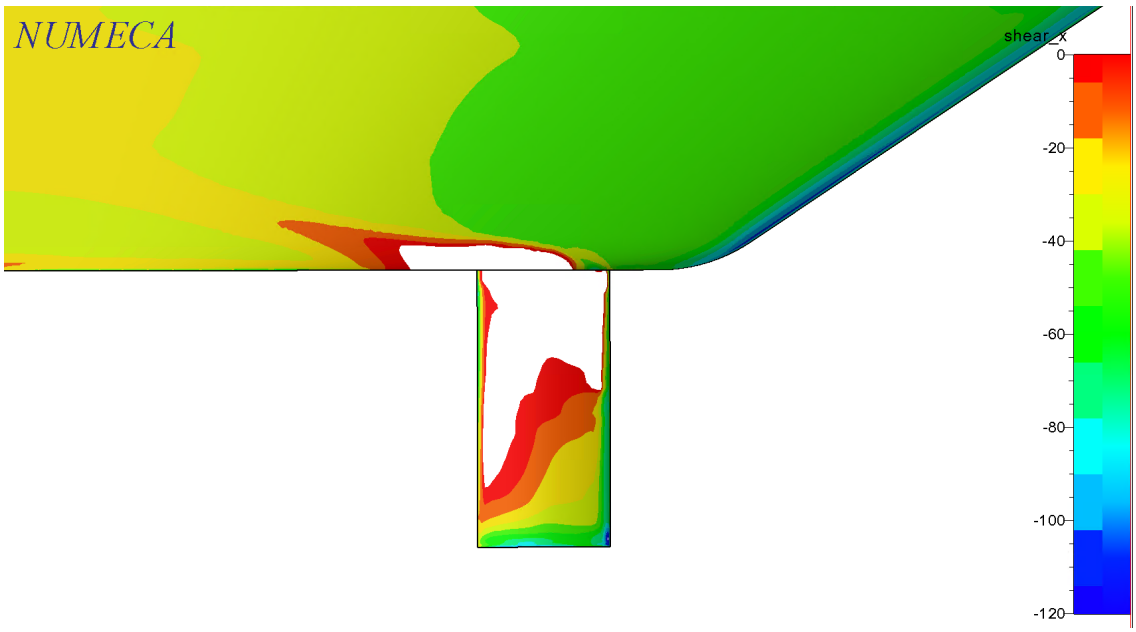

Figure 7.20: The shear in x-direction, clearly showing the centre board is stalling.

Indeed, the centre board below Adela is clearly stalling at a leeway angle of 7 degrees, increasing the drag significantly. The position so close to the tip leading edge of the keel has a big influence on the flow around the centre board. Besides the fact that the centre board is stalling, the keel-centre board configuration of the Adela is very unconventional. For those two reasons, the results of Adela at 7 degrees leeway are discarded for this validation procedure.

After examining the results of YACHT1 and Adela, it is still considered best to exclude the lift-carry-over in the lift coefficient when calculating the induced resistance.

8

Conclusions and recommendations

This chapter concludes the thesis report. The results of the experiments are summarised and discussed. What follows is a reflection on the hypothesis in chapter 2 and the research questions in chapter 3. Then, final conclusions are drawn regarding the improvement of performance prediction methods for hull-keel-centre board configurations. Lastly, recommendations are made on how Dykstra could implement this in their method of performance prediction, and how future research can contribute to acquiring more knowledge on this subject.

This project originated from a finding at Dykstra Naval Architects during the design phase of a large motor-sailor. The predicted performance of the centre board was not in line with the performance according to the CFD simulations. The centre board generated significantly more sideforce than was expected from theoretical estimations. This phenomenon is known as the lift-carry-over. Determining the influence of the lift-carry-over on the sideforce, resistance and centre of effort of the centre board, to be able to improve the performance prediction of yachts with a hull-keel-centre board configuration was the goal of this research.

8.1. The experiments

The towing tank experiments, conducted in the Delft Hydromechanics Laboratory, resulted in good results, with clear distinctions between the nine different configurations. The results are analysed by plotting several different parameters, both for the complete configurations and for the centre boards eliminated from the hull-keel. The lift and drag coefficients, lift-curve slope, effective span and resistance versus sideforce squared all give good insight in the behaviour of the configurations and the influence of the keels and centre boards. Already during the towing tank experiments, it seemed like the centre boards were (partly) stalling at a leeway angle of 9 degrees. For that reason, it was decided to test all configurations without centre board and all configurations with CB2 at additional leeway angles of 7, 8, 10 and 11 degrees. By doing this, the complete stalling region of the eliminated CB2 was obtained. It is important to know when the centre boards are stalling, since the data points at leeway angles at which the centre boards are stalling must not be included in the regression analysis. This is introduced by a boundary condition, implying that the performance is to be predicted independent of the leeway angles, meaning that the centre boards are assumed to work as effective at every leeway angle in terms of sideforce and resistance. The stalling region is not taken into account when predicting the performance of the centre board.

It is noticed that the configurations with no keel remain longer effective at bigger leeway angles than the configurations with keel1 and keel2 do, in terms of sideforce and resistance. When eliminating the centre boards from the configurations, the behaviour at each configuration can clearly be seen. The centre boards generate significantly more sideforce when placed below keel2 than when placed below the bare hull. However, they will also start stalling sooner, in terms of the leeway angle. For improving

the performance prediction methods, it is decided to only use the data from leeway angles up to 6 degrees.

In general, the presence of the lift-carry-over from centre board to keel-hull is clear. The results from the Maltese Falcon towing tank experiments suggest the centre board generates about a factor 2 more lift when placed below a hull-keel configuration than the theory by Wicker & Felner would describe. Before the data from the towing tank is used to improve the performance prediction, CFD simulations were done to validate the results. Using *FINE Marine - NUMECA*, configurations 4 and 6 were tested with CFD. The results from the CFD simulations corresponded really well to the results from the towing tank experiments. For leeway angles up to 9 degrees, the average resistance in the towing tank is 3.1% higher and the average sideforce is 3.6% lower than in the CFD simulations. Only at the stalling region, some discrepancies occurred. This may be caused by not correctly simulating the roughness of the centre board and the detachment of the flow. However, this hypothesis was not verified by for instance doing a grid refinement study or by simulating with a different turbulence model, for two main reasons. First, the data from the stalling region is discarded during the development/improvement of the performance prediction methods. Secondly, the purpose of the CFD simulations was to check whether the results of the tank experiments showed strongly deviant results, and to visualise the flow around the yacht. In the end, only the data from the towing tank experiments were used to improve and develop the performance prediction methods. If the goal was to use the data resulting from the CFD simulations, then a grid refinement study or other verification procedure would have been conducted. After validation by the CFD simulations, the results from the Maltese Falcon towing tank experiments were used to improve existing performance prediction methods, or to develop new ones.

The visualisations of the flow around the yachts proved to be a very valuable contribution to this research. The lift-carry-over from centre board to the keel and the hull could very clearly be seen by plotting the hydrodynamic pressure on the underwater body of the yacht. Also the stalling behaviour of the centre boards was visualised very clearly, by plotting the shear in x-direction. Detachment of the flow would locally result in a positive value. Perhaps most interesting, was visualising the circulation of the flow around the underwater bodies. The influence of the centre board is very clear. The overall circulation was reduced and translated downwards, from the tip of the keel to the tip of the centre board. Less circulation means that less energy is dissipated in the flow, and the foils are working more effective in terms of sideforce and resistance.

8.2. New performance prediction methods

Methods to include the lift-carry-over in conventional configurations with a hull and fin keel exist. The latest paper on this subject is written by Keuning and Verwerft in 2009 [14]. The formulas to predict this lift-carry-over were based on data from the DSYHS. But, the yachts that are being designed by Dykstra, lay to such an extend outside those systematic series, that these equations for the lift-carry-over can not be used. Besides, instead of the lift-carry-over from keel to hull, this research is meant to find the lift carried over from centre board to keel-hull. Nonetheless, these existing methods are used as a starting point. The data obtained from the Maltese Falcon towing tank experiments are used to tweak these existing methods, making them suitable for the centre board performance prediction.

Sideforce

Results from the towing tank experiments showed that heeling the yacht by 15 degrees had no influence on the lift-carry-over. When discarding the coefficients accounting for heel, only the hull coefficient remained. This coefficient was changed by adding the span of the keel in the numerator of the equation and setting the coefficient a_0 to 0.90. The equation for the lift-carry-over factor then becomes like the following:

$$K_{lift\ carry\ over} = c_{hull} = 0.90\frac{T_c + b_{keel}}{b_{CB}} + 1$$

So, the lift coefficient of the centre board can be predicted by the following equation:

$$C_{L_{lift\ carry\ over}} = C_{L_{W\&F}} \cdot K_{lift\ carry\ over}$$

With,

$$\frac{dC_L}{d\alpha} = \frac{a_0 AR_e}{\cos\Lambda\sqrt{\frac{AR_e^2}{\cos^4\Lambda} + 4 + \frac{57{,}3a_0}{\pi}}} \qquad \text{With} \qquad a_0 = 0.9\,\frac{2\pi}{57.3}$$

Centre of effort

To superpose the yaw moment and roll moment contributed by the centre board, it is important to know the centre of effort of the generated sideforce. The centre of effort of the centre board contribution was obtained by dividing the added roll and yaw moments by the added sideforce. The results showed that the CoE of the centre board contribution lies slightly in front and above the centre board itself. This underlines that the centre board can not be added one on one to the keel-hull, but that the interaction effect must be taken into account. Several methods have been developed and fitted to the data resulting from the towing tank experiments. The measured longitudinal CoE has significant scatter for different leeway angles. Nonetheless, a method has been established which estimates the average CoE, for leeway angles up to the stalling region of the centre board. It was found that both the chord length of the centre board and the lift-carry-over had an influence on the longitudinal CoE. Regarding the centre board's vertical CoE, Gerritsma's extended keel method resulted in an accurate prediction.

$X_{cp} = 0.125 \cdot C_{r,\,CB} \cdot K_{lift\ carry\ over}$ Measured from the centre board top leading edge forwards

$Z_{cp} = 0.43 \cdot T_{max}$ Measured from the waterline downwards

Resistance

The hypothesis that the induced resistance of the centre board would be much higher due to the increased lift was found to be incorrect. According to the resulting data from the Maltese Falcon towing tank experiments, the resistance was actually best predicted by simply using the lift coefficient *without* the lift-carry-over in the equation of the induced resistance. So, the following formula is used to predict the total resistance coefficient of the centre board, without taking into account the lift-carry-over phenomenon. The factor '2' in front of the viscous drag and the added fin tip drag is because these components scale with the wetted area, which is roughly twice the lateral area with which the other coefficients scale. All components have been discussed in more detail in section 2.4.

$$C_{Dtot} = 2 \cdot C_{D0} + 2 \cdot C_{Dv,\,fintip} + C_{Di}$$

With,

$$C_{D0} = C_F\left(1 + k_{Hoerner}\right) \qquad \text{With,} \quad C_F = \frac{0.075}{(Log_{10}Re - 2)^2} \quad \text{and} \quad k_{Hoerner} = 2 \cdot \left(\frac{t}{c}\right) + 60 \cdot \left(\frac{t}{c}\right)^4$$

$$C_{Dv,fintip} = 0.01875 \cdot \left(\frac{t}{c}\right)^2_{tip}$$

$$C_{Di} = k_i \frac{C^2_{L_{(W\&F)}}}{AR_e}$$

This method has been compared to the Maltese Falcon data of the upright conditions. As stated in section 1.2, heeling the Maltese Falcon model, only caused the resistance to increase with 3.9%, on average for leeway angles of 0, 3 and 6 degrees. So, also for heeled conditions, this formula could be used to estimate total resistance coefficient of the centre board.

8.3. Validation of the new performance prediction methods

At this point, new methods have been developed to make fairly accurate estimates of the contributions of several centre boards to the different Maltese Falcon configurations. Although these methods hold for all Maltese Falcon configurations, they must be validated on other yachts with a hull-keel-centre board configuration. YACHT1 and Adela are yachts which have been designed by Dykstra, and which were used to validate the newly developed prediction methods. Both YACHT1 and Adela have previously been tested by CFD simulations, with and without centre board. The data of the eliminated centre board is compared to the data predicted by the new methods. YACHT1 and Adela have very different hull-keel-centre board configurations, which gave the possibility to identify how several aspects of the prediction methods influence the estimated performance. It was good to see that for the centre boards of both yachts, the predicted performance corresponded quite well to the measured performance. Especially the lift-carry-over factor was predicted very accurately, even though this factor was for the Adela centre board almost twice as high as for the YACHT1 centre board.

The resistance showed significantly more deviations. Just as in the Maltese Falcon case, the resistance of the YACHT1 and Adela centre boards are hard to predict. This is because the centre board influences the flow around the yacht so significantly, having a big influence on the resistance. For YACHT1, the measured resistance was about half the predicted resistance. Even with the lift-carry-over excluded from the induced resistance calculation. On the other hand, the centre board of the Adela added much more resistance to the hull-keel configuration than was predicted. But, closer examination by visualising the CFD results, showed that this was due to the position below the keel. The tip vortices shedded by the keel caused the centre board to work less effective. At a leeway angle of 7 degrees it was already largely stalling, see figure 7.20.

8.4. Reflection on the research questions

All research questions have been answered in this thesis. These research questions helped to shape the structure of the research and this report. All questions will be repeated, followed by a reflection on whether they are properly answered.

1. How is the performance of vessels with a hull-keel-centre board configuration currently predicted at Dykstra, and how accurate is this prediction?

2. According to literature, what could be the theoretical explanation for the lift-carry-over in hull-keel-centre board configurations?

3. Are there other methods to predict the lift (sideforce) and drag of the appendages, and are these appropriate for the type of yachts that Dykstra is designing?

4. How can towing tank experiments and CFD simulations give more insight in the behaviour of the hull-keel-centre board configuration, and the contribution of the centre board in particular?

5. Can the resulting data be formulated in trustworthy trends and formulations, to be implemented in the Dykstra performance prediction tool?

The first question is already answered in chapter 1, while chapter 2 answers questions two and three. The methodology of the towing tank experiments and CFD simulations, discussed in chapter 3, forms the basis of the fourth research question. The chapters 4, 5 and 6, on the towing tank experiments, CFD simulations and the result analysis respectively, conclude the answer of that research question. Then finally, chapter 7 is focused on deriving new performance prediction methods for the centre board contribution, based on the resulting data from the Maltese Falcon towing tank experiments. The validation of these new prediction formulations on other yachts with a hull-keel-centre board configuration, is discussed in the last section of that chapter.

8.5. Recommendations

In the end, the goal of this research was to develop a performance prediction method for the centre board contribution, which could be used at Dykstra Naval Architects. All derived formulas for the side-force (lift-carry-over), resistance and centre of effort of the centre board contribution could easily be implemented in the performance prediction sheet, currently used at Dykstra. As discussed in the introduction of this thesis, towing tank experiments or CFD simulations of the hull with keel are conducted first, before the centre board is superposed to this hull-keel configuration. Then, a CFD simulation of the complete configuration is done to verify the centre board estimation and obtain more accurate data. So, each of those design cycles is another validation of the performance prediction equations derived in this research. The coefficients can be tweaked to make the prediction equations fit as best as possible to the CFD data.

As for future research, it would be interesting to further examine the influence of the keel on the flow around the centre board. From the CFD simulations on the Adela, it could be seen that the configuration with the centre board near the leading edge of the keel caused the centre board to act in a very disturbed flow, stalling significantly at 7 degrees leeway. This can simply be done by doing CFD simulations of only a 'box keel' with a centre board, varying the keel and centre board dimensions and the centre board location. This would be an accessible way to develop a systematic keel-centre board series.

Another aspect which requires further research is the estimation of the longitudinal centre of effort of the centre board. The resulting data from the Maltese Falcon towing tank experiments showed that this X_{cp} varied for different leeway angles. Being able to estimate the yaw moment is very important in designing a sailing yacht. So, being able to derive a more accurate estimation of the X_{cp}, with perhaps a non-linear relation to the leeway angle, would be very interesting.

A

CFD observations YACHT1.

A.1. Hydrodynamic pressure YACHT1

It can be seen that the the centre board causes the shallow keel to generate lift directly above the centre board.

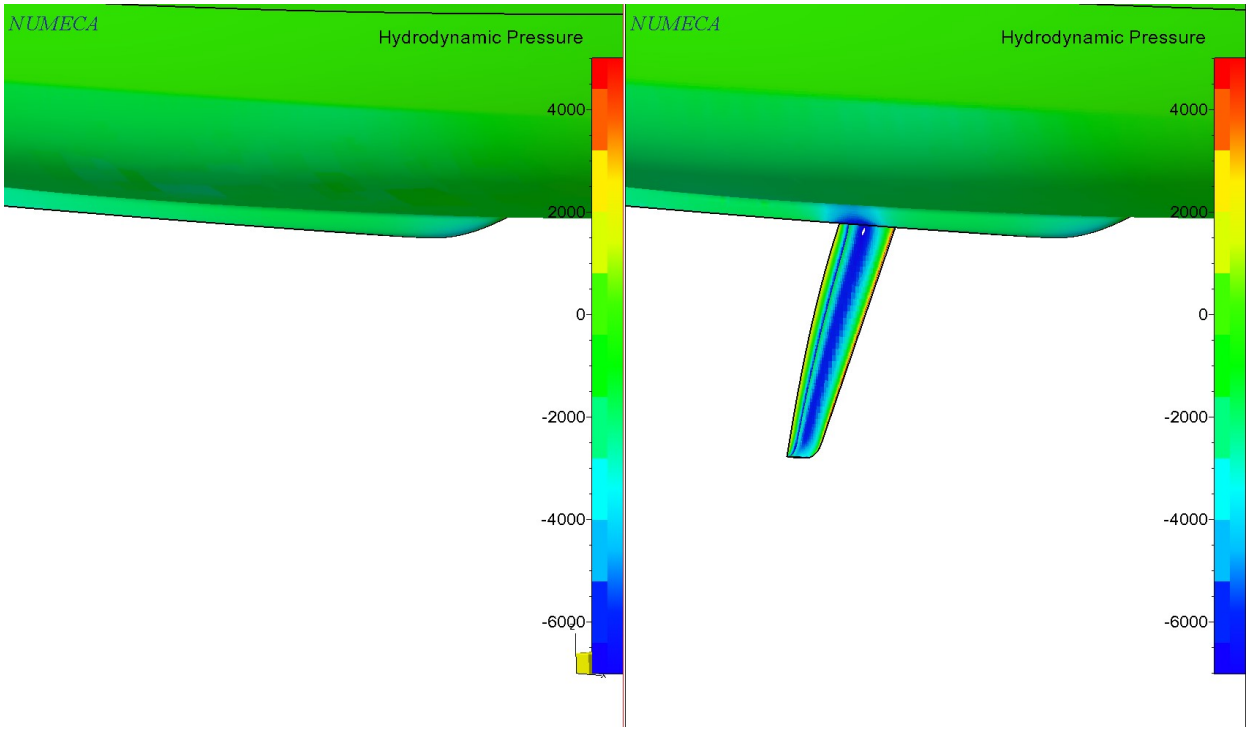

Figure A.1: The suction side of the yacht when sailing 12 knots with a leeway angle of 12 degrees.

A.2. Shear in x-direction

The shear in x-direction on the surface of YACHT1. The positive x-direction is in the sailing direction of the vessel.

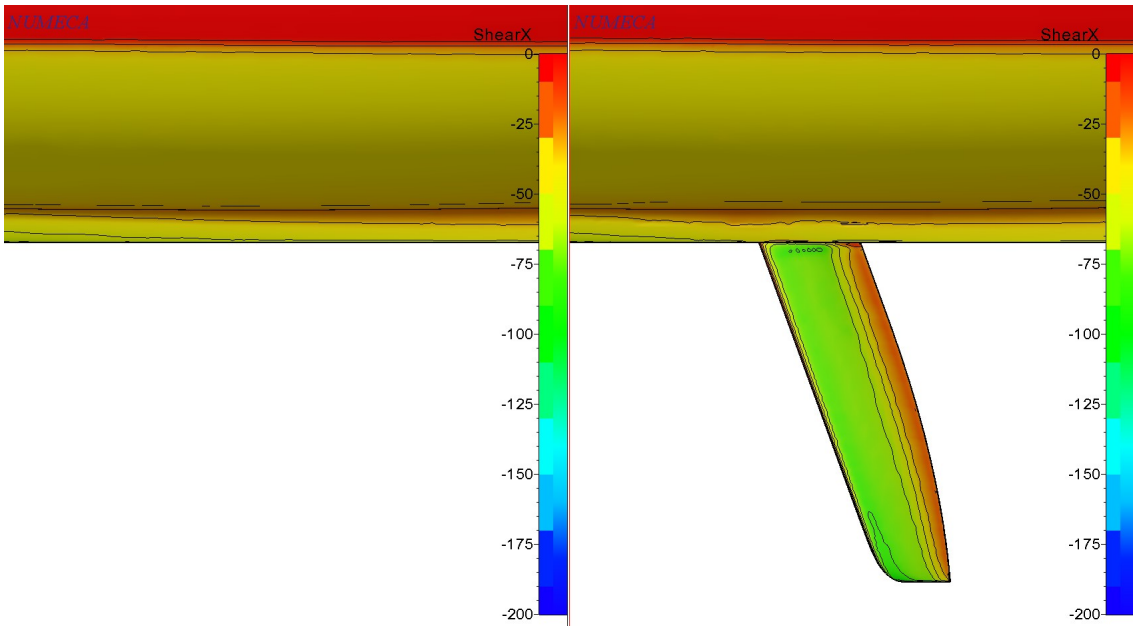

Figure A.2: The pressure side of the yacht when sailing 12 knots with a leeway angle of 4 degrees.

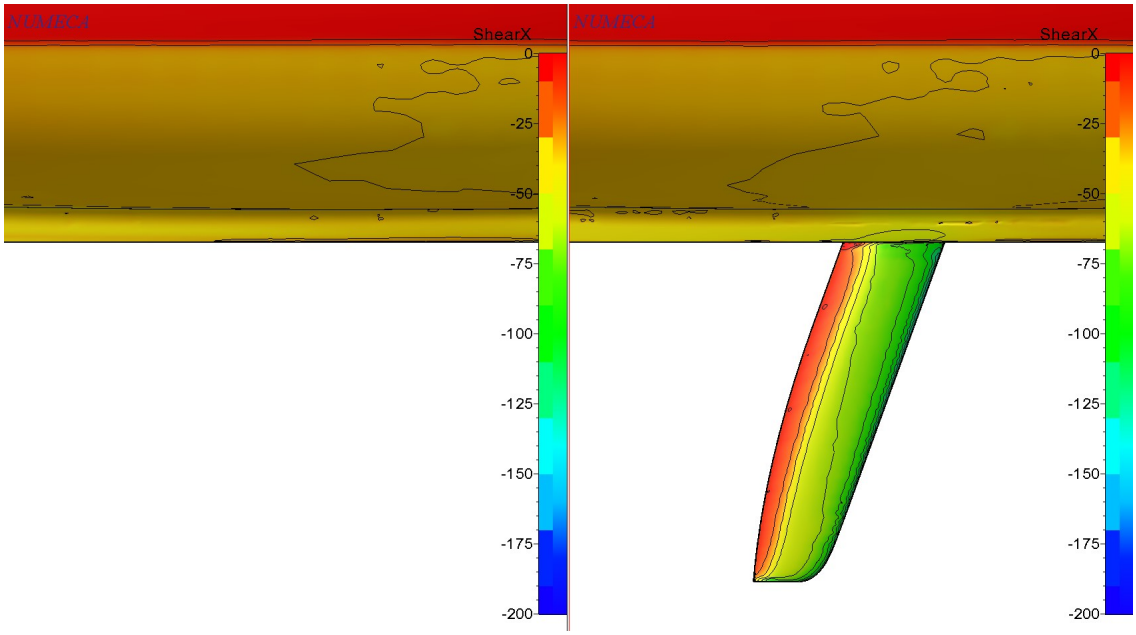

Figure A.3: The suction side of the yacht when sailing 12 knots with a leeway angle of 4 degrees.

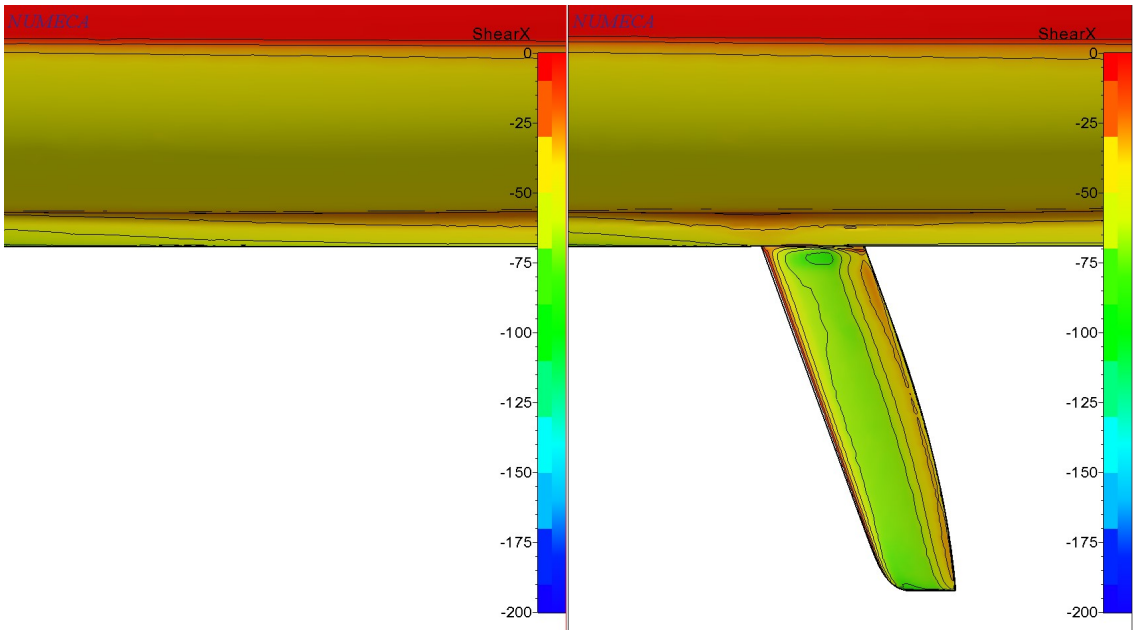

Figure A.4: The pressure side of the yacht when sailing 12 knots with a leeway angle of 8 degrees.

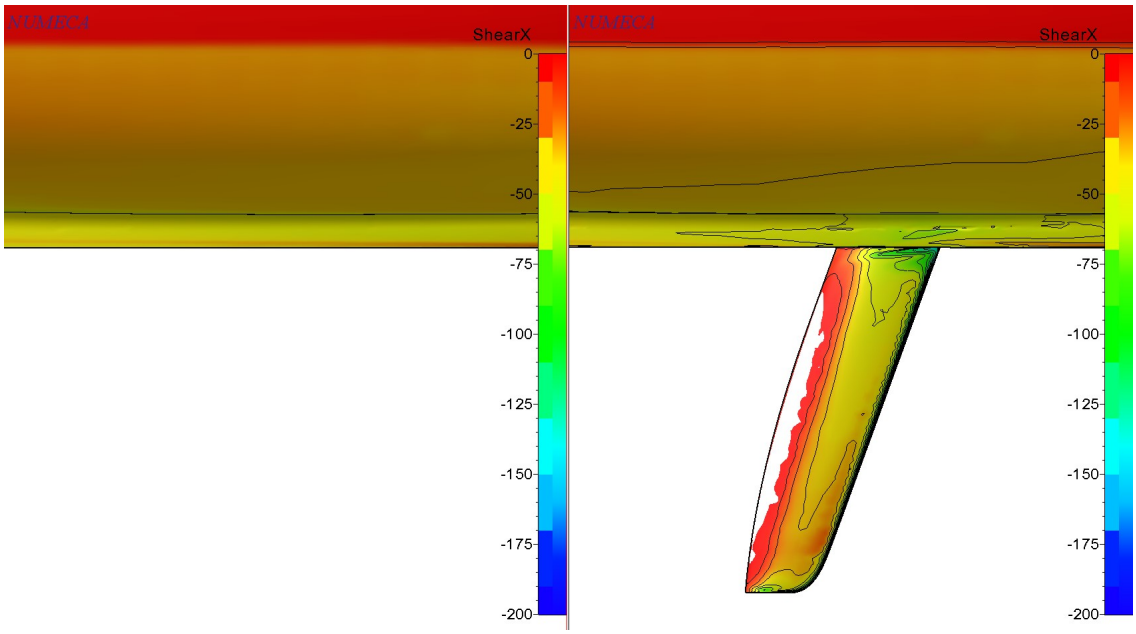

Figure A.5: The suction side of the yacht when sailing 12 knots with a leeway angle of 8 degrees.

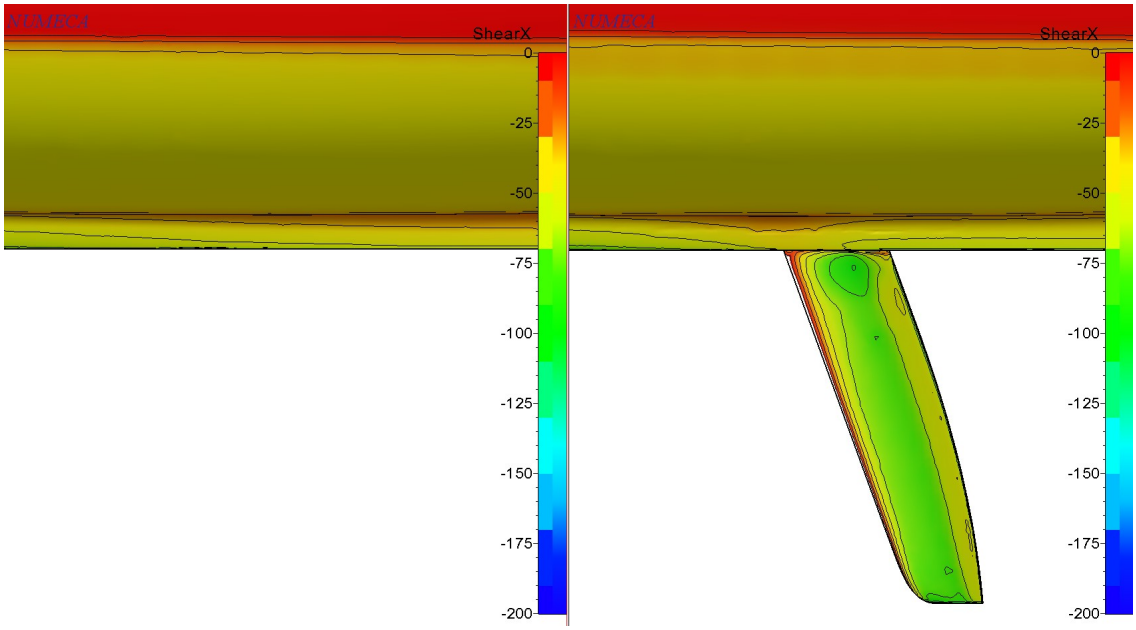

Figure A.6: The pressure side of the yacht when sailing 12 knots with a leeway angle of 12 degrees.

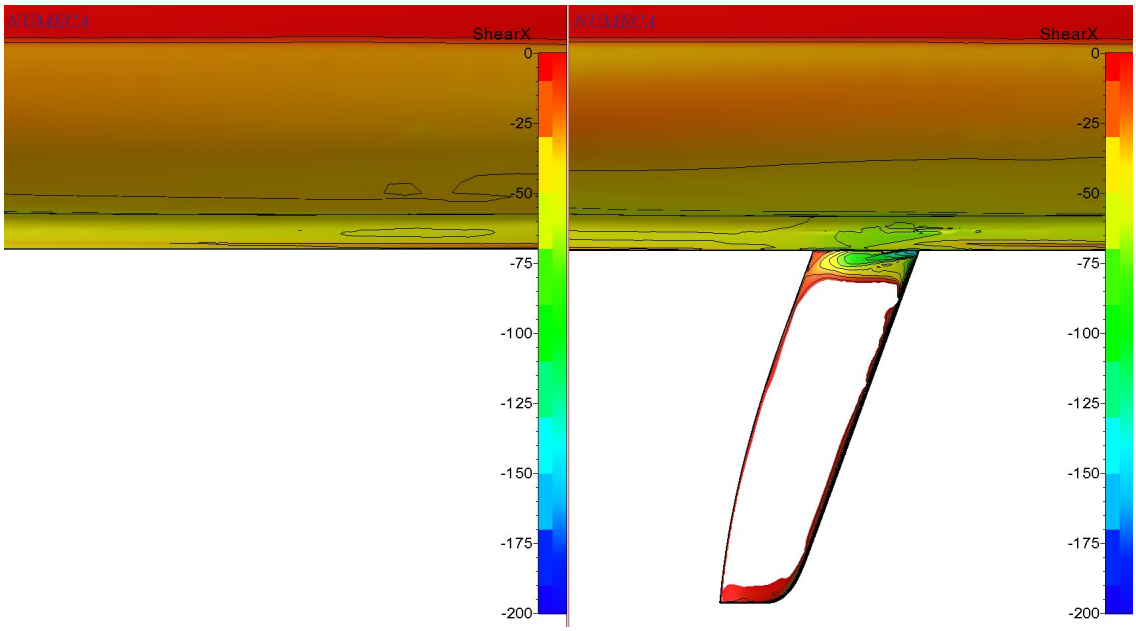

Figure A.7: The suction side of the yacht when sailing 12 knots with a leeway angle of 12 degrees.

A.3. Circulation

The circulation in the flow is made visible by showing the absolute velocity in the yz-plane. Cross sections are placed every 2 meters from 8 to 36 meters forward of the aft perpendicular. Figures A.8 and A.9 clearly show the difference in flow between the configuration without centre board (top) and with (bottom).

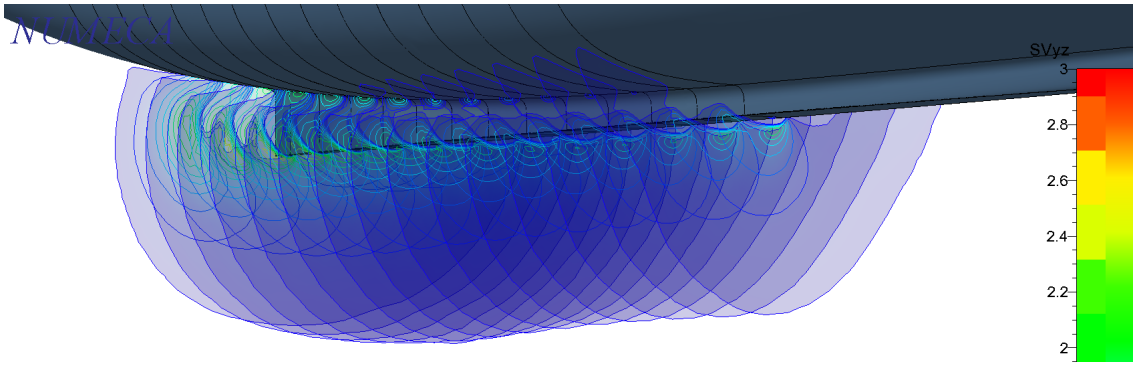

Figure A.8: The circulation of the flow indicated by the absolute velocity in the yz-plane.

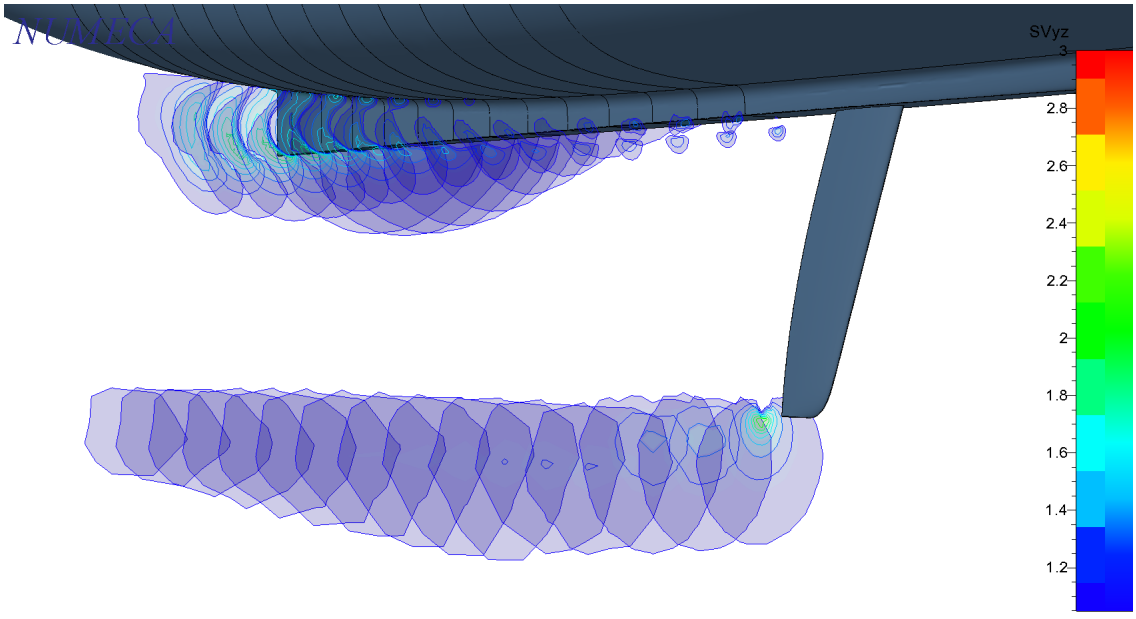

Figure A.9: The circulation of the flow indicated by the absolute velocity in the yz-plane.

Cross sections are presented for the configurations with centre board (right) and without (left). Figure A.10 shows a cross section behind the trailing edge of the centre board. Figure A.11 shows a cross section behind the trailing edge of the keel. The scale in both figures is the same.

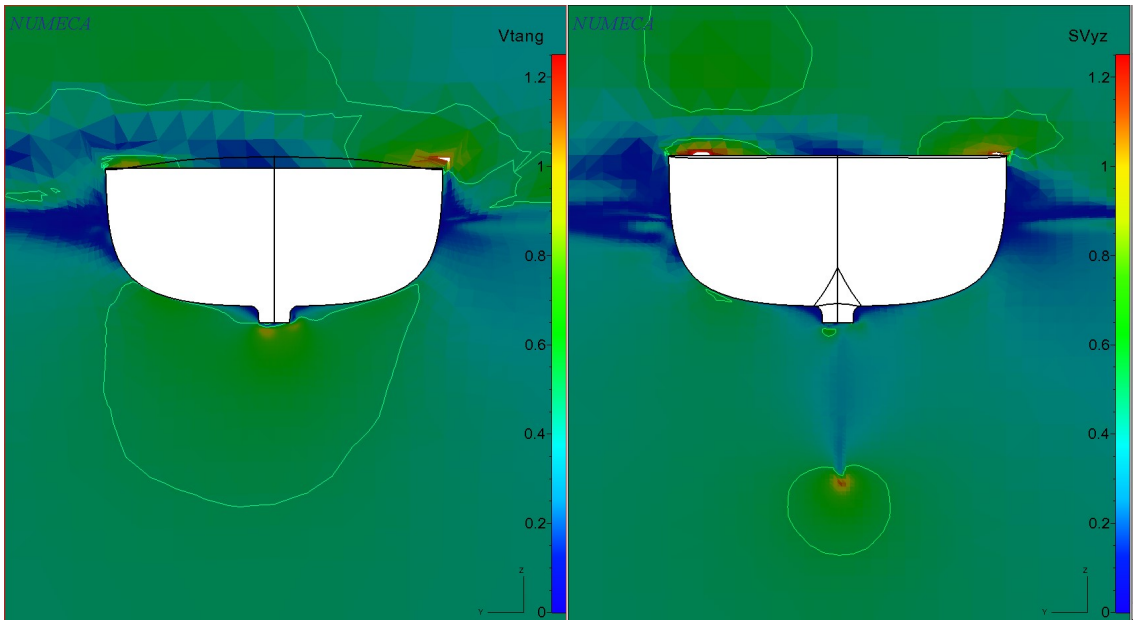

Figure A.10: The circulation of the flow indicated by the absolute velocity in the yz-plane. Vertical plane at 33 meters forward of the aft perpendicular, about 1 meter behind the trailing edge of the centre board.

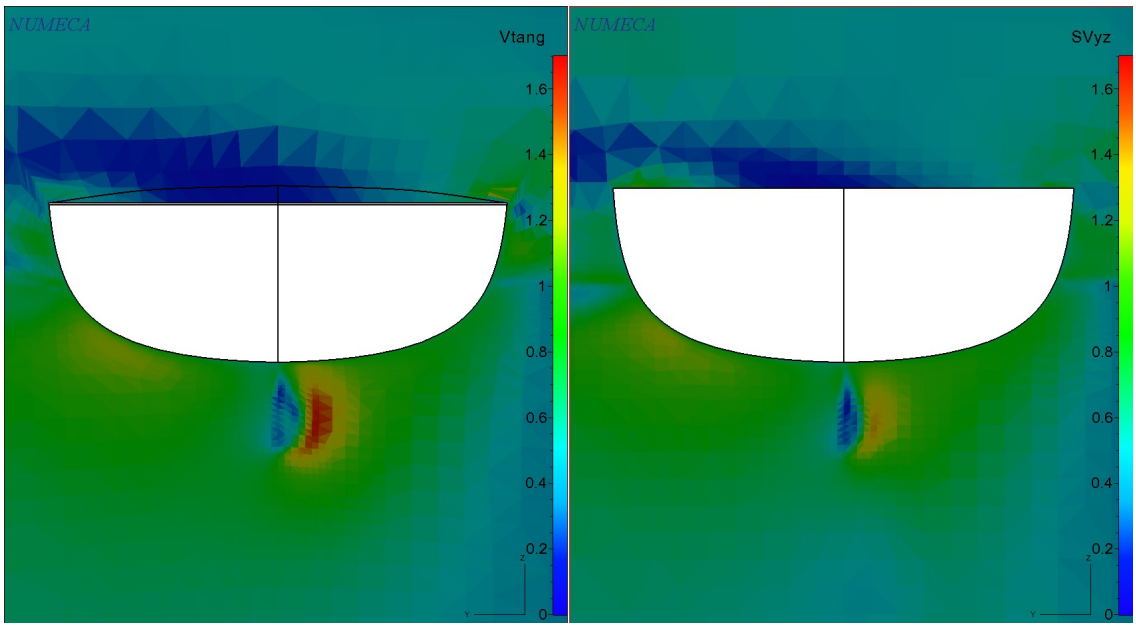

Figure A.11: The circulation of the flow indicated by the absolute velocity in the yz-plane. Vertical plane at 6.5 meters forward of the aft perpendicular, about 1 meter behind the trailing edge of the keel.

B

Layout of the Maltese Falcon

[This page was left intentionally blank]

[This page was left intentionally blank]

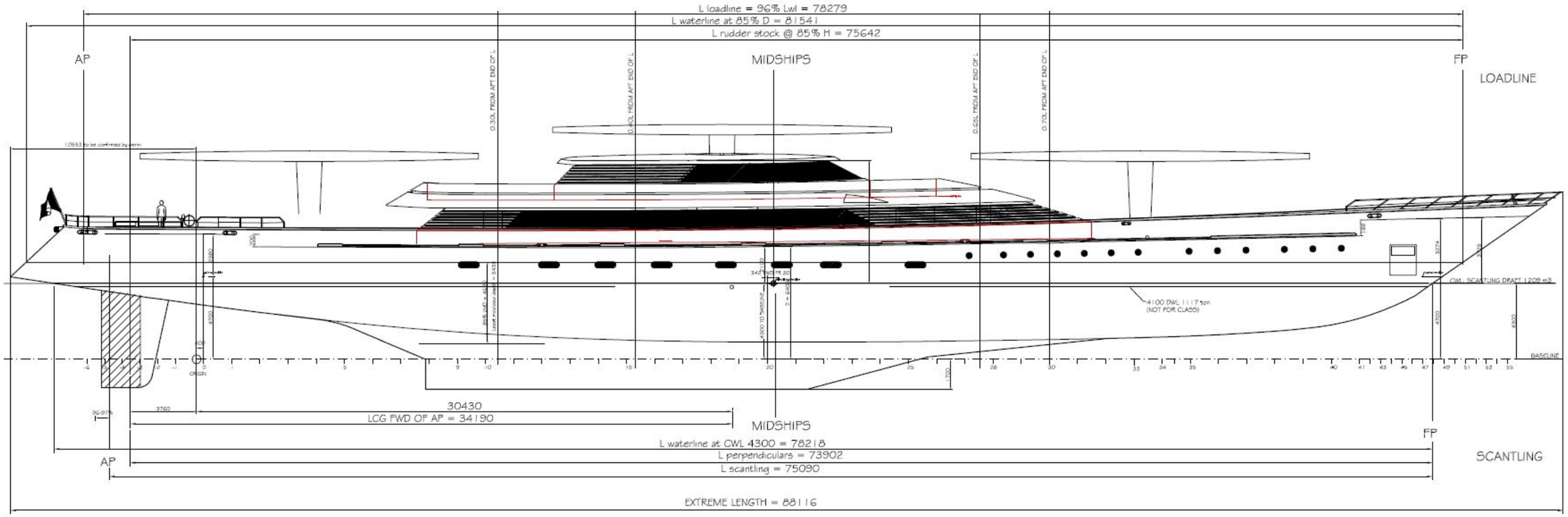

Figure 1: The main dimensions of the Maltese Falcon

C

CFD observations Maltese Falcon

[this page was left intentionally blank, to be able to show each configuration at the same leeway angle on a single page.]

C.1. Hydrodynamic pressure

The hydrodynamic pressure on the surface of the model, in configuration 5.

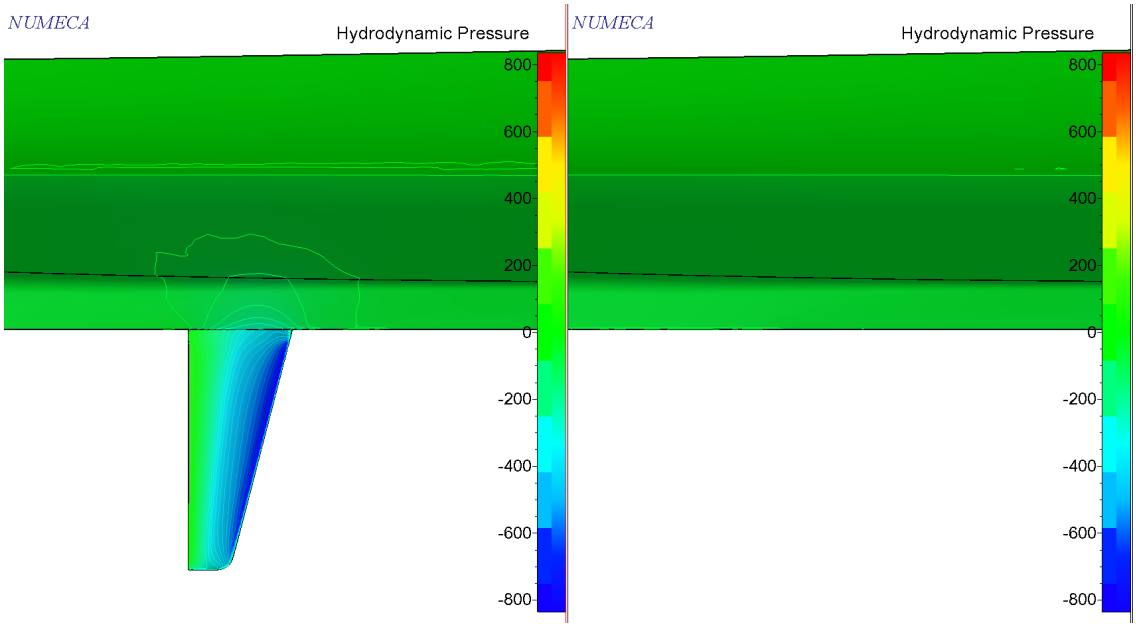

Figure C.1: Suction side. Leeway angle is 3 degrees.

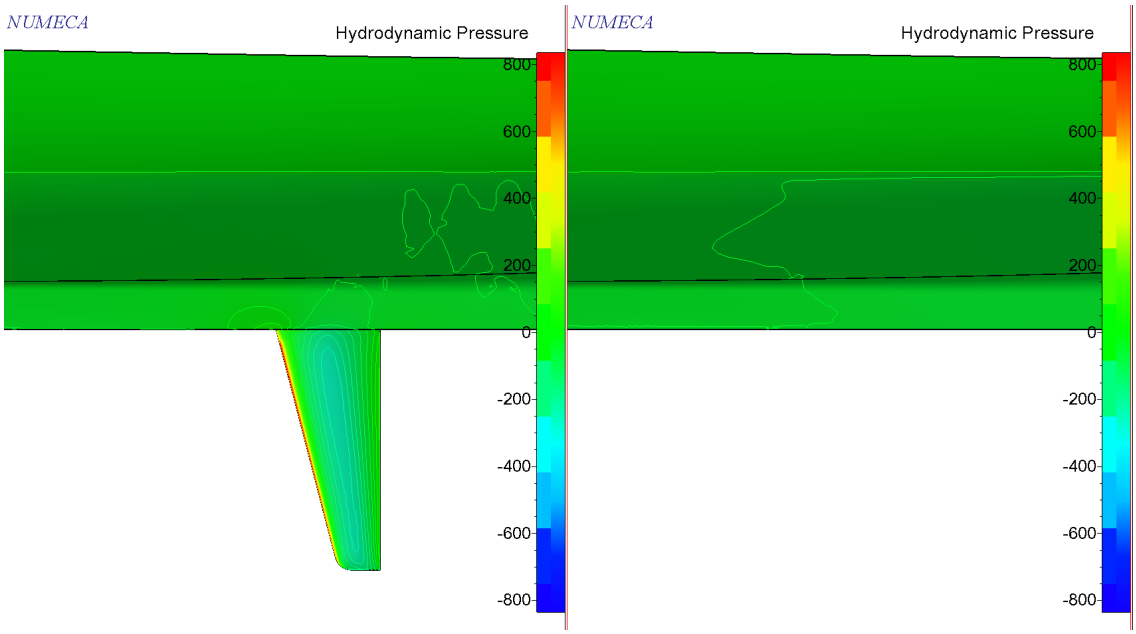

Figure C.2: Pressure side. Leeway angle is 3 degrees.

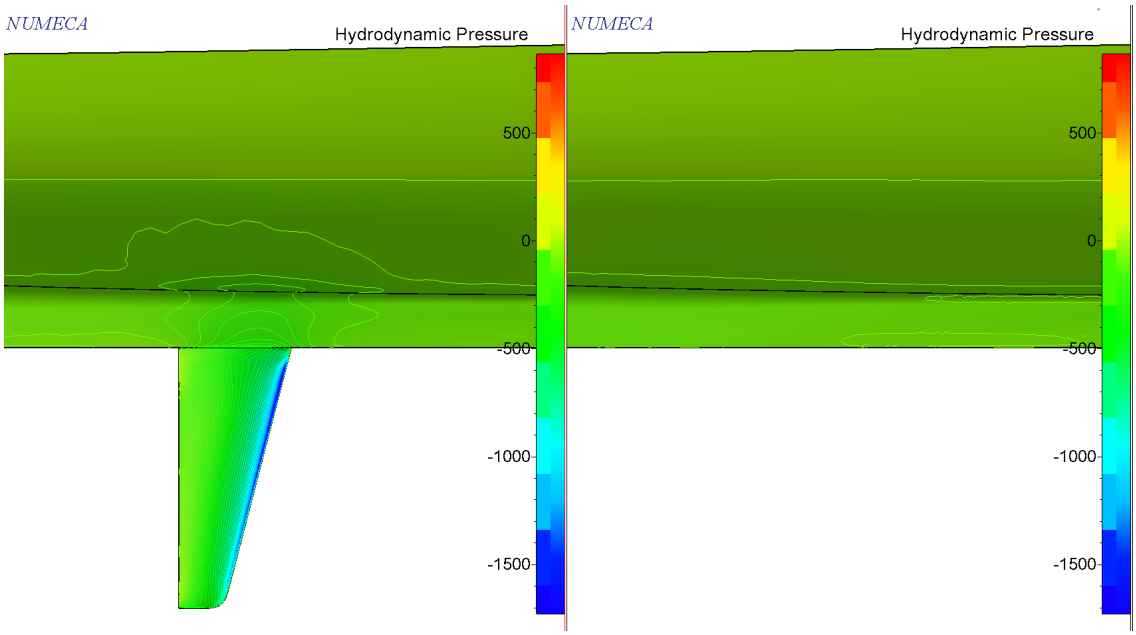

Figure C.3: Suction side. Leeway angle is 6 degrees.

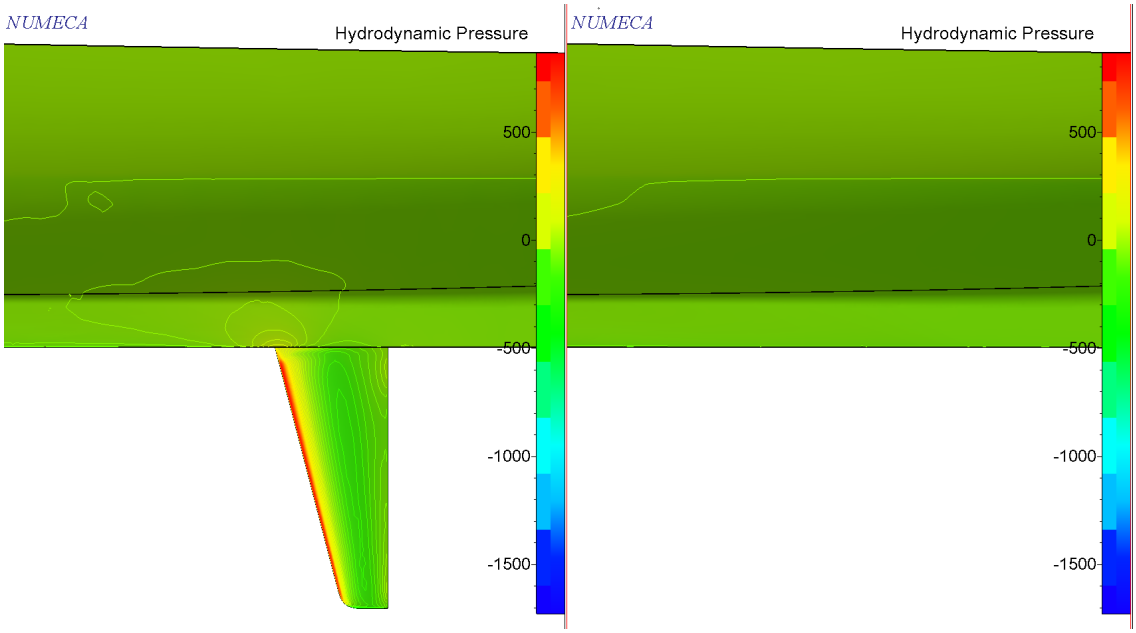

Figure C.4: Pressure side. Leeway angle is 6 degrees.

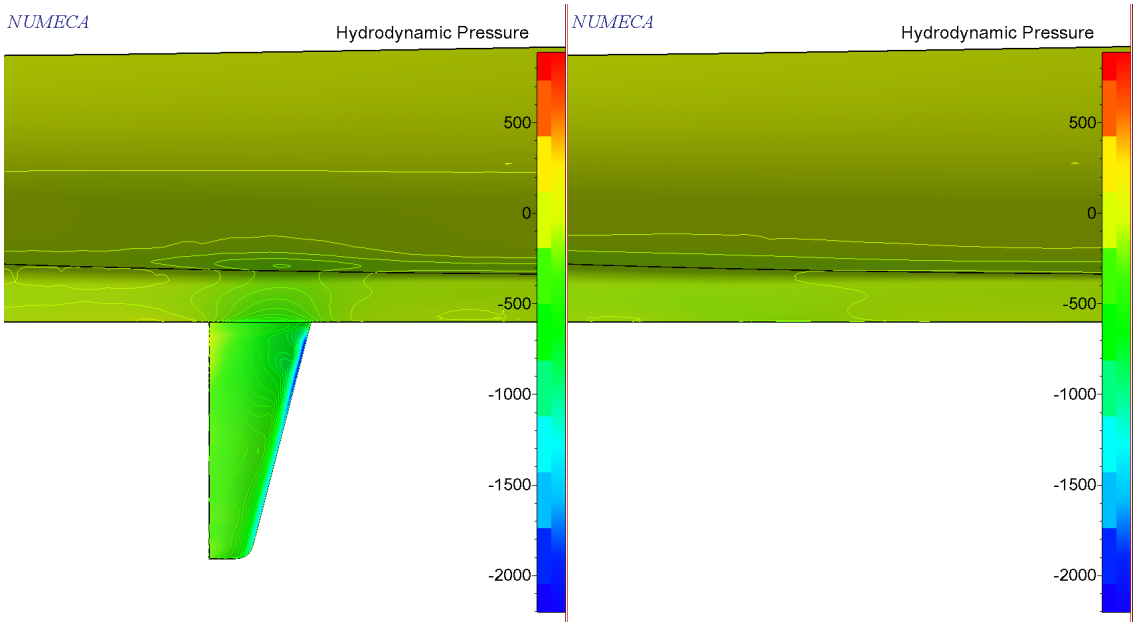

Figure C.5: Suction side. Leeway angle is 9 degrees.

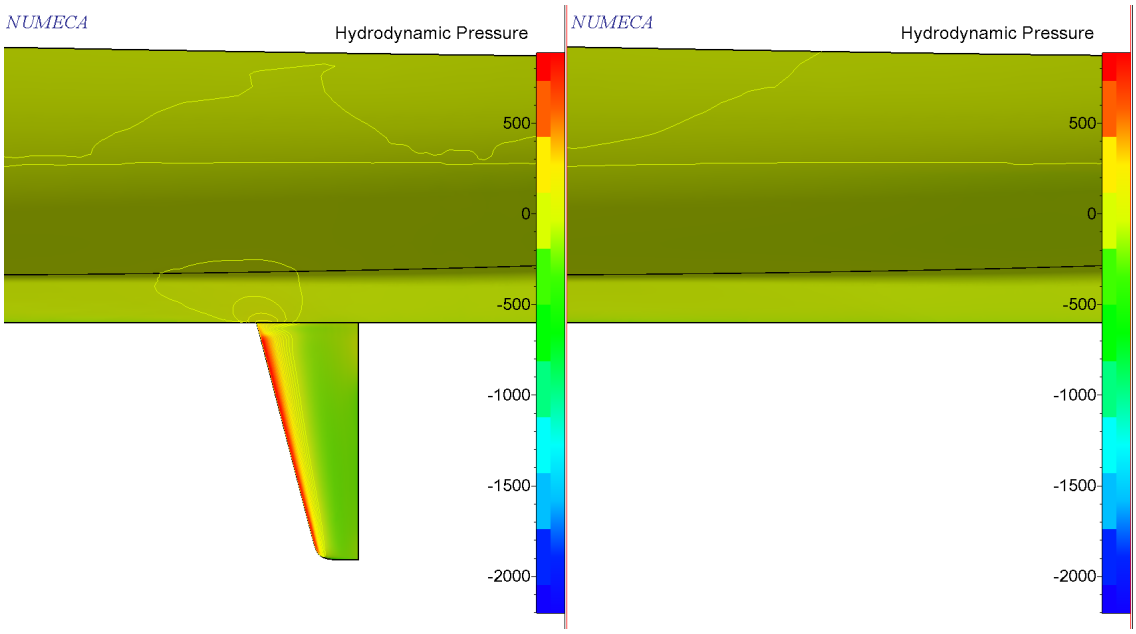

Figure C.6: Pressure side. Leeway angle is 9 degrees.

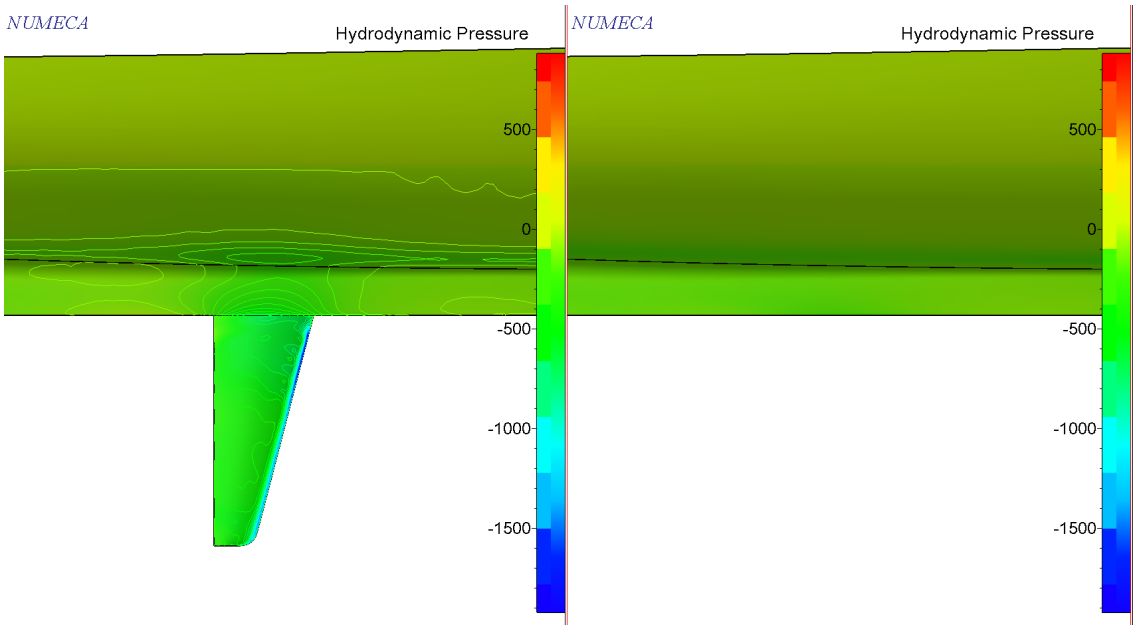

Figure C.7: Suction side. Leeway angle is 11 degrees.

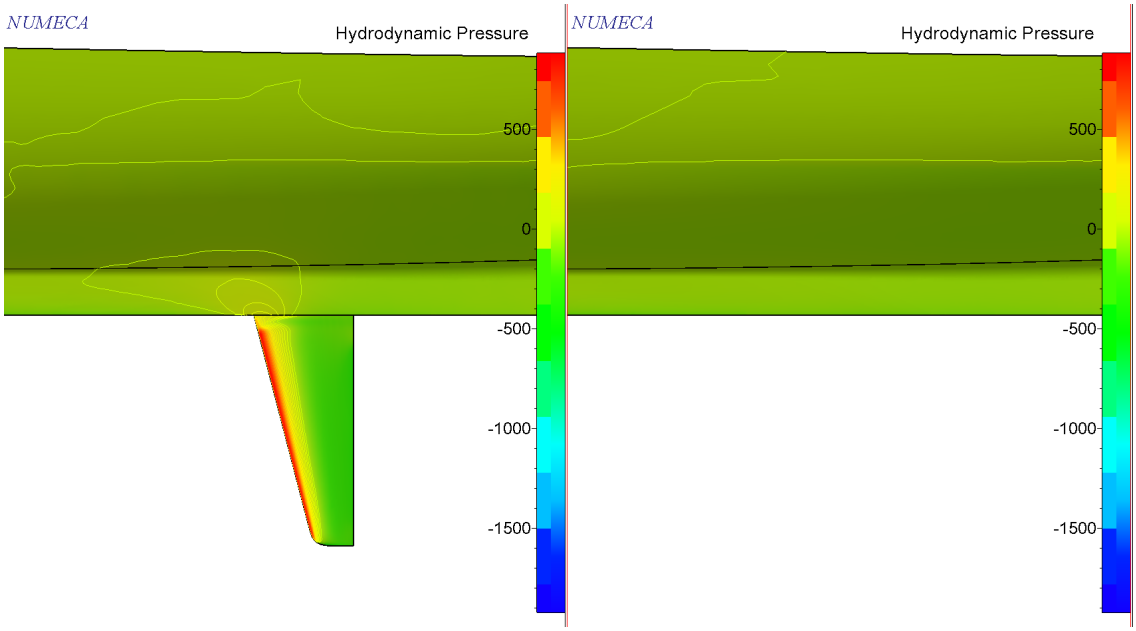

Figure C.8: Pressure side. Leeway angle is 11 degrees.

C.2. Shear in x-direction

The shear in x-direction on the surface of the model, in configuration 5. The positive x-direction is in the sailing direction of the vessel.

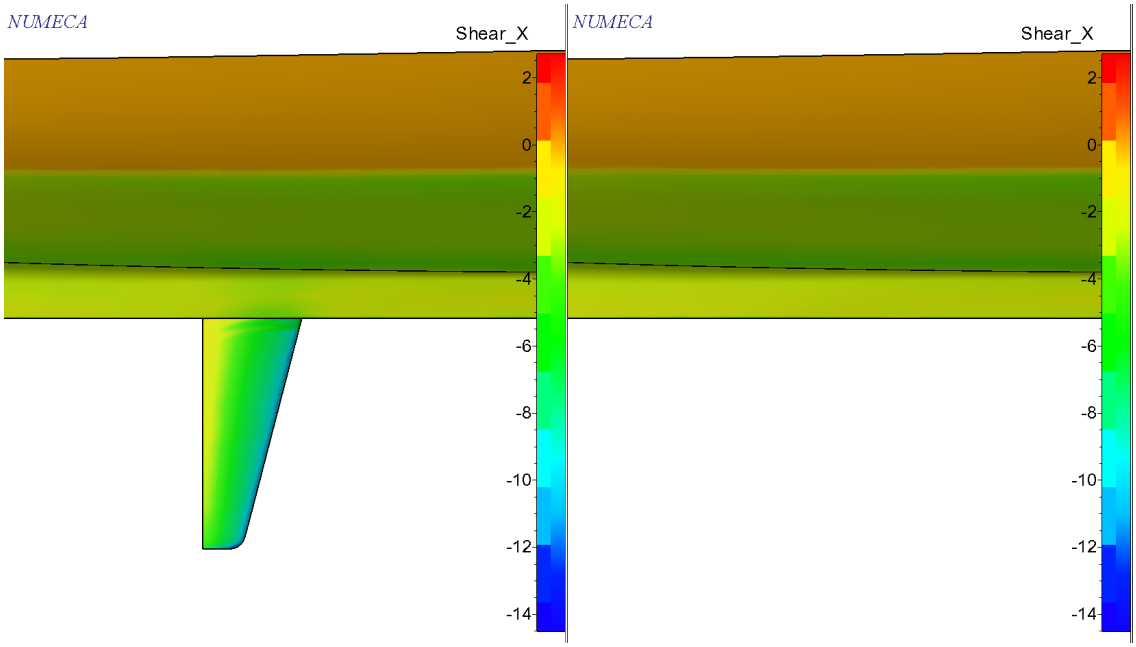

Figure C.9: Suction side. Leeway angle is 3 degrees.

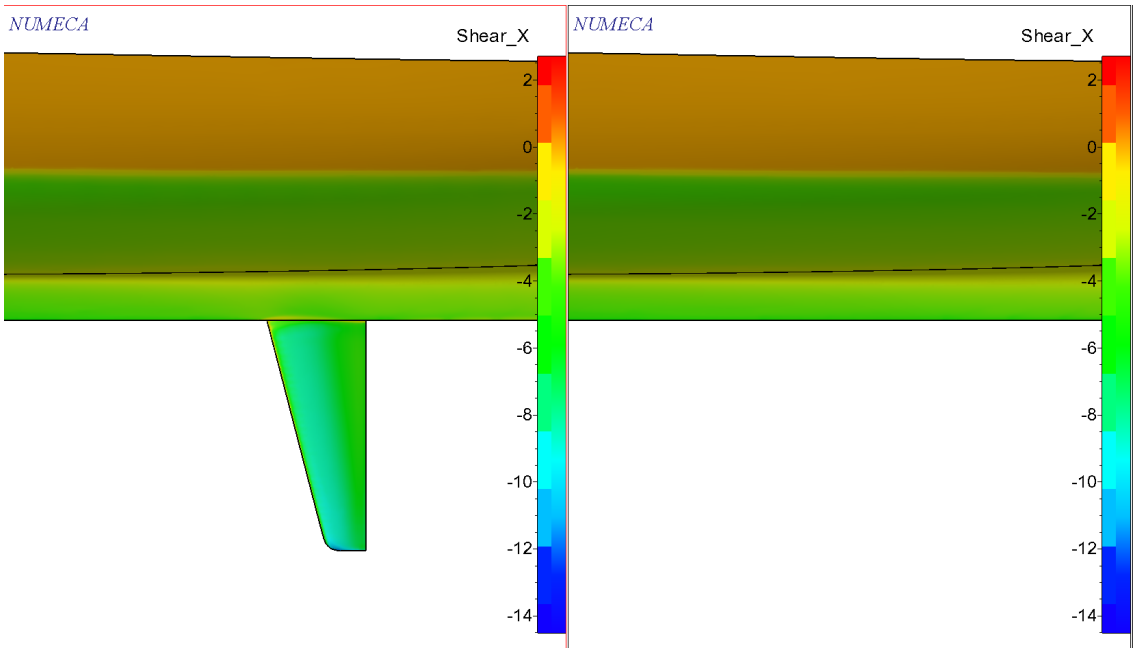

Figure C.10: Pressure side. Leeway angle is 3 degrees.

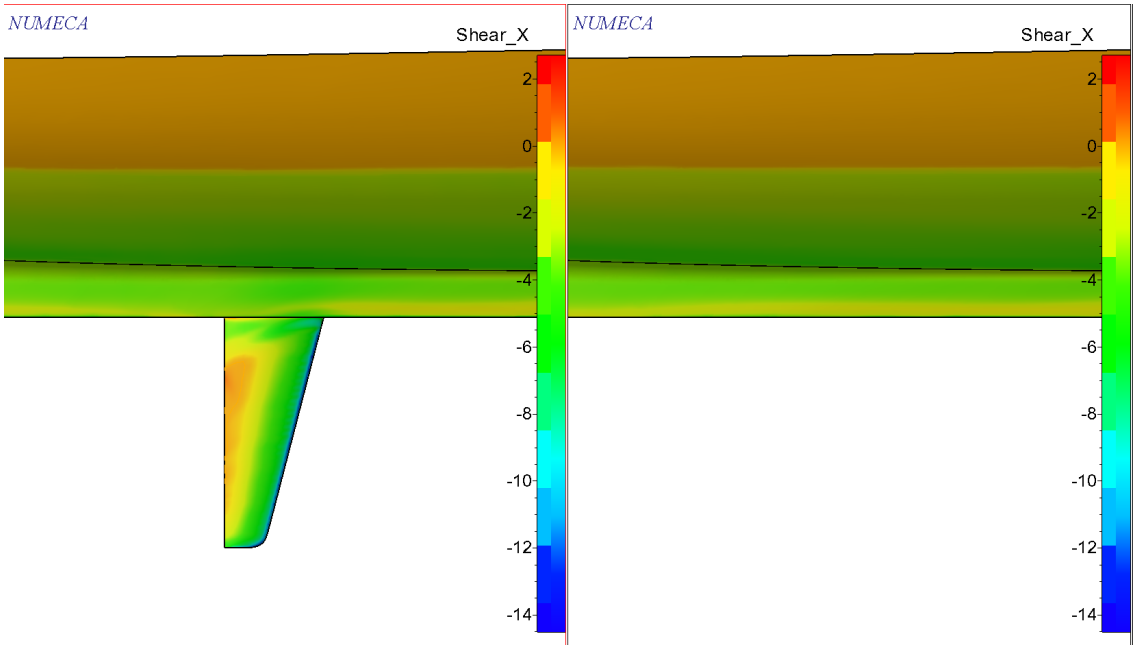

Figure C.11: Suction side. Leeway angle is 6 degrees.

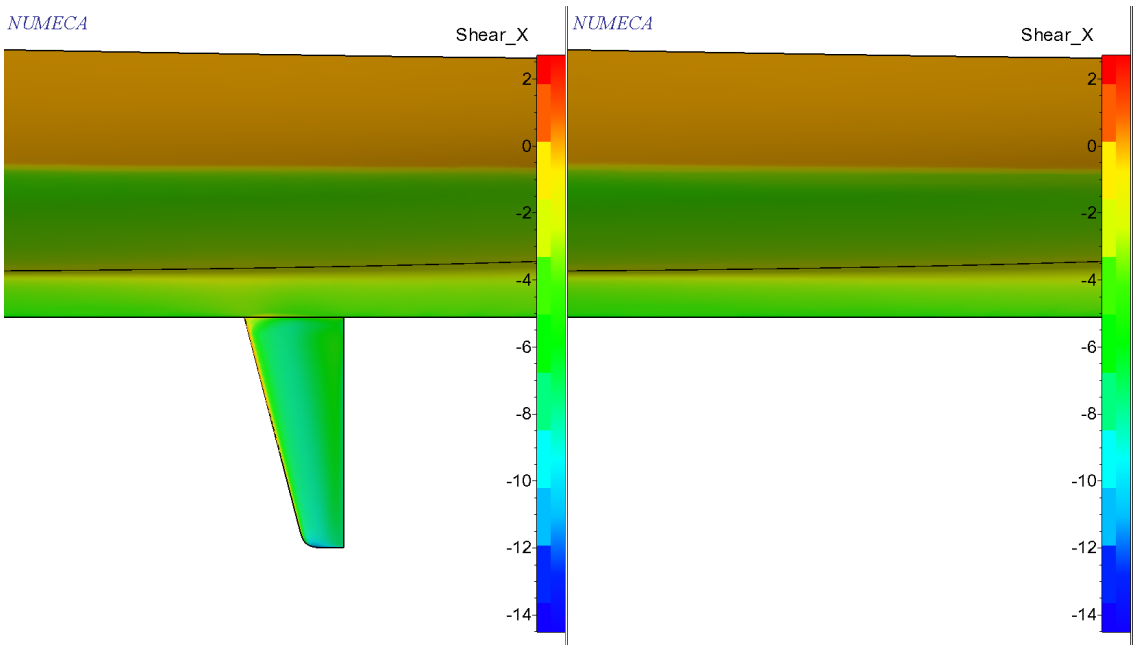

Figure C.12: Pressure side. Leeway angle is 6 degrees.

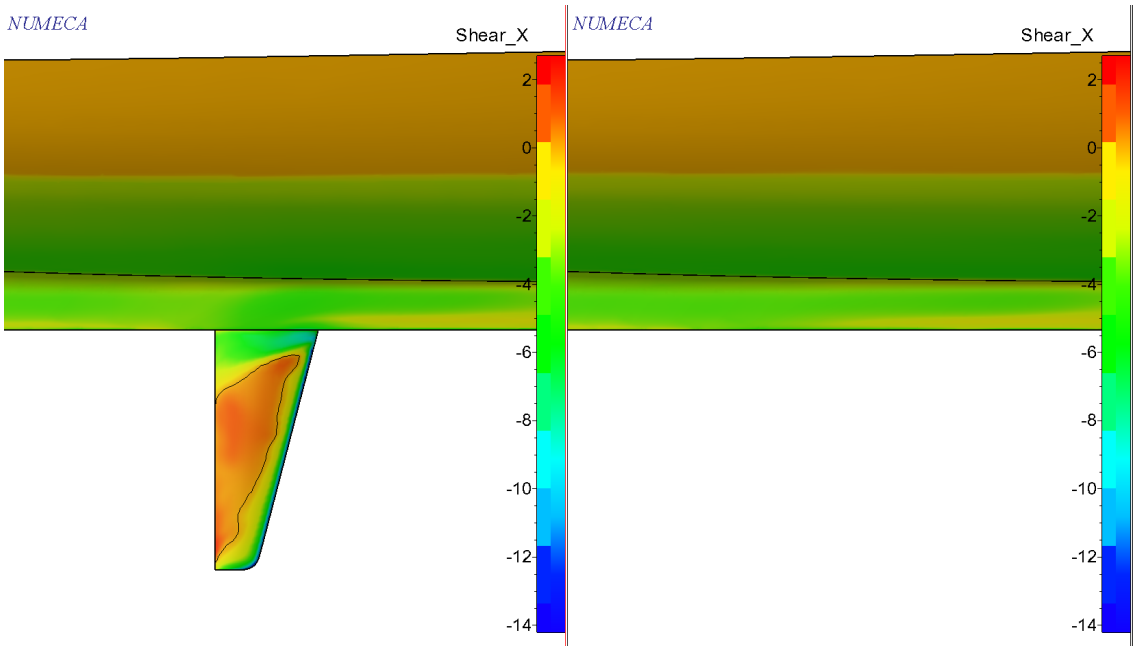

Figure C.13: Suction side. Leeway angle is 9 degrees.

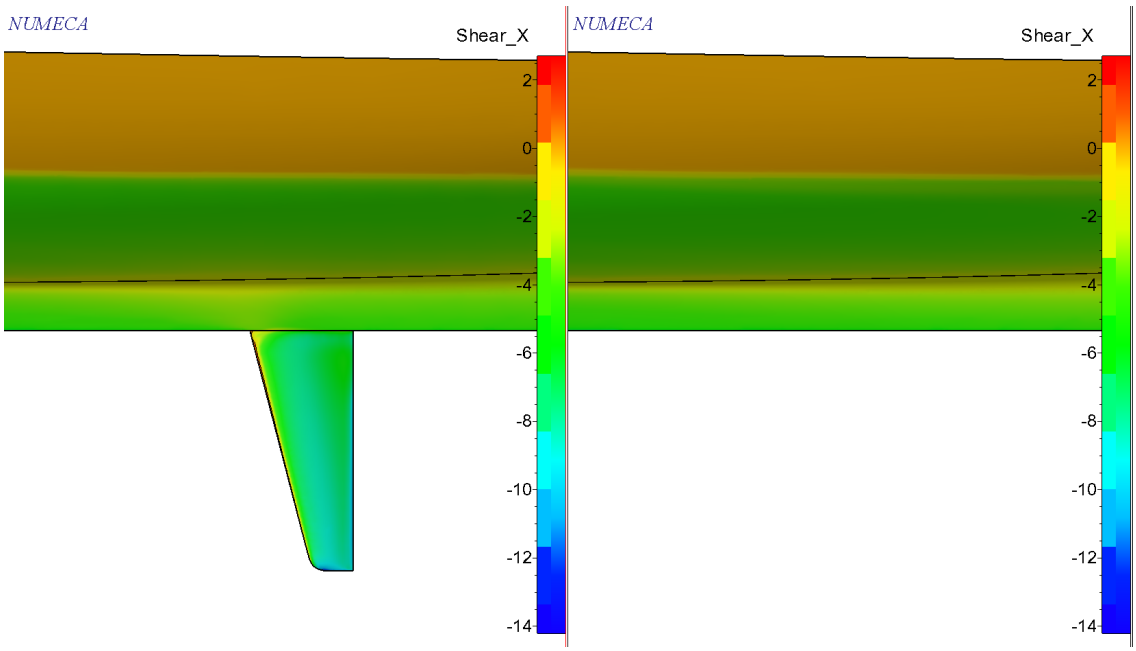

Figure C.14: Pressure side. Leeway angle is 9 degrees.

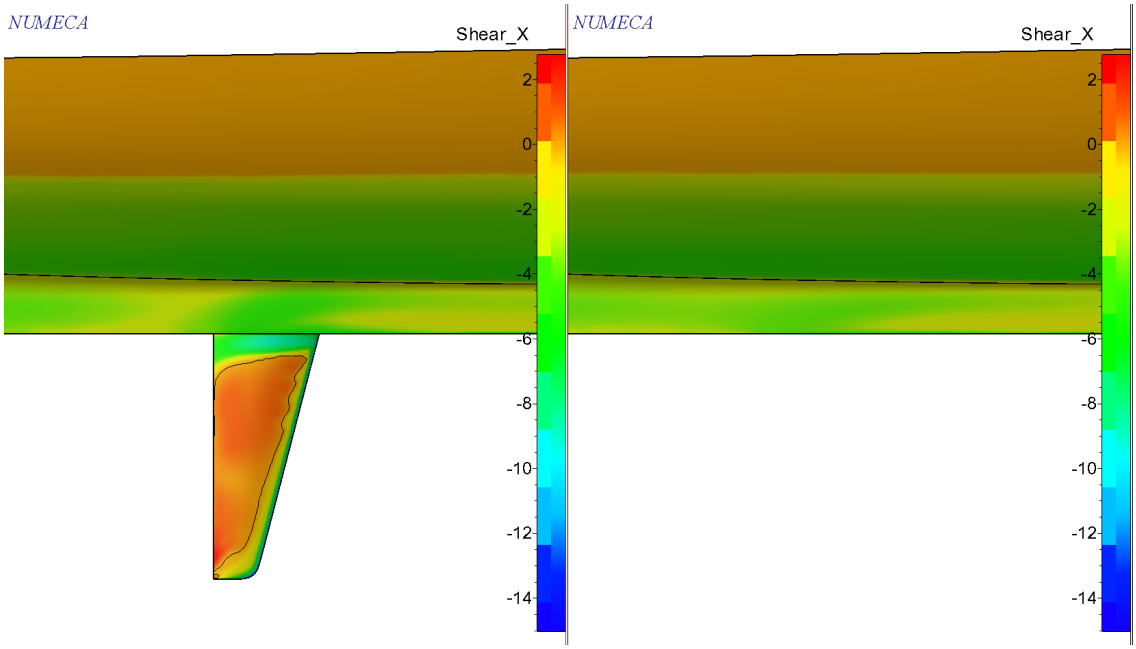

Figure C.15: Suction side. Leeway angle is 11 degrees.

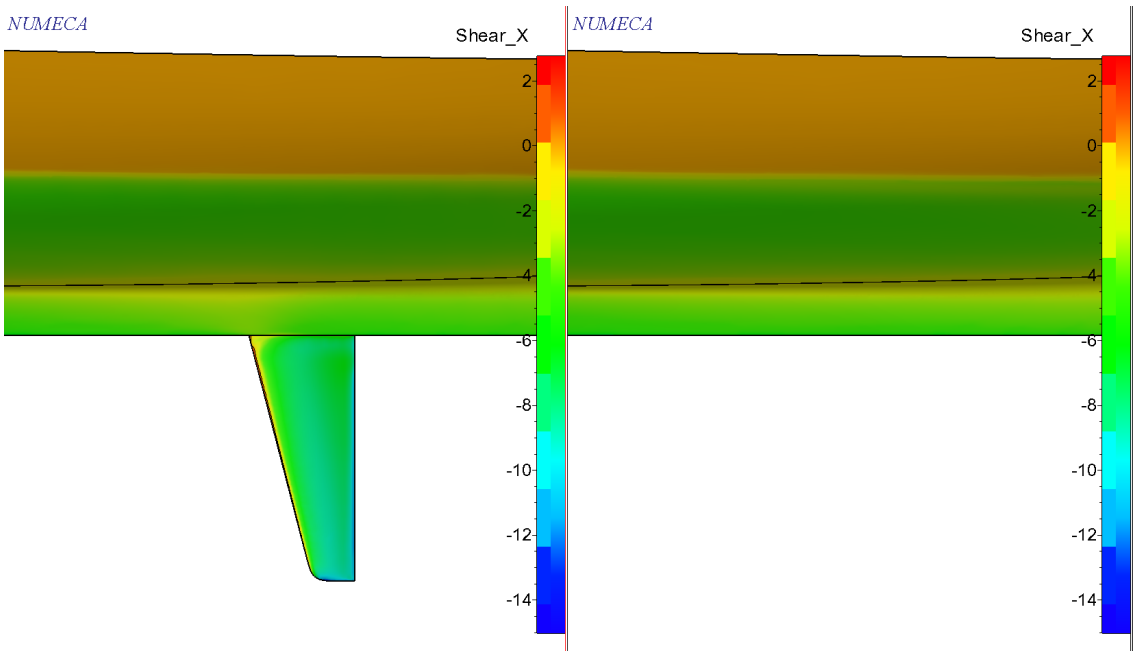

Figure C.16: Pressure side. Leeway angle is 11 degrees.

C.3. Circulation

The circulation in the flow is made visible by showing the absolute velocity in the yz-plane. Cross sections are placed every $10cm$. Figure C.17 clearly shows the difference in flow between configuration 4 (top) and 6 (bottom).

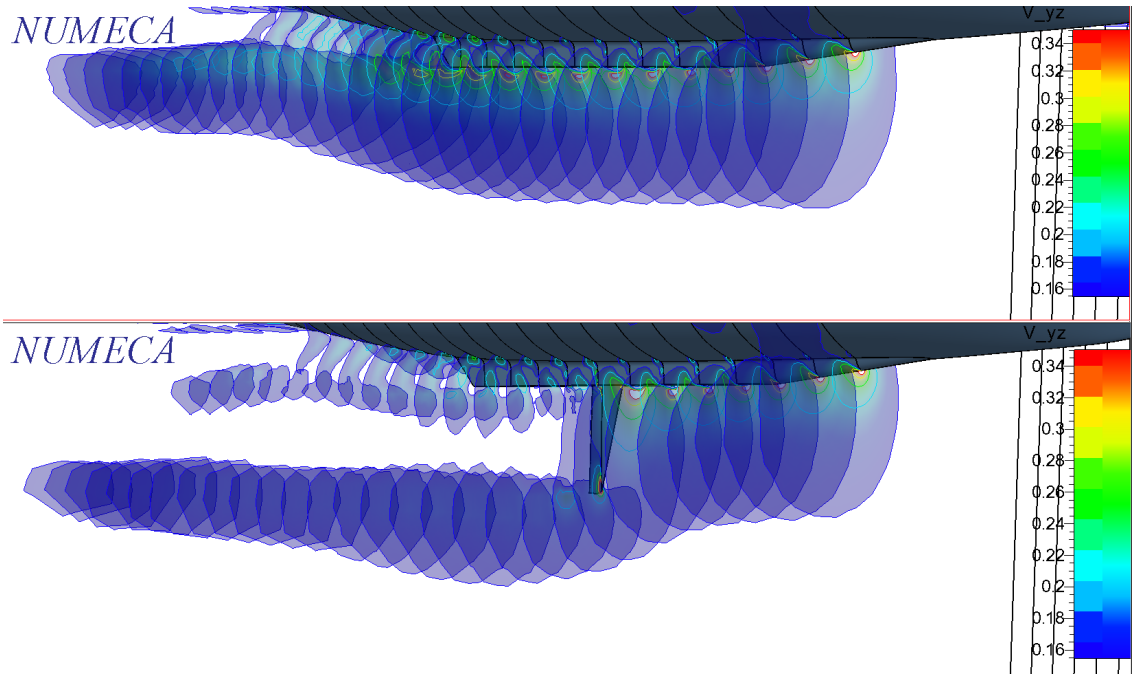

Figure C.17: Circulation in the flow around configuration 4 (top) and 6 (bottom).

Cross sections are presented for configuration 6 at left and configuration 4 at the right, both at a leeway angle of 6 degrees. Figure C.18 shows a cross section at $10cm$ behind the trailing edge of the centre board. Figure C.19 shows a cross section at $10cm$ behind the trailing edge of the keel. The scale in both figures is the same.

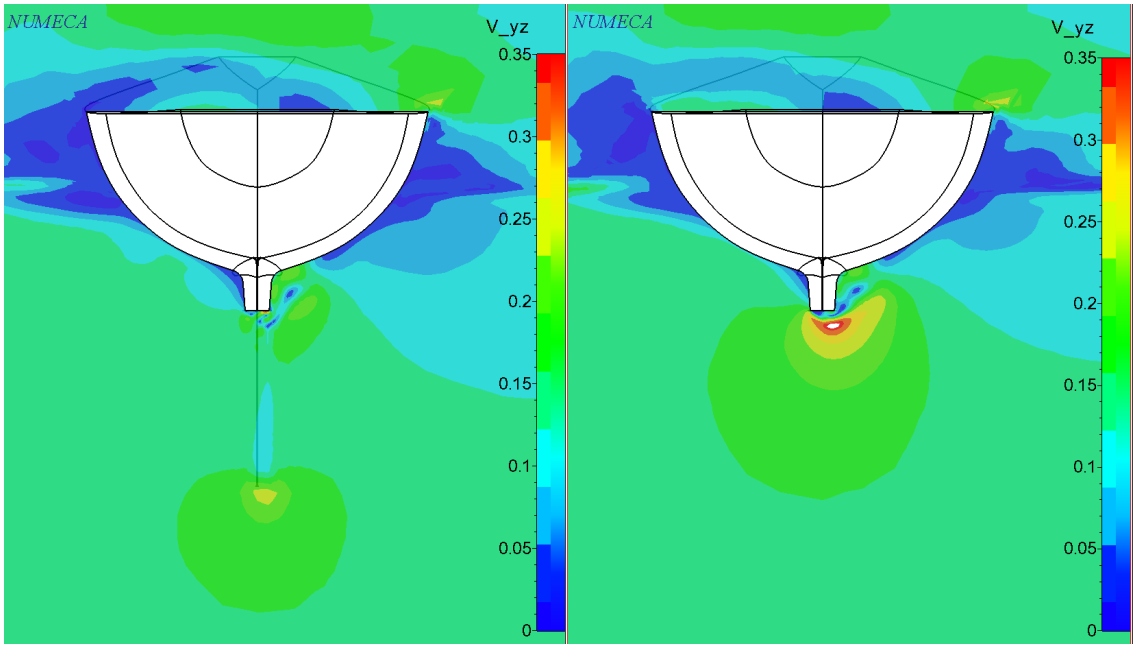

Figure C.18: Cross section at $10cm$ behind the trailing edge of the centre board. Leeway angle is 6 degrees.

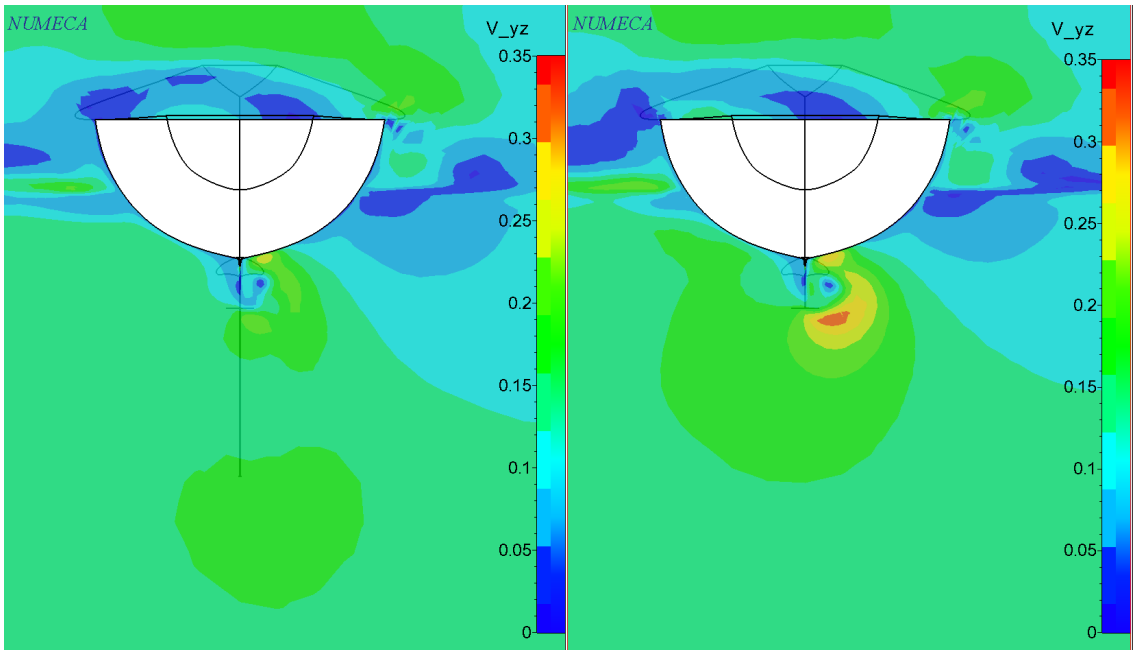

Figure C.19: Cross section at $10cm$ behind the trailing edge of the keel. Leeway angle is 6 degrees.

Bibliography

[1] B.J. Binkhorst. Keel performance in relation to keel-hull interaction. *Graduation thesis*, 1997.

[2] Christoph Böhm. *A Velocity Prediction Procedure for Sailing Yachts with a Hydrodynamic Model based on Integrated Fully Coupled RANSE-Free-Surface Simulations*. PhD thesis, October 2014.

[3] L. Larsson R.E. Eliasson. Principles of yacht design. Third edition 2007.

[4] F. Fossati. Aero-hydrodynamics and the performance of sailing yachts. First edition 2009.

[5] Prof. Ir. J. Gerritsma. Experimental analysis of five keel-hull combinations. *Ship Hydrodynamics Laboratory Delft*, December 1984.

[6] Prof. Ir. J. Gerritsma and Ir. J.A. Keuning. Model experiments with yacht keels. *Ship Hydrodynamics Laboratory Delft*, February 1985.

[7] Prof. Ir. J. Gerritsma and Ir. J.A. Keuning. Experimental determination of the performance of four keel-hull combinations. *Ship Hydrodynamics Laboratory Delft*, Oktober 1984.

[8] D. T. Greenwood. Advanced dynamics. 2006.

[9] S.F. Hoerner. Fluid dynamic drag. 1965.

[10] Ir. J.A. Keuning. Personal conversation, 2018.

[11] R. Onnink J. Gerritsma and A. Versluis. Geometry, resistance and stability of the delft systematic yacht hull series. *HISWA Symposium on Yacht Design and Yacht Construction*, 1981.

[12] M. Katgert J.A. Keuning and K.J. Vermeulen. Further analysis of the forces on keel and rudder of a sailing yacht. 2007.

[13] A.J. Keuning and U.B. Sonnenberg. Approximation of the hydrodynamic forces on a sailing yacht based on the 'delft systematic yacht hull series'. *15th International Hiswa Symposium*, 1998.

[14] A.J. Keuning and B. Verwerft. A new method for the prediction of the side force on keel and rudder of a sailing yacht based on the results of the delft systematic yacht hull series. *Chesapeake Sailing Yacht Symposium*, 2009.

[15] J.A. Keuning and G. K. Kapsenberg. Wing-body interaction on a sailing yacht. *Chesapeake Sailing Yacht Symposium*, 1995.

[16] J.A. Keuning and K.J. Vermeulen. The yaw balance of sailing yachts upright and heeled. 2003.

[17] Energétique et Environnement Atmosphérique Laboratoire de recherche en Hydrodynamique. Theoretical manual isis-cfd v6.2. *Equipe METHRIC*, July 2017.

[18] Anthony F. Molland and Stephen R. Turnock. *Marine Rudders and Control Surfaces*. Butterworth-Heinemann (imprint of Eslevier), Oxford, United Kingdom, 2007.

[19] B. Verwerft and J.A. Keuning. The modification and application of a time dependent performance model on the dynamic behaviour of a sailing yacht. *20^{th} International HISWA Symposium on Yacht Design and Yacht Construction*, November 2008.

[20] L.F. Whicker and L.F. Fehlner. Free-stream characteristics of a family of low-aspect-ratio, all movable control surfaces for application to ship design. *Technical report 933, Davind Taylor Model Basin*, 1958.